To the Graduate Council:

I am submitting herewith a thesis written by James D. Hoskins, III entitled "Testing and Modeling of Undisturbed Samples of Fine Grained Soil." I have examined the final copy of this thesis for form and content and recommend that it be accepted in partial fulfillment of the requirements for the degree of Master of Science, with a major in Civil Engineering.

Eric C. Drumm

Eric C. Drumm, Major Professor

We have read this thesis
and recommend its acceptance:

William F. Kane

Richard M. Bennett

Accepted for the Council:

Lee Minkel

Vice Provost
and Dean of The Graduate School

STATEMENT OF PERMISSION TO USE

In presenting this thesis in partial fulfillment of the requirements for a Master's degree at The University of Tennessee, Knoxville, I agree that the Library shall make it available to borrowers under rules of the Library. Brief quotations from this thesis are allowable without special permission, provided that accurate acknowledgment of the sources is made.

Permission for extensive quotation from or reproduction of this thesis may be granted by my major professor, or in his absence, by the Head of Interlibrary Services when, in the opinion of either, the proposed use of the material is for scholarly purposes. Any copying of use of the material in this thesis for financial gain shall not be allowed without my written permission.

Signature James O. Hoskins, III

Date 18 August 1989

# Testing and Modeling of Undisturbed Samples of Fine Grained Soil

A Thesis

Presented for the

Master of Science

Degree

The University of Tennessee, Knoxville

James Dickason Hoskins, III

December 1989

## DEDICATION

This thesis is dedicated to my grandparents,

Weezie and Dundee, and to my wife, Susan.

## ACKNOWLEDGMENTS

The completion of this thesis would not have been possible if it were not for the support, encouragement, and intellectual guidance of my major professor, Dr. Eric C. Drumm. I am also indebted to Mr. Curtis Allen, who eagerly gave of his time, assistance, and knowledge and without whom my laboratory work may never have been completed. I would like to thank Dr. William Kane and Dr. Richard Bennett for their support and guidance. Special thanks is given to Dr. Larry Powell, Mr. Ted Triplett, and Dr. Kevin O'Conner for their guidance and the United States Bureau of Mines Twin Cities Research Center for financial support. In addition, the managing of this manuscript, along with other assistance, by Miss Yvonne Honeycutt is greatly appreciated.

A deep hearted thanks is extended to my family in Charlotte, N.C. and both sets of my grandparents here in Knoxville. I can never fully express the appreciation I wish to convey to Weezie and Dundee for providing a home away from home, meals, and a fun place to just sit around and talk about the old days and modern times.

Finally, I would like to thank my wife, Susan, for her encouragement, support, and patience.

## ABSTRACT

In the geotechnical field, common problems can become very complicated and usually difficult to solve directly. One such problem is the occurrence of surface subsidence due to high extraction or longwall methods of coal mining. This surface subsidence can cause serious damage to structures and agricultural areas. Concern about longwall-induced surface subsidence has prompted research aimed at minimizing or preventing the structural damage. Such research is concerned with designing a new foundation system able to withstand the effects of surface subsidence. To design such a system, several important areas must be analyzed. These areas include the behavior of foundation itself, the foundation-soil contact and the soil beneath the foundation.

To analyze such a system using simplified hand calculations is very inefficient and will probably yield poor results. In such cases, a numerical analysis may provide the engineer with a method of solution. However, numerical analysis methods that do account for the behavior usually associated with geologic materials involve an advanced constitutive model and may require extensive laboratory testing to determine the model parameters. The properties selected to represent the highly nonlinear, inelastic soil can be expected to significantly affect the analysis results. It is the purpose of this thesis to determine the Sandler cap model parameters (DiMaggio and Sandler, 1971) for a soil from Sesser, Illinois that will be used in this numerical analysis and to suggest an alternate method or simplified procedure by which these parameters can be determined.

## TABLE OF CONTENTS


| CHAPTER | | PAGE |
|---|---|---|
| 1. | INTRODUCTION | 1 |
| | 1.1 Statement of Problem | 1 |
| | 1.2 Purpose of Study | 1 |
| | 1.3 Notation | 3 |
| 2. | PREVIOUS RESEARCH | 5 |
| | 2.1 Modeling Introduction | 5 |
| | 2.2 Elastic Models | 7 |
| | 2.3 Hypoelastic Model | 8 |
| | 2.4 Elastic-Plastic Models | 10 |
| | 2.5 Development of Elastic-Plastic Models | 12 |
| | 2.6 Cap Model | 15 |
| 3. | LABORATORY CONSIDERATIONS | 20 |
| | 3.1 Typical Triaxial Set Up | 20 |
| | 3.2 Triaxial Devices | 23 |
| | 3.3 Triaxial Stress Paths | 27 |
| | 3.4 Volume Change and Area Corrections | 31 |
| | 3.5 Additional Testing Considerations | 36 |
| 4. | SAMPLING AND TESTING PROCEDURE | 38 |
| | 4.1 Field Sampling | 38 |
| | 4.2 Sample Preparation | 40 |
| | 4.3 Testing Procedure-Drained | 41 |
| | 4.4 Testing Procedure-Undrained | 48 |
| | 4.5 Data Acquisition | 49 |
| | 4.6 Data Reduction | 53 |
| 5. | PARAMETER DETERMINATION PROCEDURE | 54 |
| | 5.1 Determination Procedure | 54 |
| | 5.2 Actual Parameter Determination for Sesser Soil | 59 |
| | 5.3 Back Prediction Procedure | 76 |
| | 5.4 Brief Summary of Published Cap Model Parameter for Various Materials | 79 |

CHAPTER PAGE

6. SIMPLIFIED PARAMETER DETERMINATION PROCEDURE ..... 83
6.1 Steps and Justification ..... 83

7. CONCLUSIONS AND SUGGESTIONS ..... 87
7.1 Summary ..... 87
7.2 Conclusions and Suggestions ..... 88

REFERENCES ..... 91

APPENDICES ..... 96
APPENDIX A Sesser Soil Properties ..... 97
APPENDIX B Sample Preparation Data ..... 99
APPENDIX C Additional Test Graphs ..... 105
APPENDIX D REDUC Computer Program ..... 109
APPENDIX E Equipment Usage Procedure ..... 122
APPENDIX F Triaxial Test Procedures ..... 130

VITA ..... 135

## LIST OF TABLES


| TABLE | | PAGE |
|---|---|---|
| 2.1 | Summary of Cap Model Parameters | 19 |
| 4.1 | Sample Drainage Condition Factor | 42 |
| 5.1 | Preliminary Testing Plan | 60 |
| 5.2 | Volumetric Strain Table for Determination of Parameter D | 77 |
| 5.3 | Summary of Initial Sesser Soil Cap Model Parameters | 78 |
| 5.4 | Brief Summary of Published Cap Model Parameters for Various Materials | 80 |

## LIST OF FIGURES


| FIGURE | | PAGE |
|---|---|---|
| 2.1 | Comparison of observed soil behavior and linear elastic model | 9 |
| 2.2 | Comparison of observed soil behavior and non-linear elastic model | 9 |
| 2.3 | Elastic and plastic strain diagram - first unload cycle | 11 |
| 2.4 | Elastic and plastic strain diagram - second unload cycle | 11 |
| 2.5 | Boundary surface of Cam clay model | 14 |
| 2.6 | Failure surfaces for DiMaggio-Sandler cap model | 17 |
| 2.7 | Failure surfaces for cap model and showing yield surface | 17 |
| 3.1 | Typical drained triaxial testing set-up | 21 |
| 3.2 | Typical undrained triaxial testing set-up | 22 |
| 3.3 | Cylindrical triaxial device schematic | 24 |
| 3.4 | "Cubical" triaxial device schematic | 26 |
| 3.5 | Hollow cylinder stress schematic | 26 |
| 3.6 | Triaxial stress paths in $\sigma_1$ - $\sqrt{2}\sigma_3$ stress space | 28 |
| 3.7 | Triaxial stress paths in p-q stress space | 28 |
| 3.8 | Triaxial stress paths in $J_1$ - $\sqrt{J_{2D}}$ stress space | 29 |
| 3.9 | Basic schematic of volume change device | 32 |
| 3.10 | Triaxial chamber contraction and expansion correction curves | 35 |
| 4.1 | Map location of Sesser, Illinois, USA | 39 |
| 4.2 | $t_{90}$ construction plot | 44 |
| 4.3 | Hydrostatic compression test showing load-unload cycle | 46 |
| 4.4 | Typical X - Y - Y' plotter calibration curve | 51 |

FIGURE PAGE

4.5 Typical X - Y - Y′ plotter calibration curve ..... 51

4.6 Typical X - Y - Y′ plotter calibration curve ..... 52

5.1 Example of specimen coding system ..... 61

5.2 CTC-20-CD (LUR)-TH-SS-1 stress-axial strain curve ..... 62

5.3 CTC-20-CD (LUR)-TH-SS-2 stress-axial strain curve ..... 62

5.4 CTC-20-CD (LUR)-TH-SS-1 stress-lateral strain curve ..... 64

5.5 CTC-20-CD (LUR)-TH-SS-2 stress-lateral strain curve ..... 64

5.6 HC-1 stress-octahedral strain curve ..... 66

5.7 HC-2 stress-octahedral strain curve ..... 66

5.8 CTC stress-strain curves ..... 68

5.9 TC stress-strain curves ..... 68

5.10 RTC stress strain curve ..... 69

5.11 Triaxial stress paths ..... 71

5.12 Drucker-Prager I and II surfaces ..... 72

5.13 Plot of plastic yield caps ..... 75

# CHAPTER 1

# INTRODUCTION

## 1.1 Statement of Problem

In the geotechnical field, common problems can become very complicated and usually difficult to solve directly. In such cases, a numerical analysis may provide the engineer with an alternate method of solution. However, many of the numerical analysis methods used for engineering problems do not account for inelastic and strain hardening behavior that is ordinarily associated with geologic materials. Numerical analyses that do account for such behavior usually involve an advanced constitutive model such as a plasticity based model and require extensive laboratory testing to determine the model parameters.

One elastic-plastic model which has worked well in modeling the behavior of geologic materials, such as soil and rock, is the cap model. For the cap model (DiMaggio and Sandler, 1971; Sture et al., 1979) to be used in a numerical analysis nine to ten material parameters must be determined. These parameters have traditionally come from the results of a series of drained triaxial tests. If the material is a fine grained soil, it can take up to six weeks to determine these parameters.

## 1.2 Purpose of Study

Coal, one of the United States' most abundant energy resources, has been mined in this country for centuries. Until recently, the majority of coal was mined using a method called room-and-pillar mining. The room-and-pillar

method involves mining an entry straight into the seam of coal and then, at set intervals, branching to the left and right to connect with adjacent entries. This method leaves a series of rectangular pillars of coal which support the roof. A major problem associated with room-and-pillar mining is that without high extraction mining methods, thirty to fifty percent of the coal, in the form of pillars, is left in the mine for roof support. When the mine is abandoned, the pillars are either left in place to keep the roof from collapsing or they are extracted using a method called "robbing the pillars." Since extracting the pillars can be dangerous due to roof collapse, the pillars are often left in the mine. In the past, with the roof supported, the room and pillar method of mining usually had no immediate adverse effects on the surface. However, the pillar strength usually degrades with time leaving abandoned mining operations responsible for surface subsidence years later.

A newer method of coal mining, called longwall mining, is currently utilized in some areas of the United States. Longwall mining allows the roof to collapse behind the continuous mining machine. Because no coal is left in the mine to support the roof, higher rates of coal recovery and greater efficiency can be achieved thus making this method more economical. One problem with the longwall method is that the roof is allowed to collapse, thereby producing surface effects, specifically surface subsidence. Surface subsidence may not be considered important in some remote areas; however, subsidence does pose serious problems in populated and agricultural areas. Because subsidence occurs in a wave type fashion, there is usually considerable damage done to any

structures under which subsidence occurs due to the differential movement of the foundation.

Concern about longwall-induced surface subsidence has prompted research aimed at minimizing or preventing the structural damage. To help develop a foundation system that may prevent or minimize subsidence-induced structural damage, a numerical analysis involving an advanced constitutive model can be applied. To conduct a numerical analysis of the foundation system, several aspects of the material response must be evaluated. These areas include the behavior of the foundation structure itself, the behavior of the foundation and soil contact or interface, and the behavior of the soil under the foundation.

The properties selected to represent the highly nonlinear, inelastic soil behavior can be expected to significantly affect the analysis results. It is the purpose of this thesis to determine the model parameters that will be used in this numerical analysis and to suggest an alternate method or simplified procedure by which these parameters can be determined.

## 1.3 Notation

When dealing with numerical analysis methods, the mathematical terminology and equations can become very complicated and difficult to understand. It is the intent of this section to provide basic definitions for the notation used in this thesis. Details and derivations can be found in the literature (Fung, 1969; Desai and Siriwardane, 1984; and Chen and Baladi, 1985).

K = bulk modulus

= unloading modulus for hydrostatic compresstion test

$E$ = modulus of elasticity

$M$ = constrained modulus

$\mu$ = Poisson's ratio

$UM_1$ = unloading modulus in the axial direction

$UM_{2,3}$ = unloading modulus in the lateral direction

UM-HC = unloading modulus for the hydrostatic compression test

$\sigma_1, \sigma_2, \sigma_3$ = principal stresses, $\sigma_1$ referring to the axial stress and $\sigma_{2,3}$ the lateral stress compressive = positive

$\tau$ = shear stress

$\sigma_{oct.}$ = octahedral normal stress

$= 1/3\ (\sigma_1 + \sigma_2 + \sigma_3)$

$\tau_{oct.}$ = octahedral shear stress

$\varepsilon_1, \varepsilon_2, \varepsilon_3$ = principal strain, $\varepsilon_1$ referring to the axial strain and $\varepsilon_{2,3}$ the lateral strain

$\varepsilon_v$ = volumetric strian

$= \varepsilon_1 + \varepsilon_2 + \varepsilon_3$

$\varepsilon_e$ = elastic strain

$\varepsilon_p$ = plastic strain

$I_1$ = first invariant of strain tensor

$= \varepsilon_{11} + \varepsilon_{22} + \varepsilon_{33}$

$I_{2D}$ = second invariant of deviatoric strain tensor

$$= \frac{1}{6}\left[\left(\varepsilon_{11} - \varepsilon_{22}\right)^2 + \left(\varepsilon_{22} - \varepsilon_{33}\right)^2 + \left(\varepsilon_{11} - \varepsilon_{33}\right)^2\right] + \varepsilon_{12}^2 + \varepsilon_{23}^2 + \varepsilon_{13}^2$$

$J_1$ = first invariatn of stress tensor

$= \sigma_{11} + \sigma_{22} + \sigma_{33}$

$J_{2D}$ = second invariant of deviatoric stress tensor

$$= \frac{1}{6}\left[\left(\sigma_{11} - \sigma_{22}\right)^2 + \left(\sigma_{22} - \sigma_{33}\right)^2 + \left(\sigma_{11} - \sigma_{33}\right)^2\right] + \sigma_{12}^2 + \sigma_{23}^2 + \sigma_{13}^2$$

deviatoric stress = $\sigma_1 - \sigma_3$ (where $\sigma_2 = \sigma_3$)

# CHAPTER 2

# PREVIOUS RESEARCH

## 2.1 Modeling Introduction

In the field of engineering, one of the most common, and sometimes the most difficult, responsibilities placed upon the engineer is the prediction of system behavior under certain loading conditions. For the engineer to predict or estimate this behavior, either a sample of the material must be placed under actual loading conditions and the behavior observed, or a mathematical model used to predict how the material will behave under the anticipated loading conditions.

While the use of a mathematical model may require some initial testing and verification, it is still considerably more general and efficient than the observational approach if different loading conditions and variations in materials exist. This is not to say that actual testing of materials under various conditions is not important. Testing and observation of material behavior must occur for the development and modification of newer models and for their verification.

One notable testing and observational series was conducted by H. Tresca in the 1860's (Tresca, 1872). Tresca's studies mainly focused on the behavior of a material in a shearing or punching test. These tests were usually performed on differing types of metal with one test being performed on sand. Tresca's work, along with other researchers, greatly enhanced the understanding of metal behavior in the late 1800's (Scott, 1983). From these studies, laws and

equations governing the behavior of metals were developed. As a result, other materials, such as concrete, wood, rock, and soil, were assumed to obey laws and equations for metal.

Since steel is a product of man, it is easily understood how it can be manufactured to meet certain specifications and have certain desirable properties. A linear elastic relationship (model) is commonly used to model the behavior of steel because design methods have been developed to assure that the stress remains in the elastic range. In practice, when dealing with a material such as steel, unless failure occurs, it should never reach those loads which cause plastic behavior. Hence, the plastic state may be ignored for most design purposes. Therefore, the linear elastic model is considered a good model for the representation of steel response.

If linear elastic, isotropic, material behavior is assumed, stresses and strains within the material are related by generalized Hooke's law:

$$\varepsilon_x = \frac{1}{E}\left[\sigma_x - \mu\left(\sigma_y + \sigma_z\right)\right] \qquad 2.1$$

$$\varepsilon_y = \frac{1}{E}\left[\sigma_y - \mu\left(\sigma_z + \sigma_x\right)\right] \qquad 2.2$$

$$\varepsilon_z = \frac{1}{E}\left[\sigma_z - \mu\left(\sigma_x + \sigma_y\right)\right] \qquad 2.3$$

The modulus of elasticity (E) and Poisson's ratio ($\mu$) are easily determined for steel samples through simple and quick laboratory tests.

Soil or rock may be modeled as a linear elastic material, but severe limitations occur. Soil is often loaded such that the nonlinear, inelastic

response is important. While the linear elastic models may perform well for steel, they do not predict the behavior of geologic materials very well; it is for this reason that other models have been investigated, developed, and used for predicting the behavior of geologic materials.

## 2.2 Elastic Models

From the study of the behavior of metals, elasticity theory was used in many early models to predict the behavior of soil. The elasticity based models are still used in problems dealing with stress and deformation behind retaining walls and under foundations (Chen and Baladi, 1985). These models are mostly strain dependent, therefore producing a linear response. Two such models are the Cauchy elastic model and the Green elastic model. The Cauchy elastic model is a stress-strain model, in which stress is a function of strain. With the Green elastic model, a material is assumed to have a state of non-stress called its natural state. Once the material deforms under some load, it goes from the natural state to some different state of stress. When the load is removed, the elastic material returns to the natural state. This complete elastic rebound implies that all the energy supplied to the material during the loading phase is recoverable during the unloading phase (Desai and Siriwardane, 1984).

Since the aforementioned models are linear, they may give a fair estimation for analysis involving low stresses, but as the stresses increase, the error in the model response increases. Even if a nonlinear-elastic relation is used, such as the hyperbolic model (Konder, 1963), these elastic models fall short when dealing with geologic materials for two main reasons. First, the

elasticity based models do not allow any permanent or plastic strain, which actually begins to occur at low stresses. Second, these elasticity based models are stress path dependent thus, making them unsuitable for many problems. Figures 2.1 and 2.2 compare typical linear and non-linear hyperbolic elastic model response with observed soil behavior.

## 2.3 Hypoelastic Model

In the previously mentioned models, the stress state which the material is experiencing is solely dependent on the deformation, or strain, that the material is currently experiencing. Simple laboratory tests will show that geologic materials, as well as some other materials, do not conform to this elastic criteria. For the most part, geologic materials are dependent on the stress path followed during loading or unloading.

Recognizing this stress path dependency, a concept called hypoelasticity was proposed in which deformation can be taken step-by-step (Truesdall, 1955). From this step-by-step (incremental) loading, the stress a material experiences during loading is expressed as a function of stress and increment of strain. Using the hypoelasticity concept allows the total deformation (strain) of a material to be separated into its elastic and plastic strain components.

$$\varepsilon_v = \varepsilon_v^e + \varepsilon_v^p = \left(\varepsilon_1^e + \varepsilon_2^e + \varepsilon_3^e\right) + \left(\varepsilon_1^p + \varepsilon_2^p + \varepsilon_3^p\right) \qquad 2.4$$

This strain separation is not possible using the elastic models and is essential in stress path dependent materials.

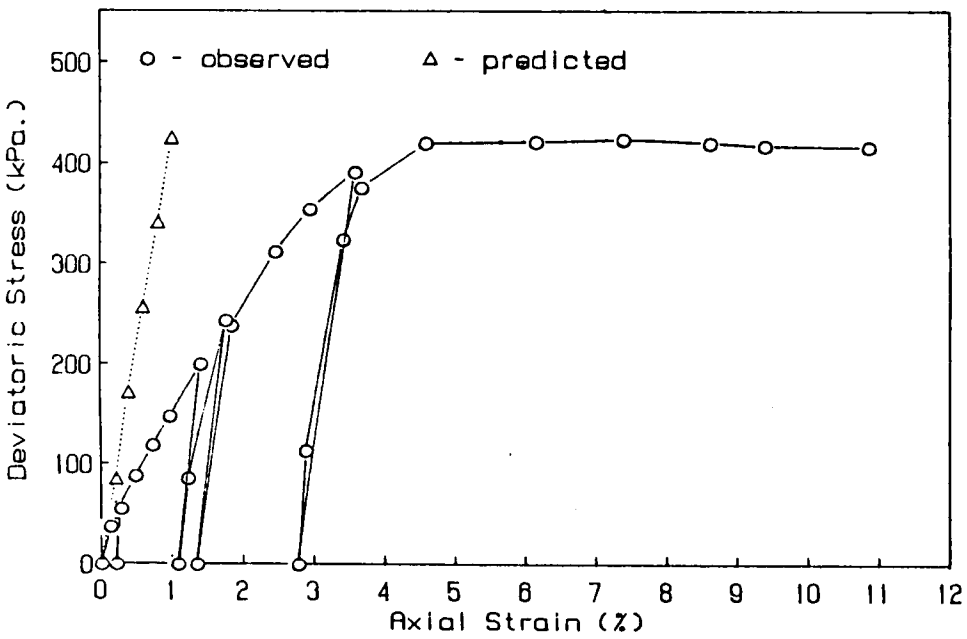


**Figure 2.1. Comparison of observed soil behavior and linear elastic model.**

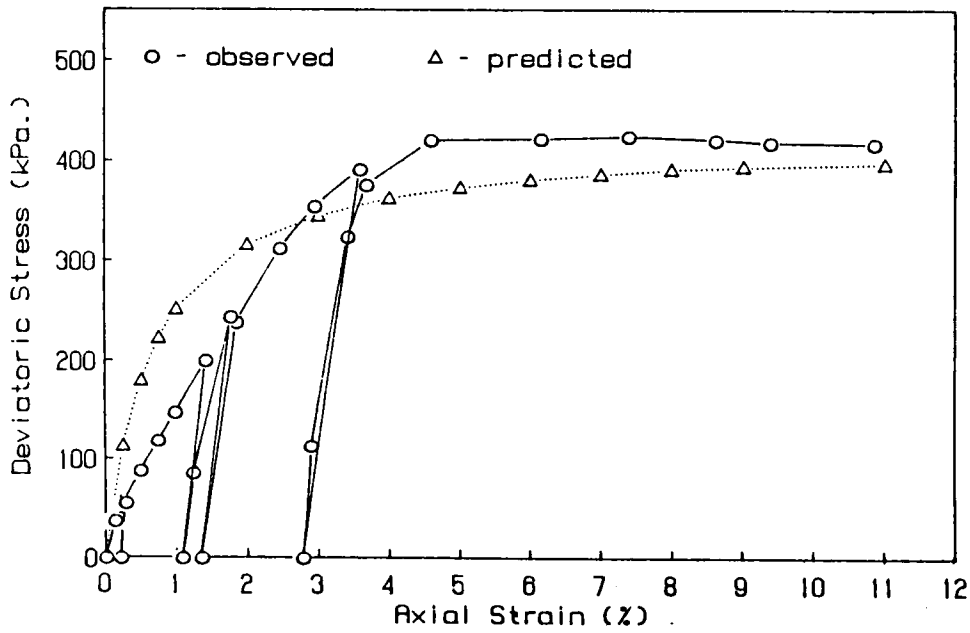


**Figure 2.2. Comparison of observed soil behavior and non-linear elastic model.**

The hypoelastic model may be able to predict the behavior of most geologic materials that are stress path dependent rather than strain dependent. Since the implementation of the model in a numerical analysis technique results in a non-symmetrical stiffness matrix, the computations can become very complicated and lengthy. One advantage of the hypoelastic model is that the parameters may be determined from conventional triaxial tests (Desai and Siriwardane, 1984).

## 2.4 Elastic-Plastic Models

Through simple laboratory tests, it can be shown that soil is neither a purely elastic material nor a purely plastic material but an ever changing combination of both. When a sample of soil is loaded, as in a conventioanl triaxial test ($\sigma_1$ increased while $\sigma_2 = \sigma_3 = k$), the soil initially exhibits an elastic response at very low stresses. If the sample were loaded to point 1, Figure 2.3, since the sample is below yield, the unloading stress-strain curve would follow back down the loading curve as shown in Path A, Figure 2.3, resulting in no permanent deformation. If loaded above yield, point 2, and subsequently unloaded, the unloading curve would drop sharply, as shown in Path B, Figure 2.3, resulting in some amount of now permanent strain. From the load-unload curve, the total strain corresponding to point 2 can be separated into an elastic region (recoverable strain) and a plastic region (irrecoverable strain). If the soil sample were reloaded to an even higher state of stress, point 3, then unloaded and reloaded again, as shown as Path C in Figure 2.4, one would see that the elastic strains are about the same as depicted in Figure 2.3, but the plastic

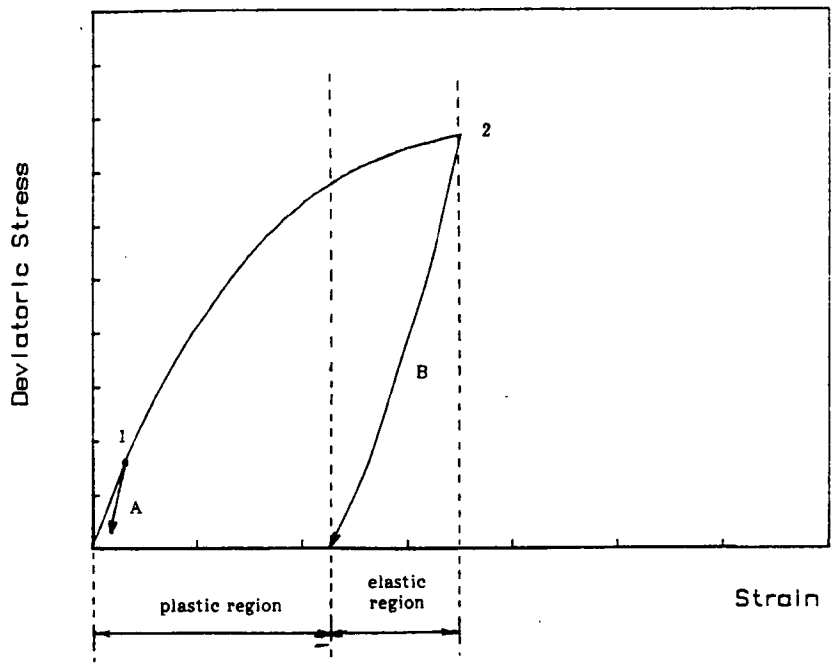


Figure 2.3. Elastic and plastic strain diagram - first unload cycle.

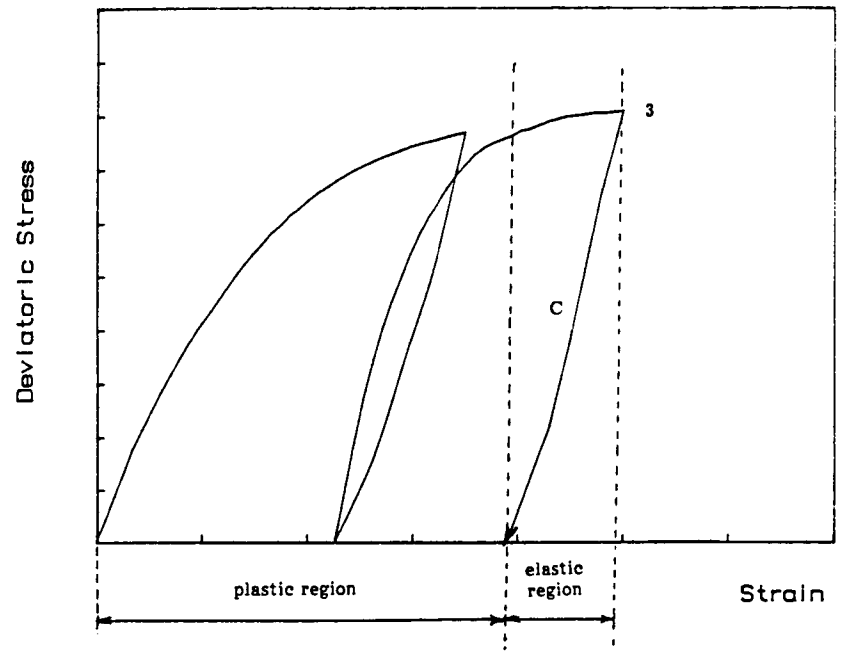


Figure 2.4. Elastic and plastic strain diagram - second unload cycle.

region has increased. Therefore, it can be concluded, the best models for geologic materials are those that encompass both elastic and plastic conditions, an elastic-plastic model.

## 2.5 Development of Elastic-Plastic Models

Through the 1800's, the theory of plasticity took shape from the studies of metals by various individuals. By 1950, most soil mechanics was still based on the linear elastic, isotropic, material conditions. A good review of the studies leading to the development of a plasticity based soil model can be found in Scott (1983).

In the 1950's, two plasticians, D.C. Drucker and W. Prager, tried to apply the theory of plasticity to the behavior of soils (Drucker and Prager, 1952). Based on the three-dimensional Mohr-Coulomb model, Drucker and Prager proposed a perfectly plastic model that was simple to use and incorporated the associated flow rule, thus assuring Drucker's postulates (Drucker, 1950; Drucker, 1950) guaranteeing unique solutions. The major limitation of the Drucker-Prager model is that plastic volumetric strains produced by shearing loads are usually over-predicted (greater) compared with those strains observed in laboratory tests (Ko and Sture, 1981). The model is also limited in its inability to predict hysteretic behavior within the failure surface (DiMaggio and Sandler, 1971; Chen and Baladi, 1985). The predicted response of this model, along with a few other proposed models (Shield, 1953; Haythornthwaite, 1960), was so far from observed soil behavior that no other notable research on soil models was

reported by plasticity researchers after the mid 1950's. Rather, this research would be taken up by soil engineers (Scott, 1983).

In the early 1960s, a group from Cambridge University, headed by K. H. Roscoe, developed a model which used the associated flow rule and incorporated a strain-hardening yield function (Roscoe et al., 1958). This strain-hardening yield function was based on the volumetric plastic strain which took place during shearing. The yield function would increase with an increase in the compressive strain. The model, which was further developed by fellow Cambridge workers, A. N. Schofield and C. P. Wroth, was called the Cam clay model (Schofield and Wroth, 1968). The Cam clay model was further developed for axially symmetrical conditions, as in the conventional triaxial compression test and placed in a three dimensional p-q-e (e=void ratio) space, as shown in Figure 2.5.

The Cam clay model has several important features. One feature is that the model is used in the p-q stress space, in two dimensions, where

$$p = \frac{\sigma_1 + 2\sigma_3}{3} = \frac{J_1}{3} \qquad 2.5$$

where $\sigma_2 = \sigma_3$

$$q = \sigma_1 - \sigma_3 = \sqrt{3}\, J_{2D} \qquad 2.6$$

It should be noted that this definition of q differs by a factor of 2 from the familiar form,

$$q = \frac{\sigma_1 - \sigma_3}{2} \qquad 2.7$$

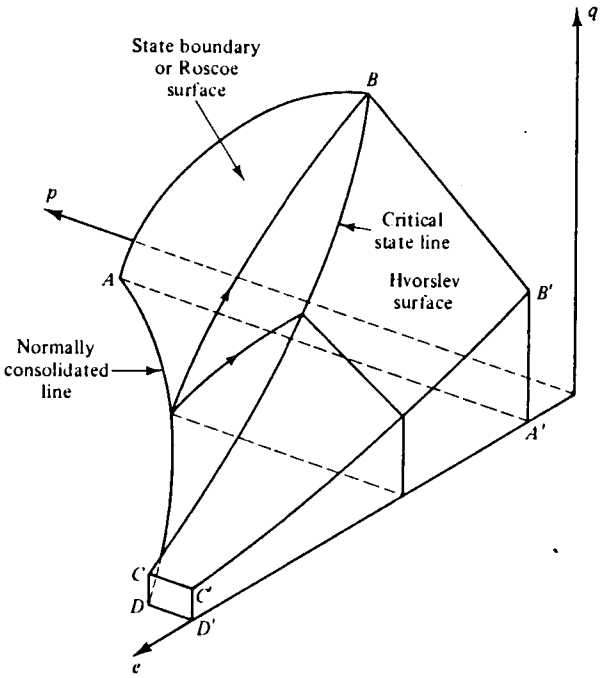


**Figure 2.5 Boundary surface of Cam clay model.**
**(after Roscoe et al., 1958; Desai and Siriwardane, 1984)**

The other important feature of the Cam clay model is the incorporation of the critical state concept. In simplest terms, the critical state concept, proposed by Roscoe et al., (1958), states that a sample attains a certain constant volume or void ratio during shearing. Once a sample reaches the critical state, the volume of the sample will remain constant, even if shearing is continued. Several variations of the Cam clay model were proposed by other Cambridge workers. One of the most notable models was a modified Cam clay model proposed by Roscoe and Burling (1968).

Numerous other elastic-plastic models have been proposed such as third invariant models (Nayak and Zienkiewicz, 1972; Lade and Duncan, 1975), a bounding surface model (Dafalias and Popov, 1976), and the nested surface model (Prevost, 1978). Although each of these models has certain advantages, only the cap type models will be described herein.

## 2.6 Cap Model

The cap model was first developed to model soil and rock behavior under loads caused by ground shocks, such as that of a nuclear explosion (Baron et al., 1973). The model was developed to show the elastic and plastic behavior of the materials caused by the load-unload-reload cycle from the ground shocks. In general, the cap model is very effective in simulating the behavior of geologic materials accounting for the non-linear response, elastic and plastic strains, shear dilatancy, and strain hardening behavior experienced during different loading or unloading conditions. Consequently, the cap model is perhaps the most widely used elastic-plastic model.

The first working cap model was proposed by DiMaggio and Sandler (1971). DiMaggio and Sandler used a stress invariant representation of the Mohr-Coulomb failure surface with a plastic yield condition as proposed by Drucker and Prager (1952). Material constants are used to define the failure surface as well as the plastic, or strain hardening, features of the model. Following the DiMaggio-Sandler model, several modifications of the original DiMaggio-Sandler model have been introduced over the past seventeen years, but most are just variations of the original cap model.

The cap model introduced by DiMaggio and Sandler (1971), consisted of a fixed failure envelope composed of two surfaces. The first surface was a Drucker-Prager failure surface defined by

$$f_1 = \alpha J_1 - \sqrt{J_{2D}} - K_1 = 0 \qquad 2.8$$

The second surface was a Von-Mises surface defined by

$$f_1 = \sqrt{J_{2D}} - K_2 = 0 \qquad 2.9$$

where $\alpha$, $K_1$ and $K_2$ are material constants. These two straight-line surfaces are connected by a smooth curve, Figure 2.6. This defined surface is usually called the fixed failure surface. The total failure surface was defined by Equation 2.10, where $\alpha$, $\gamma$, and $\beta$ are material parameters.

$$f_1 = \sqrt{J_{2D}} - \alpha + \gamma e^{(J_1 \beta)} = 0 \qquad 2.10$$

A modified cap model was introduced by Sture et al., (1979). Instead of using the Von-Mises surface, as used in the Dimaggio-Sandler cap model, a second Drucker-Prager surface was used (Sture et al., 1979), Figure 2.7. This

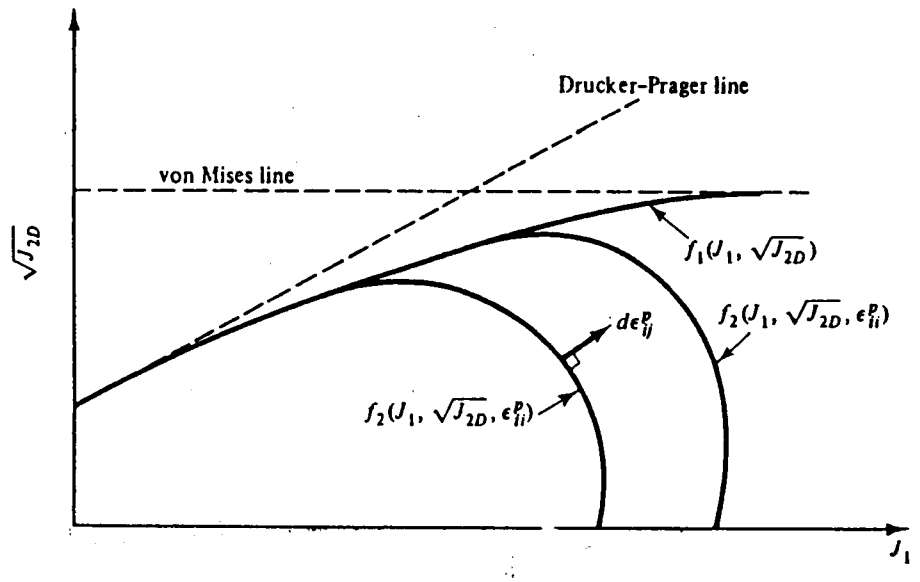


Figure 2.6. Failure surfaces for DiMaggio-Sandler cap model.
(after DiMaggio and Sandler, 1971; Desai and Siriwardane, 1984)

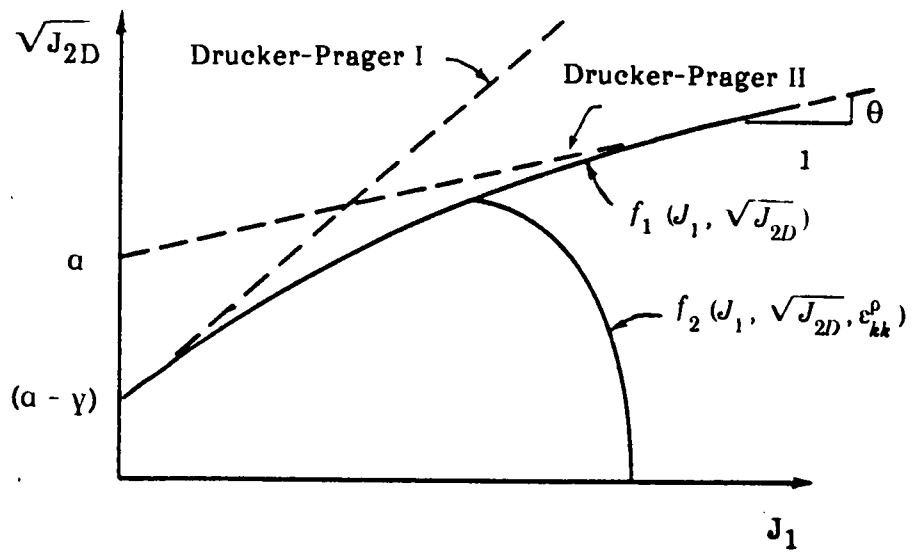


Figure 2.7. Failure surfaces for cap model and showing yield surface.

surface added an additional parameter corresponding to the slope of the second Drucker-Prager surface, is defined by Equation 2.11 where $\alpha$, $\gamma$, $\beta$ and $\theta$ are material parameters.

$$f_1 = \sqrt{J_{2D}} - \alpha + \gamma e^{(J_1 \beta)} - \theta J_1 = 0 \qquad 2.11$$

A yield surface, which resembles a portion of an ellipse, extends from the failure surface to the abscissa, as shown in Figure 2.7. This yield surface, usually termed an elliptical end cap or cap, is able to translate as loading occurs. The movement of the elliptical cap is a function of the total volumetric plastic strain through a hardening parameter, k. In general terms, these caps represent equal amounts of total volumetric plastic strain, thus defining a yield surface (Sture et al., 1979). The yield surface is defined by,

$$f_2 = \sqrt{J_{2D}} - \frac{1}{R} \left\{ \left[ X(k) - L(k) \right]^2 - \left| J_1 = L(k) \right|^2 \right\}^{1/2} \qquad 2.12$$

where R = aspect ratio of the cap

k = hardening parameters

X = intersection with $J_1$

L = intersection with $f_1$

As previously stated, the cap model is defined by ten parameters. Two parameters define the elastic behavior of the soil in the elastic region of the model. Four parameters define the fixed failure surface and the remaining four parameters are associated with the shape of the hardening caps. Table 2.1 briefly describes the physical significance of each of the ten material parameters used in the cap model.

**Table 2.1**

**Summary of Cap Model Parameters**
**(Zaman et al., 1985)**

| Parameter | Physical Significance |
|---|---|
| E | modulus of elasticity |
| $\mu$ | Poisson's ratio |
| $\alpha$ | asymptotic strength |
| $\theta$ | slope of surface at large $J_1$ |
| $\beta$ | degree of curvature in transition zone |
| $\gamma$ | $\alpha$-$\gamma$ cohesive strength |
| R | aspect ratio of cap |
| D | total volumetric plastic strain rate |
| W | maximum volumetric plastic strain |
| Z | $J_1$ corresponding to inital cap |

# CHAPTER 3

# LABORATORY CONSIDERATIONS

## 3.1 Typical Triaxial Set Up

A basic schematic of the triaxial systems set-up used for drained and undrained testing is shown in Figure 3.1 and Figure 3.2 respectively. The air pressure system was controlled by a Brainard-Kilman pressure panel with three out-line connections, all with pipette and annulus measuring systems. A triaxial cell capable of withstanding 1034.3 kPa. (150.0 psi) and having 5.08 cm (2.0 inch) diameter sample plattens was used. The triaxial system consisted of a 1.27 cm (0.5 inch) diameter loading ram running through a roller bearing bushing system. The ram was controlled by a loading system utilizing pneumatically pressurized oil. An electronic measurement system consisting of a 4448 Newton (1000 pound) load cell and a 0.00254 cm (0.001 inch) increment LVDT was used. The load cell measured the axial load while the LVDT measured the axial displacement of the sample. During drained tests, a Wykeham-Farrance volume change device was used, while a 517.1 kPa. (75.0 psi) pore pressure transducer was used during undrained tests. The signals from these electronic devices were displayed on a three channel digital display unit and recorded with a two pen, X-Y-Y' plotter.

Calibration of all equipment was verified prior to the beginning of any triaxial test series. Calibration of the load cell was conducted using a calibrated compression machine. The load cell was calibrated to a convenient setting of 0.5 mV. per 4.45 Newton (0.5 mV. per pound). The calibration of

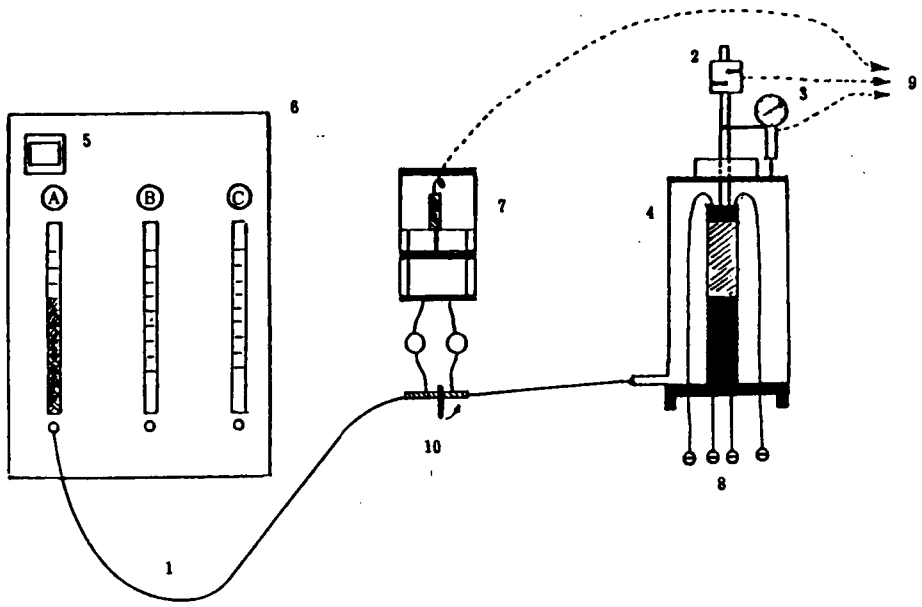


1. Cell pressure line running from the pipette, which is filled with deaired water, through the volume change device and to the cell.
2. 4448 Newton (1000 pound) load cell.
3. LVDT with 0.00254 cm (0.001 inch) dial gage.
4. Triaxial cell.
5. Digital pressure display (usually used for cell pressure and back pressure readings).
6. Pressure control panel.
7. LVDT controlled electronic volume change device.
8. Sample drainage lines - closed. (NOTE: volume change was not measured from the water leaving the sample since the samples were only partially saturated).
9. Electronic lines leading to digital display unit.
10. Deaired water flow control valve.

Figure 3.1. Typical drained triaxial testing set-up.

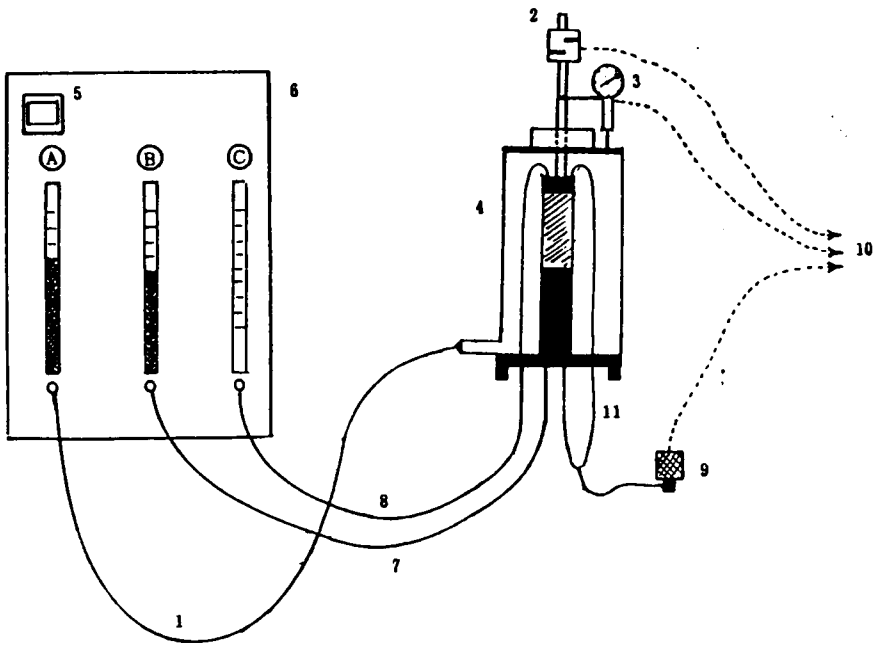


1. Cell pressure line running from the pipette, which is filled with deaired water, to the cell.
2. 4448 Newton (1000 pound) load cell.
3. LVDT with 0.00254 cm (0.001 inch) dial gage.
4. Triaxial cell.
5. Digital pressure display (usually used for cell pressure and back pressure readings).
6. Pressure control panel.
7. Back pressure line (number 1) running from pipette filled with deaired water to bottom of the sample.
8. Vacuum line OR additional back pressure line (number 2) at 13.79 kPa. (2.0 psi) below back pressure line number 1.
9. Pore pressure transducer.
10. Electronic lines leading to digital display unit.
11. Sample drainage lines. Two are used for saturation purposes and the other two are used for pore pressure measurements.

Figure 3.2. Typical undrained triaxial testing set-up.

the axial displacement LVDT was conducted using a calibrated, high precision micrometer and again calibrating it to a convenient setting of 1.0 mV per 0.00254 cm (1.0 mV per 0.001 inch). The volume change device was calibrated by use of a two-pipette system. The gain setting of the volume change device was set using the guidelines proposed by Lade (1988), discussed later. Calibration of the pore pressure transducer was factory set to read pressure, in psi, directly. The calibration of the pore pressure transducer was periodically checked by comparing the pressure reading from the pressure panel with that of the pore pressure digital display unit. Full details of the calibration of the three aforementioned pieces of equipment can be found in Appendix E.

### 3.2 Triaxial Devices

Recent developments in geologic testing equipment have eliminated several limitations existing in the traditional cylindrical triaxial device. Such limitations include the inability to test samples in tension and independently vary the intermediate principal stress. Some recent developments in triaxial equipment have addressed these limitations. These differing types of triaxial equipment will be briefly discussed with respect to the cylindrical triaxial device in this section.

The conventional cylindrical triaxial device is the most widely used triaxial device. This cylindrical device consists of a large cylindrical plexiglass chamber in which the sample, encased in a rubber membrane, is placed. The chamber, shown in Figure 3.3, is then filled with water. The sample is initially loaded by applying a pressure to the water surrounding the sample; this pressure

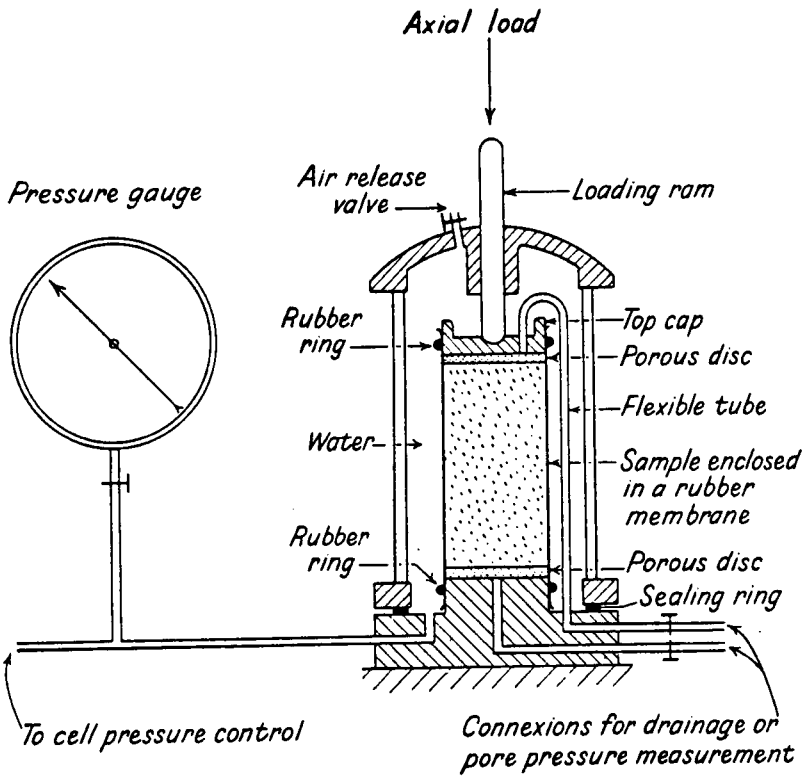


Figure 3.3. Cylindrical triaxial device schematic.
(after Bishop and Henkel, 1962)

creates an equal stress over the entire surface of the sample. After consolidation under this initial hydrostatic state of stress, the sample is typically sheared to failure by increasing the axial load.

With the conventional triaxial device, the lateral stresses acting on the sample are always equal; this places restrictions on the types of loadings that can be applied. The "truly triaxial" or "cubical" triaxial device (Ko and Scott, 1967) was developed such that the stresses on the sides may be different ($\sigma_2$ does not have to equal $\sigma_3$ or $\sigma_1$). Figure 3.4 shows the basic schematic of a "cubical" triaxial device.

The "cubical" triaxial device consists of a rigid frame in which a cube of soil, surrounded by a membrane, is placed. The load can be applied independently to six sides of the cube. This design allows the sample to be loaded from any face and strain measured along any face of the sample.

An alternate triaxial device which allows control of the intermediate principal strains is the hollow cylinder device. Using the hollow cylinder device permits testing under continuous rotation of principal stress direction. The sample is encased, inside and outside, in a thin rubber membrane. Different from the conventional triaxial device, the inside of the sample may be pressurized at a different stress than the outside of the sample. The sample can be loaded axially with straight compression, cycled compression, or compression combined with a torsional stress (Al-Hussaini, 1981). Figure 3.5 shows a basic schematic of the stresses involved with the hollow cylinder device.

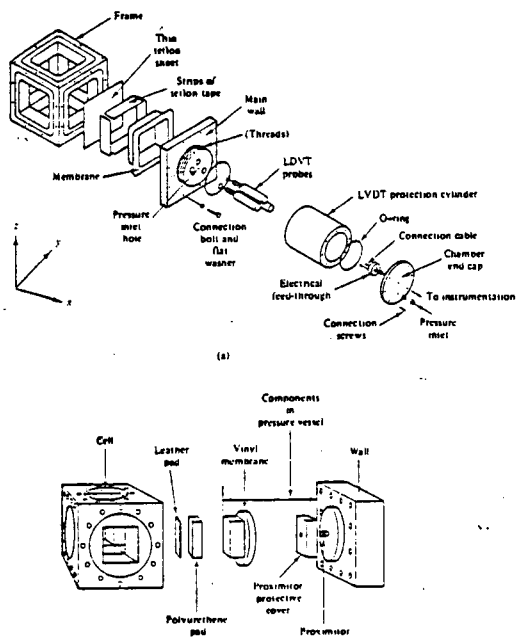


Figure 3.4. "Cubical" triaxial device schematic.
(after Desai and Siriwardane, 1984)

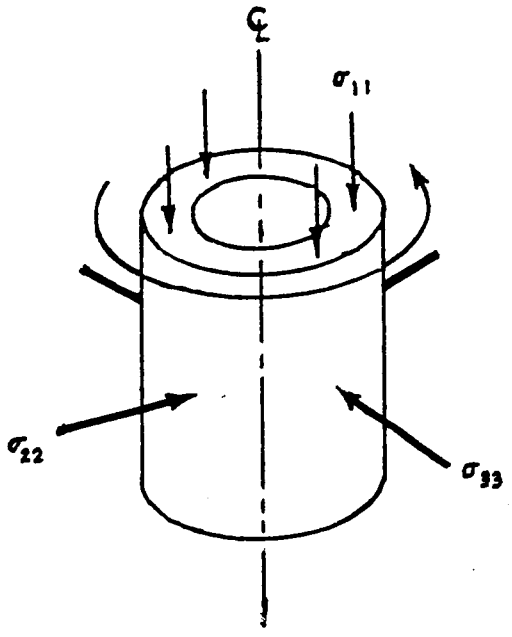


Figure 3.5. Hollow cylinder stress schematic.

## 3.3 Triaxial Stress Paths

Depending upon the manner in which the stresses are varied, there are several stress paths along which a sample of soil may be tested. Some of the stress paths are easy to simulate, while others require special equipment such as the "truly triaxial" device or hollow cylinder device, described above.

The following is a description of the stress paths that can be run with the conventional triaxial device. Other stress paths may be possible using the conventional triaxial device, but accuracy and precision are minimized unless special attachments are used for tension tests. Each stress path is depicted in various stress-strain spaces in Figures 3.6, 3.7, and 3.8.

### Hydrostatic Compression (HC)

In the hydrostatic test, stress increments of equal magnitude are applied to all sides of the specimen. Starting with the axial stress and lateral stress equal to zero or some other low stress, a small increment of stress is then applied both axially and to the sides. The loading is continued in an incremental manner.

### Conventional Triaxial Compression (CTC)

The specimen is loaded hydrostatically to the predetermined confining stress. Once the sample has been loaded hydrostatically, the confining stress is kept constant while the axial stress is increased. Loading is continued at a constant rate until failure occurs.

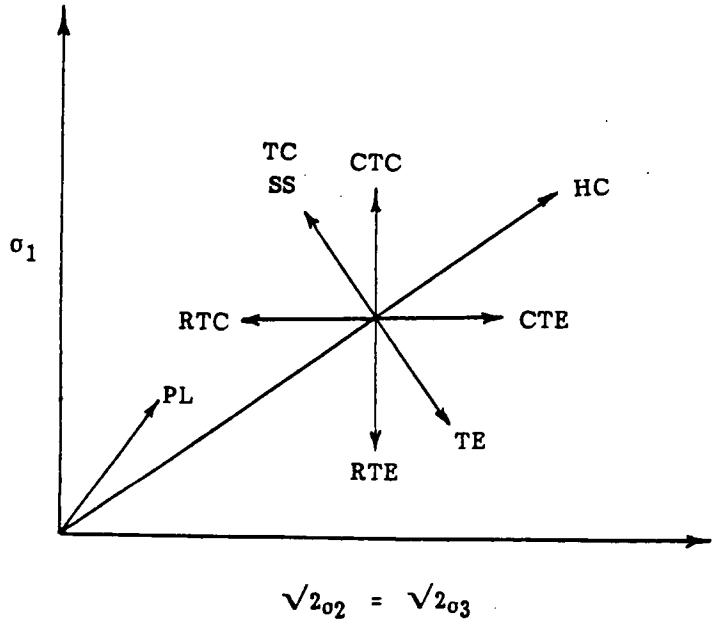


Figure 3.6. Triaxial stress paths in $\sigma_1 - \sqrt{2}\sigma_3$ stress space.

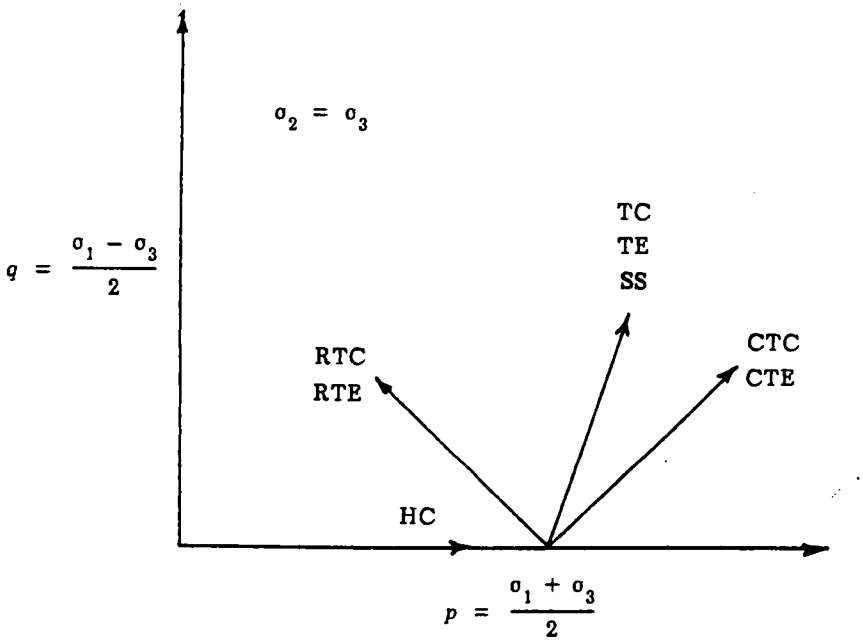


Figure 3.7. Triaxial stress paths in p-q stress space.

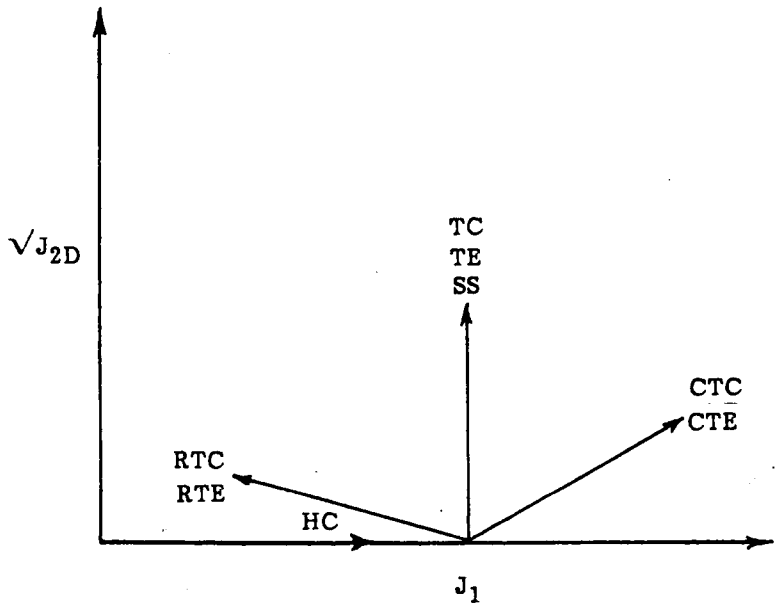


Figure 3.8. Triaxial stress paths in $J_1$ - $\sqrt{J_{2D}}$ stress space.

**Reduced Triaxial Compression (RTC)**

The specimen is loaded hydrostatically to the predetermined confining stress. Then the sample is unloaded incrementally by decreasing the side stress and keeping the axial stress constant. The axial load is kept constant by increasing the deviatoric stress the same amount the lateral stress is decreased. This incremental decreasing of the load, while keeping the axial load constant, is continued until failure occurs or the confining stress reaches zero.

**Triaxial Compression (TC)**

The specimen is loaded hydrostatically to the predetermined confining stress. With the lateral stress the same as the axial stress initially, the side stress is then reduced while the axial stress is increased an equal amount to keep the octahedral stress constant throughout the test.

$$\sigma_{oct} = \frac{\sigma_1 + \sigma_2 + \sigma_3}{3} \qquad 3.1$$

In addition, the following stress paths cannot be evaluated using traditional equipment. A detailed description of these stress paths may be found in the text by Desai and Siriwardane, (1984). These stress paths are:

- Conventional Triaxial Extension (CTE)
- Triaxial Extension (TE)

- Reduced Triaxial Extension (RTE)
- Simple Shear (SS)
- Proportional Loading (PL)

A complete description of the triaxial tests procedures for this thesis can be found in Appendix F.

### 3.4 Volume Change and Area Corrections

As shown in Figure 3.9, the volume change device used for this research consisted of an outer plexiglass chamber with an inner piston connected to a LVDT. The inner piston was allowed to rise and fall as changes in the sample or cell volume took place. The overall set-up, including the triaxial cell and pressure supply, is similar to that described by Bishop and Henkel (1962) for testing both fully and partially saturated samples. The difference is that the mercury volume change device has been replaced by an electronic volume change device.

As stated by Lade (1988), volume change devices must meet two sets of requirements. The two sets of requirements include the volume capacity and precision of measurements, along with the operational requirements. While the volume change device meets the first set of requirements, discussed below, several of the operational requirements are not met. These requirements include the ease of initial assembly, maintenance, and disassembly. Though not meeting these requirements, they did not have any effect on triaxial test results.

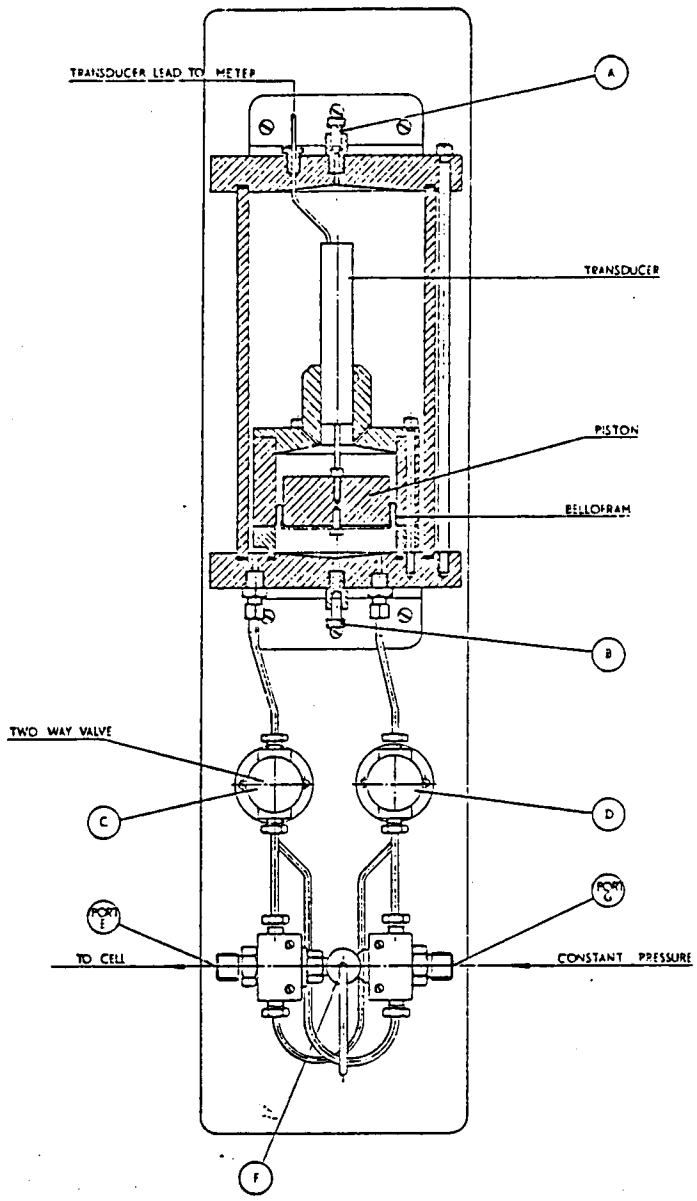


Figure 3.9. Basic schematic of volume change device.

According to Lade (1988), the resolution of the volume change device should be directly related to the resolution of the axial displacement measuring device; that is, the volumetric strain should be as precise as the axial strain. To check this precision, Lade outlines a series of requirements that must be met in terms of volume change device capacity, sample dimensions, and axial displacement measuring device precision. Considering 5.08 cm (2.0 inch) diameter and 10.16 cm long (4.0 inch) samples, along with a 0.00254 cm (0,001 inch) increment axial displacement dial gage, the axial strain precision was determined to be 0.025 cm/cm (0.025 in./in.). Therefore, the volumetric strain precision must be 0.025 cc/cc (0.025 $in.^3/in.^3$) or greater and the volume change precision should be 1.0 mV. per 0.051482 cc (0.00314 $in.^3$). Using a gain setting of 60.0 mV. per cc, the actual volume change precision was 1.0 mV. per 0.01667 cc (0.0010171 $in.^3$). Since the actual volume change precision was greater then the required volume change precision, the 60.0 mV. per cc gain setting was used for each triaxial test. The full calculations can be found in Appendix E.

With the soil samples used in this research being partially saturated, the volume change of the sample was measured as the water entering or flowing out of the cell (corrections will be discussed later). If the samples were saturated, the volume change device could be connected to the pore lines running from the top and bottom of the sample. Volume change measurements could then be taken directly without corrections.

Several testing corrections must be considered when conducting triaxial tests on partially saturated samples with volume change measurements. These corrections may vary depending on the type of triaxial device used in the

testing. The corrections stated below should be considered when using the conventional triaxial device.

The volume change indicated on the digital display unit should not be taken as the actual volume change if different lateral stresses were used in the test due to the contraction and/or expansion of the triaxial chamber wall. Expansion and contraction will vary from chamber to chamber due to differing materials used for the chambers, use of restricting bands, wall thickness, and other differences based on the model or manufacturer of the triaxial chamber. A contraction and expansion curve should be determined for each triaxial system to be used. This curve is determined by filling the chamber with deaired water, no sample, and pressurizing the cell at different confining stresses. The volume change for each different stress is recorded and graphed. When pressurizing the cell, it is important to record volume change while increasing the pressure and decreasing the pressure (Bishop and Henkel, 1962). A typical volume change curve for this research is shown in Figure 3.10.

Area corrections refer to the change in the cross-sectional area of the sample during testing. If volume change measurements are not taken during testing, the cross section area can be assumed to vary according to the following equation.

$$A = \frac{A_o}{\left(1 - \varepsilon_1\right)} \qquad 3.1$$

where $A$ = corrected area

$A_O$ = initial sample area

$\varepsilon_1$ = axial strain

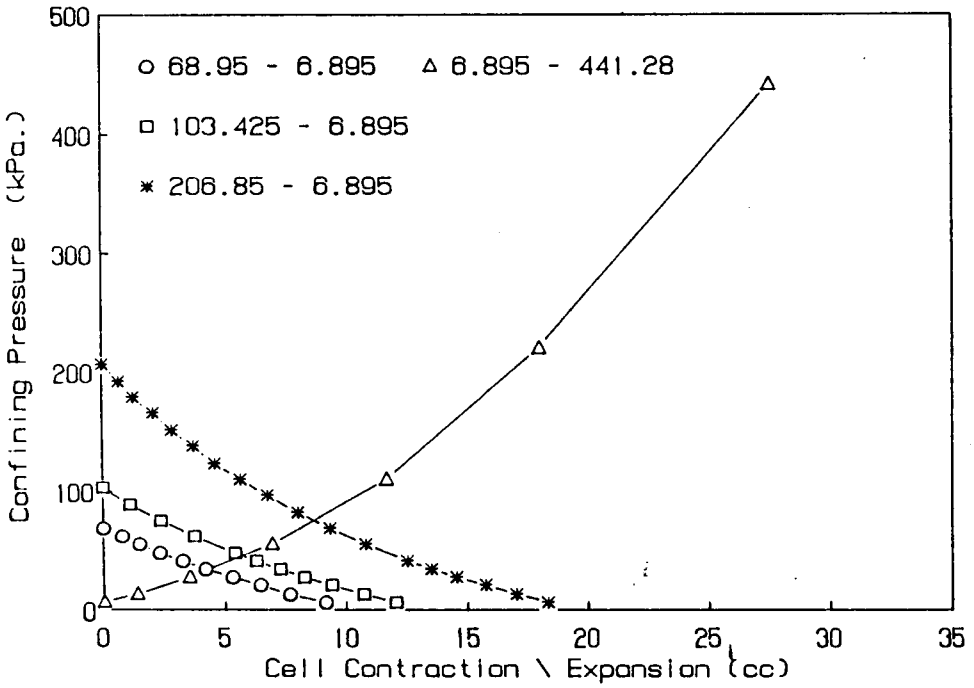


**Figure 3.10. Triaxial chamber contraction and expansion correction curves.**

If volume change measurements are taken during testing, the following equation can be used to find the corrected area.

$$A = \pi\left\{\left[R_o + \left(\varepsilon_3\right)\left(R_o\right)\right]^2\right\} \qquad 3.2$$

where A = corrected area

$R_O$ = initial sample radius

$\varepsilon_3 = \varepsilon_2$ = lateral Strain

### 3.5 Additional Considerations

Other corrections that should be considered are ram friction, cylindrical sample shape, and membrane strength. These three areas of concern have been mentioned as having some effect on triaxial results (Bishop and Henkel, 1962).

The loading system used for this research consisted of a 1.27 cm (0.5 inch) diameter steel loading ram running through a lubricated roller bushing system. The friction associated with this type of system is usually negligible and was neglected in this investigation.

Once the soil samples were extruded, they were trimmed lengthwise using a small coping saw. The ends of the sample were smoothed with a knife blade to form an approximate cylinder. Further steps beyond visual examination were not used to assure a cylindrical sample.

The correction for membrane strength or effect on triaxial samples and tests is usually very small and is usually neglected (Bishop and Henkel, 1962). Only membranes of similar thickness were used in the testing series. No other corrections were made with respect to membrane effect.

There are other suggested modifications (Baldi et al., 1988) that may be used in the testing set-up and procedure that may provide better results. Several of these suggestions are listed below.

1. Using an internal load cell, one that is contained in the triaxial chamber, may eliminate errors due to friction of the loading ram and the bushings.

2. Using pore pressure measuring devices mounted to read pore pressure at the side of the sample and at the base of the sample to account for any differential pore pressures.

3. Using internal axial displacement measuring devices that measure the very small strains which may take place.

4. Using corrections for determining the amount of water absorbed by the membrane surrounding the sample and determining if any of the absorbed water was transferred to the sample for determining moisture content changes.

However, it seems to the author that the uncertainties associated with the testing of soils override the need for such fine tuned testing of soil. Until the engineer or scientist determines that a laboratory triaxial test can represent the actual behavior of soil in the field, the testing methods and equipment presently in use should be adequate.

# CHAPTER 4

# SAMPLING AND TESTING PROCEDURE

## 4.1 Field Sampling

The soil samples used for the research in this thesis were undisturbed samples collected in Sesser, Illinois, which is located in the southern part of Illinois, USA, Figure 4.1.

The samples were collected for the purpose of characterizing the soil behavior in the general area of Sesser, Illinois. As mentioned in Section 1.2, the cap model parameters and other information obtained from the testing of these samples is to be used in an ongoing research program at The University of Tennessee, Knoxville, to study the effects of longwall mining induced surface subsidence.

The samples were collected in an area where two test house foundations had been built approximately three and a half years earlier. These test foundations consisted of concrete strip footings with 1.22 m (4 feet) high concrete masonry unit (concrete block) walls. Placed on these walls were wooden boxes filled with soil to simulate the load structure of the typical house. It should be mentioned that a floor joist system was present within these structures, but there was no roof to these structures, which lead to the accumulation of water around the foundation during periods of high rainfall.

In the boundaries of one of the test foundations, the topsoil was stripped off using a flat blade shovel. Using the floor joists as a reaction point, an automobile scissors jack was used to push lubricated, metal, thin walled sample

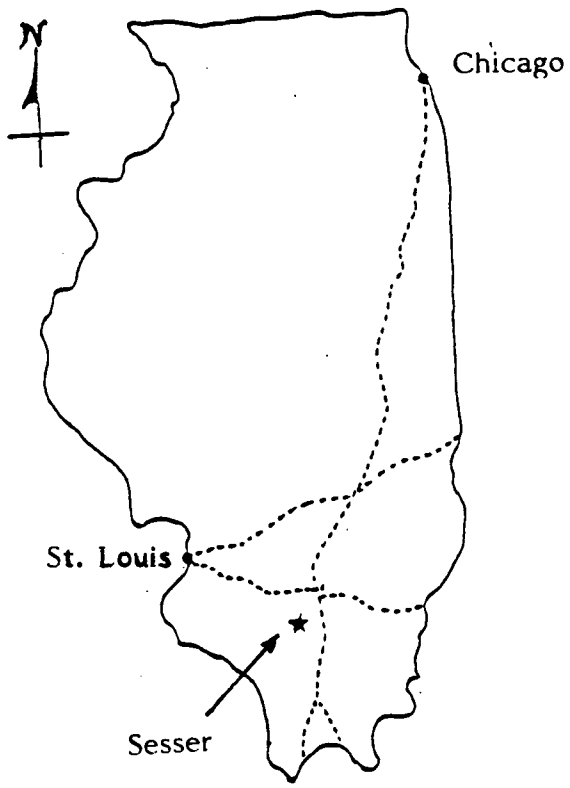


Figure 4.1. Map location of Sesser, Illinois, USA.

tubes measuring 11.43 cm (4.5 inches) long with an inside diameter of 5.08 cm (2.0 inches) into the soil. The soil surrounding the tubes was then carefully excavated and the tubes were removed. Once the tubes were removed from the soil, they were placed in a plastic bag, sealed, placed in another plastic bag, and again sealed. The sealed samples were placed in PVC pipe sections, measuring 12.7 cm (5.0 inches) long and having an inside diameter of 6.35 cm (2.5 inches). The pipe sections were sealed with PVC pipe caps. The samples were then transported back to Knoxville, Tennessee, where they were stored in a moisture room until tested.

Samples were collected in Sesser on two consecutive trips, June 25, 1988, and July 7, 1988. Conditions on June 25, 1988, were sunny, extremely dry, with temperatures around 37.8°C (100°F). Conditions on July 7, 1988, were overcast, varying weather with occasional heavy rain, and temperatures around 36.7°C (98°F).

### 4.2 Sample Preparation

For testing, each sample was removed from the moisture room and extruded from the metal tube by use of a slow-moving, hydraulic piston. Once the sample was removed from the tube, it was trimmed to a nominal length of 10.16 cm (4.0 inches). Final preparation measurements of the length and diameter of the sample were taken. The trimmings were saved for initial moisture content measurements. The sample was then weighed and carefully placed in a thin, rubber membrane and placed in the triaxial cell.

The triaxial cell was sealed and slowly filled with deaired water pressurized to 6.895 kPa. (1.0 psi). This low fill pressure was used to prevent any consolidation of the sample usually caused by a high fill pressure. Once the cell was completely filled and all visible air bled out, the sample was tested.

### 4.3 Testing Procedure - Drained

The triaxial tests conducted for use in determining cap model parameters, in the traditional manner, were drained tests on partially saturated samples. The following brief procedure is in accordance with ASTM (D 2850-87) standard testing procedure (ASTM, 1988). Small deviations from ASTM standards were necessary due to equipment differences and the need for conducting tests not described by ASTM.

**Conventional Triaxial Compression (CTC).** Once the sample was ready to be tested, the drain lines were opened, and the cell pressure was applied. The cell pressure was applied to a column of water in a pipette which fed water through the volume change device and into the cell, as shown in Figure 3.1. Thus, the volume change which occurred during consolidation could be measured with both the pipette and the volume change device. For samples at low confining stresses, the sample was usually consolidated in 8 to 12 hours; for samples at high confining stresses, the sample was usually consolidated in 12 to 18 hours. In all cases, the sample was allowed to consolidate for a period of 24 hours to assure full consolidation. The final axial deformation and volume change readings after consolidation were recorded. Following the consolidation

phase, the sample was loaded axially at a predetermined rate of 0.0254 cm (0.01 inches) per hour.

Referring to work by Bishop and Henkel (1962), true clays such as Wield clay and Cambridge clay failed in about 48 hours for drained triaxial tests. From this failure data and assuming the soil would begin to fail at an axial strain of approximately 10 %, a loading rate of 0.0254 cm (0.01 inch) per hour was selected, giving a failure time of about 35 to 55 hours, depending on the confining stress.

If oedometer test data is available, an actual time to failure should be computed using the following equation (Bishop and Henkel, 1962).

$$t_f = \frac{20\ h^2}{n\ C_v}$$

where 2h = height of the sample

$C_v$ = coefficient of consolidation

$t_f$ = time to failure

n = drainage condition factor (from Table 4.1)

**Table 4.1**

**Sample Drainage Condition Factor (Bishop and Henkel, 1962)**

| Drainage Conditions | n |
|---|---|
| Drainage from one end only | 0.75 |
| Drainage from both ends only | 3.0 |
| Drainage from radial boundry only | 32.0 |
| Drainage from one end and radial boundry | 35.8 |
| Drainage from both ends and radial boundry | 40.5 |

During the test, the load, axial deformation, and volume change were recorded by an electronic two pen plotter (X-Y-Y' plotter). Periodic manual readings were taken to check the calibration factors and as a back-up method. Once the test was complete, data points from the recorded graph were entered into a data reduction program and reduced into appropriate stress-strain units.

**Hydrostatic Compression (HC).** In the hydrostatic compression test, there is no consolidation phase, but the sample may become slightly consolidated when the chamber is filled with water. For water to flow into the chamber, the water must be under pressure, unless gravity filling is used. During filling, when the fill water reaches the top of the chamber and air is being bled out, the fill pressure is transferred to the sample.

As mentioned when describing the CTC test, the fill pressure was 6.895 kPa. (1.0 psi). Therefore, the sample can be considered to be consolidated at 6.895 kPa. (1.0 psi). Once the chamber was filled with deaired water, all the measuring devices were zeroed, and the cell pressure was increased to 13.79 kPa. (2.0 psi).

Recording axial deformation at set time intervals, a dial reading versus square root of time graph was plotted and $t_{90}$ was determined, as shown in Figure 4.2. Described by Taylor (1948), $t_{90}$ is the point at which 90% consolidation has occurred. Once this point was reached, the final axial deformation and volume change for that step was recorded and the next load step was applied to the sample and another graph started. This procedure was followed for each increasing (loading) load step. In the case of decreasing

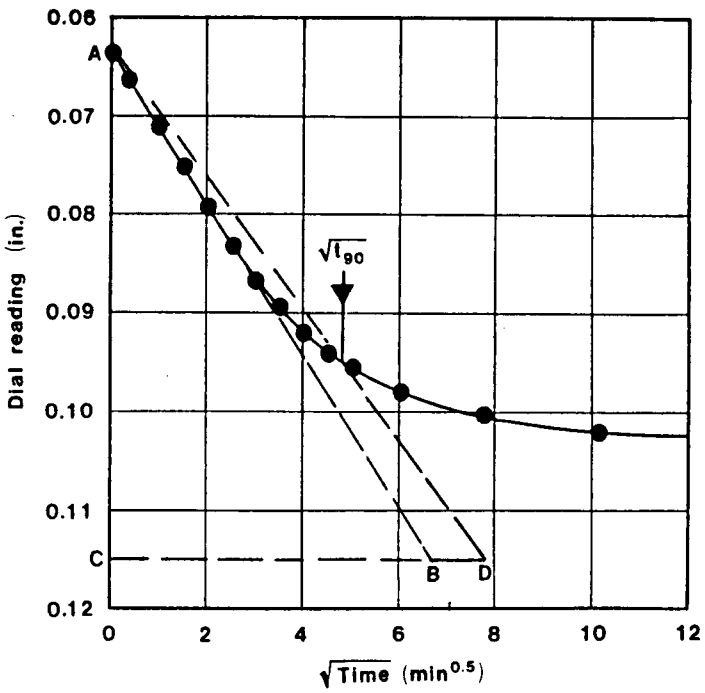


Figure 4.2. $t_{90}$ construction plot.
(after Taylor, 1948; Das, 1986)

(unloading) load steps, a similar graphing procedure was used to determine $t_{90}$, although $t_{90}$ cannot truly be called 90% consolidation, but rather 90% of the axial unloading movement had occurred. Again, at $t_{90}$, the next unload or load step was applied. The loading steps should be similar to that of a traditional oedometer test. The load steps, in kPa., were 6.895, 13.79, 27.58, 55.16, 110.32, 55.16, 27.58, 13.79, 27.58, 55.16, 110.32, 220.64, 110.32, 55.16, 27.58, 13.79, 27.58, 55.16, 110.32, 220.64, 441.28 (in psi: 1.0, 2.0, 4.0, 8.0, 16.0, 8.0, 4.0, 2.0, 4.0, 8.0, 16.0, 32.0, 16.0, 8.0, 4.0, 2.0, 4.0, 8.0, 16.0, 32.0, and 64.0). The final axial deformation and volume change for each step was recorded. This data was then reduced and graphed in a similar fashion as the conventional triaxial compression test data.

Hydrostatic compression tests were stopped at 441.28 kPa. (64.0 psi) since 551.6 kPa. (80.0 psi) was the limit of the pressurized air supply. The HC test may be run to even higher stresses to make certain cap model parameter evaluations less complicated and time consuming.

It was found through testing that it is important to unload to the same stress each cycle. For example, on the first cycle if the sample is unloaded to 10.0 kPa (1.45 psi) and on the next cycle unloaded to only 50.0 kPa (7.25 psi), the slopes of the unloading curve will not be consistent, as shown in Figure 4.3. This inconsistency is due to the nonlinearity of the unload behavior. When unloading in the second cycle to only 50.0 kPa (7.25 psi), 50.0 kPa (7.25 psi) was on the hysteresis loop on the first unloading cycle. The HC tests conducted for this research were unloaded to different stress, thus promoting the aforementioned statement.

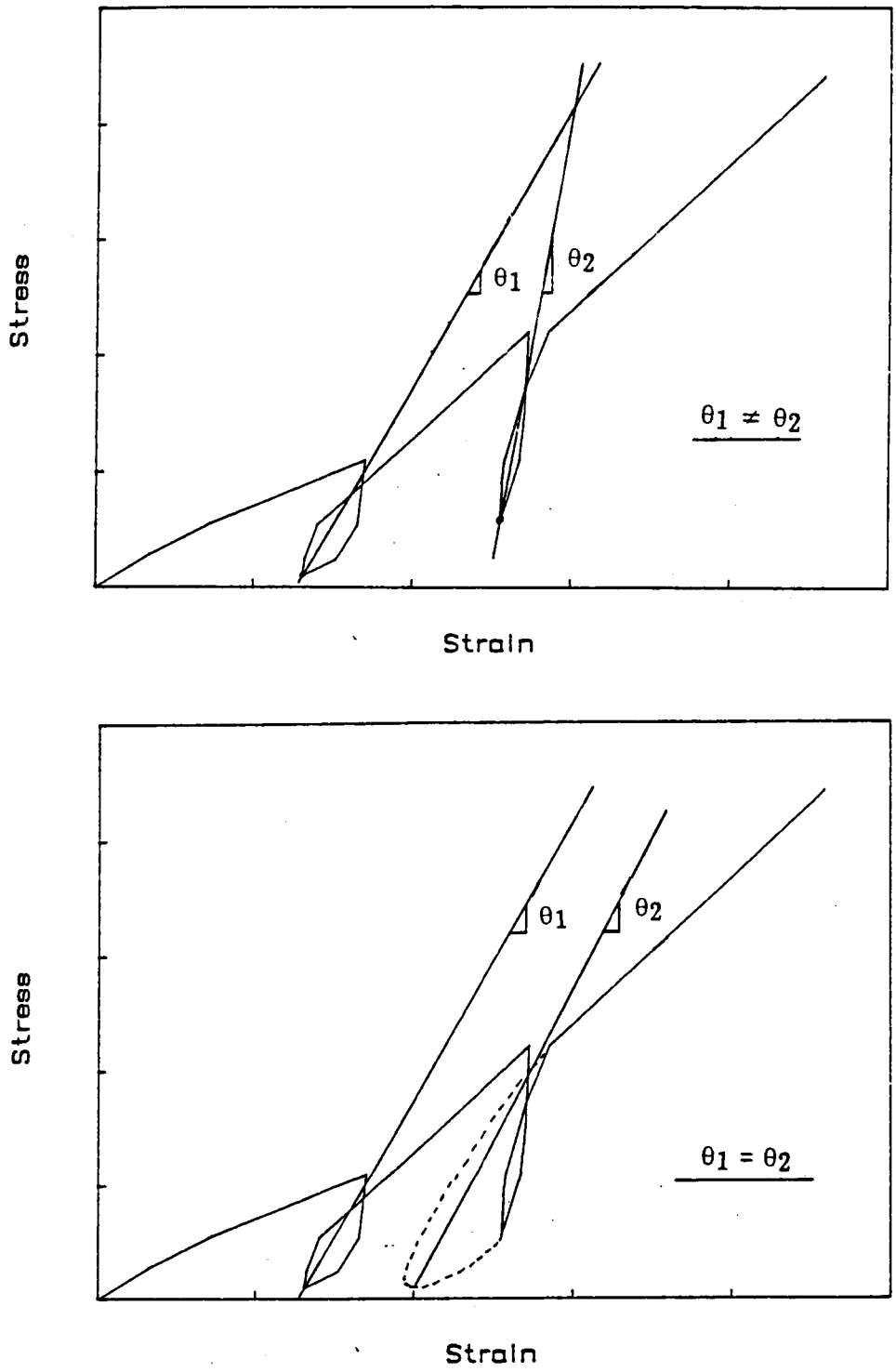


**Figure 4.3. Hydrostatic compression test data showing load-unload cycle.**

The HC tests conducted for this research were not unloaded to 6.895 kPa (1.0 psi) or 0.0 kPa (0.0 psi) due to unavoidable drift which may occur in the pressure system.

It was also found through testing that when samples were unloaded below 13.79 kPa. (2.0 psi), an apparent drift in the data acquisition system occurred. The author does not know if this is attributed to the resolution of the testing equipment or actual behavior of the soil.

**Triaxial Compression (TC).** As stated in an earlier section, the triaxial compression test is run along a stress path such that the octahedral stress remains constant. This test is started by first consolidating the sample at some predetermined consolidation pressure as described previously. Following the consolidation phase, the triaxial compression test was run immediately. Initially, the octahedral stress is equal to the consolidation stress, then the cell pressure (lateral stress) is decreased as the axial stress is increased, keeping the octahedral stress constant.

The octahedral stress is kept constant by first loading the sample axially at the same rate the CTC drained tests were loaded. As the axial stress reaches convenient intervals, usually 1.724 to 3.448 kPa. (0.25 to 0.5 psi), the cell pressure is decreased accordingly to keep the octahedral stress constant. Again at convenient intervals, such as 6.895 kPa. (1.0 psi), the axial and lateral stresses are recorded along with the axial displacement and volume change.

This procedure requires an extensive amount of monitoring, since load steps must be applied manually and the data must be recorded manually. This is

especially true if the soil being tested is a fine-grained soil, due to the requirement of complete sample drainage.

**Reduced Triaxial Compression (RTC).** The reduced triaxial compression test is similar to the TC test, with the exception of the variation of axial stress. In the TC test, the axial stress is increased to keep the octahedral stress constant; conversely, in the RTC test, the axial stress is increased to maintain the same value at which it was consolidated.

The axial stress is kept constant by first loading the sample axially at the same rate as the CTC drained tests. As the axial stress reaches convenient intervals, usually 1.724 to 3.448 kPa. (0.25 to 0.5 psi), the cell pressure is decreased accordingly to keep the axial stress the same as the consolidation stress. Again at convenient intervals, such as 1.0 psi, the axial and lateral stress is recorded along with the axial displacement and volume change. This procedure, as for the TC test, requires an extensive amount of monitoring.

## 4.4 Testing Procedure - Undrained

Since the samples obtained from the Sesser, Illinois site were partially saturated, a sample had to be fully saturated before undrained testing with pore pressure measurements could take place. Several methods of saturation were used in trying to saturate the samples.

The first method of saturation is a method using back pressure to increase the degree of saturation (Lowe and Johnson, 1960). In this method, deaired water is forced into the sample, thus driving the air in the sample into solution. This is accomplished by incrementally increasing the cell pressure and pore

pressure at a constant rate; the difference in the two pressures being the effective stress. It is important to use intervals in which no consolidation, beyond the planned consolidation, takes place. This method can be modified by placing a vacuum at the top of the sample to expedite the saturation process.

Another method used is similar to the previously mentioned procedure except that, instead of using a vacuum, a second back pressure line forces deaired water into the top of the sample (Lowe and Johnson, 1960). A differential of no more than 13.79 kPa. (2.0 psi) is used in the back pressure lines.

With soils such as low permeability clays, these methods may not provide complete saturation of the soil, unless extremely high back pressures are used. In this case, very small holes are drilled, running 3/4 the length of the sample around the perimeter of the sample and stuffed with woolen wicks. The sample is then turned over and a single hole is drilled, running 3/4 the length of the sample down the middle of the sample and stuffed with woolen yarn. The wicks are placed at these set intervals to reduce the length of the path the water must travel through the sample (Lowe and Johnson, 1960).

Each of these methods was attempted, however, none were able to saturate the clayey samples from Sesser. The highest value of the Skempton pore pressure parameter B that was achieved was 0.8.

### 4.5 Data Acquisition

Data for the triaxial tests was displayed on a digital display unit (DDU) and simultaneously recorded by a X-Y-Y', two pen plotter. Throughout the test,

manual spot checks for the CTC tests were made. Solely manual methods were used to record the data for the HC, TC, and RTC tests. Other pertinent data, such as the sample preparation data (i.e. unit weight, initial height and diameter of the sample, and initial sample water content, etc.), were recorded on sample preparation sheets and can be found in Appendix B.

The recording of data on the X-Y-Y' plotter required extensive initial calibration. Because gain settings on the plotter were not in accordance with actual increments marked on the dials of the recorder, actual measurements were taken manually while being recorded by the plotter. From the graphs, a new calibration curve was plotted for that particular channel. This procedure was repeated for the remaining two channels. The calibration curves turned out to be straight lines to which a single conversion factor could relate the markings on the plotter paper to actual digital readout. These calibration factors were checked, and modified if need be, by manual measurements each time a test was run. Figures 4.4, 4.5, and 4.6 show typical calibration curves used. This additional correction factor is likely a result of the plotter not being calibrated for use with the signal coming from the DDU.

For drained triaxial tests, the axial load, axial displacement, and volume change signals were displayed on the three channel DDU and graphed using the X-Y-Y' plotter. The X-Y-Y' plotter graphed two curves, an axial displacement-axial load plot and an axial displacement-volume change plot.

For undrained tests, the axial load and axial displacement were displayed on the three channel DDU. The signal from the pore pressure transducer was displayed on a single channel DDU. All three signals were simultaneously

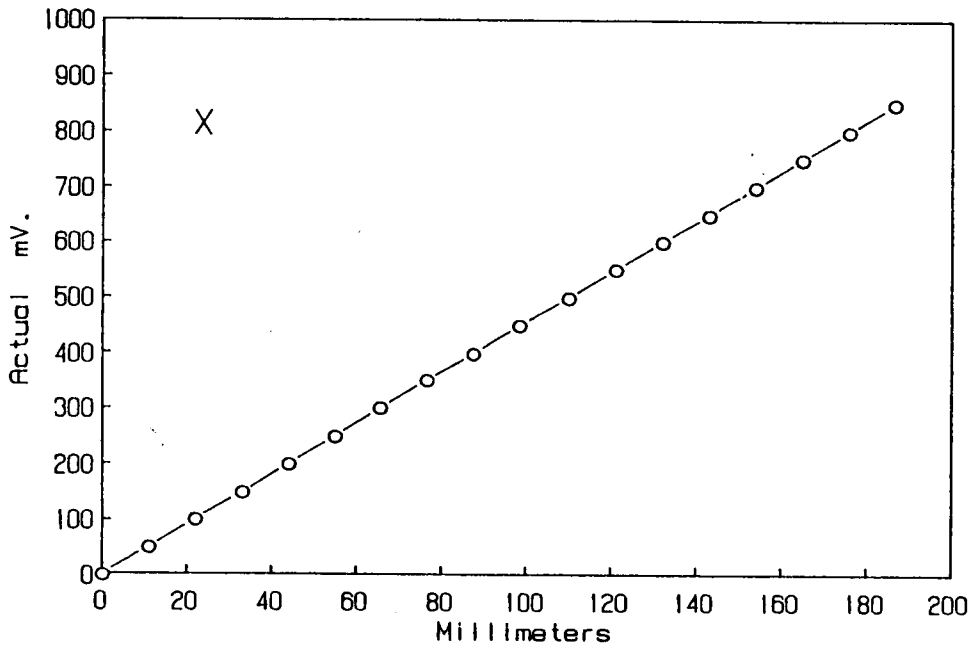


Figure 4.4. Typical X-Y-Y' plotter calibration curve.

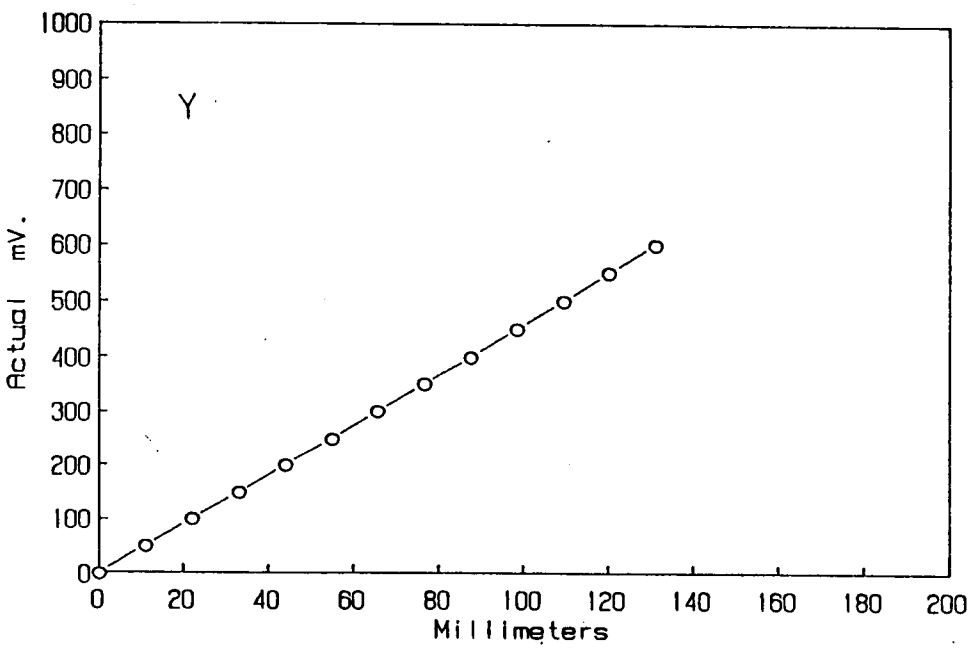


Figure 4.5. Typical X-Y-Y' plotter calibration curve.

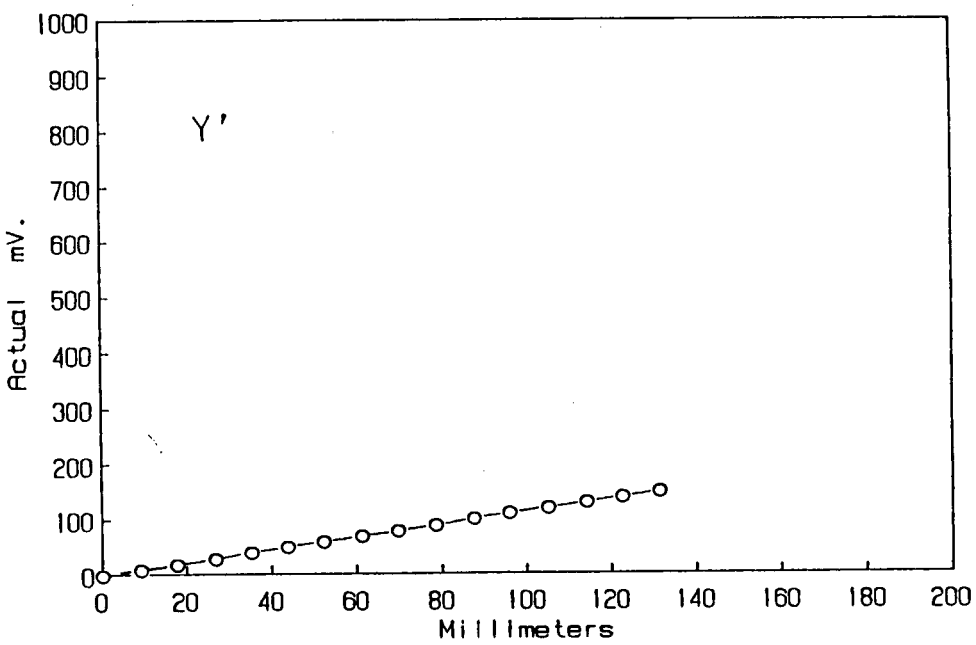


**Figure 4.6. Typical X-Y-Y′ plotter calibration curve.**

displayed on the X-Y-Y' plotter. This plotter graphed two curves, an axial displacement-axial load plot and an axial displacement-pore pressure plot.

### 4.6 Data Reduction

For the CTC tests, digitized data points were selected from the X-Y-Y' plotter graphs and multiplied by the calibration factor to obtain data points in mVs units. These points were then entered into the computer program REDUC, found in Appendix D. This program, depending on the type of test run, reduces the data into the following data points: stress-strain, invariants of stress, volume change, volumetric strain, and incremental volumetric strain. For the HC test, the data output includes data points for stress-strain, volume change, volumetric strain, octahedral stress, and octahedral strain.

Following reduction of the data, a graphics program was utilized to graph the stress-strain curves and the $J_1$-$\sqrt{J_{2D}}$ stress path. The other graph used in the data reduction was a hand graph in which each stress path was plotted in the $J_1$-$\sqrt{J_{2D}}$ stress space.

# CHAPTER 5

# PARAMETER DETERMINATION PROCEDURE

## 5.1 Determination Procedure

To utilize the cap model to simulate the behavior of soil under different loading or unloading conditions, the parameters of the model must be determined. For the cap model, nine to ten material parameters must be calculated (DiMaggio and Sandler, 1971; Sture et al., 1979).

A series of triaxial tests must be conducted along different stress paths to determine all the parameters needed for the cap model. This test series may be conducted using any of the triaxial devices mentioned in Section 3.2, but the remaining discussion will focus on the determination of the cap model parameters using a conventional triaxial device.

When trying to determine cap model parameters in the traditional manner, the first two tests that should be run are a drained conventional triaxial test and a hydrostatic compression test. Both tests are run in a load-unload-reload manner. Three to eight additional tests should be conducted along different stress paths to define the fixed failure surface. All of the above mentioned tests are drained tests with volume change measurements.

**Elastic Parameters.** The first two material parameters that should be determined are the modulus of elasticity (E) and Poisson's ratio ($\mu$). These two parameters describe the elastic behavior of the soil.

The modulus of elasticity can be determined by running a conventional triaxial test. Since the soil only exhibits elastic behavior at very low stresses,

the test is run in a load-unload-reload manner; that is, the sample is axially loaded to some point, unloaded to the confining stress, and then reloaded again past the first unload point. This load-unload-reload cycle is usually repeated three to five times. The results are plotted in the principle stress difference-axial strain space and the principle stress difference-lateral strain space. The modulus of elasticity is usually taken as the slope of the unloading curve from the principle stress difference-axial strain plot. Two other values, the unloading moduli for the axial and lateral direction are also determined from this data. The unloading modulus for the axial direction (UM $_1$) is the same as the modulus of elasticity. The unloading modulus for the lateral direction (UM $_{2,3}$) is determined as being the slope of the unloading path in the principle stress difference-lateral strain plot. These two unloading moduli will allow the separation of total volumetric strain into its elastic and plastic components for the remaining CTC, the TC and RTC tests.

The determination of the modulus of elasticity allows calculation of Poisson's ratio from the drained hydrostatic data (Zaman et al., 1985). From the hydrostatic test, which is also run in a load-unload-reload fashion, the slope of the unloading curve, plotted in $\sigma_{oct.} - \varepsilon_v$ space, will give the bulk modulus (K). The bulk modulus is related to the modulus of elasticity and Poisson's ratio by the following:

$$K = \frac{E}{3\left(1 - 2\mu\right)} \qquad 5.1$$

Considering the HC data graphed in the $\sigma_{oct.}$ - $\varepsilon_v$ space, the unloading modulus for the HC test can be taken as the bulk modulus. An alternate method would be to plot the data in the $\sigma_{oct.}$ - axial and lateral strain space and determine an unloading for both the axial and lateral direction, as calculated for the CTC data.

**Fixed Failure Surface Parameters.** Parameters that constitute the fixed failure surface, defined by Equation 2.12, are $\alpha$, $\beta$, $\gamma$, and $\theta$. These parameters are determined by running a series of triaxial tests along different stress paths. It is not significant what number or combination of tests are run, just as long as the failure points from the tests sufficiently define the fixed failure surface. Usually, at least four to seven tests must be run to define the failure surface with a sufficient degree of accuracy. For the engineer with a great deal of experience with the cap model, the number of tests may be less. Once the combination of tests is determined, the data is plotted in the $J_1$ - $\sqrt{J_{2D}}$ space to determine the numerical value of the four parameters stated above. This is accomplished by fitting two Drucker-Prager curves or a Von Mises and a Drucker-Prager I surface to the data, which ever best fits the data.

Parameters $\alpha$, $\gamma$, and $\theta$ (if used) are determined from the geometry of the fixed failure surface. Since this surface is mainly made up of two straight line surfaces, a transition curve connects them. The transition curve is defined by the parameter $\beta$.

$$\beta = \frac{-1}{J_1} \ln\left(\frac{\alpha - \theta J_1 - \sqrt{J_{2D}}}{\gamma}\right) \qquad 5.2$$

It should be noted that if the Von Mises and Drucker Prager I surface fits the data better, as in the original DiMaggio-Sandler cap model, the parameter $\theta$ is zero.

**Yield Surface and Hardening.** The parameter R refers to the shape factor for the hardening caps; this parameter is associated with the total volumetric plastic strains which occur when the sample is subjected to the stresses encountered along different stress paths. A record of the total volumetric strain is obtained for each stress increment for any stress path run (i.e. each test run). Using the unloading moduli determined from the CTC-LUR test, this total volumetric strain can be separated into its elastic and plastic components. This separation is done by dividing the stress increment by UM $_1$ which gives the elastic axial strain. The elastic axial strain subtracted from the total axial strain gives the plastic axial strain. The same procedure is followed for the lateral direction except using UM $_{2,3}$ is replaced with UM $_1$. Remembering that the lateral direction plot is of both $\varepsilon_2$ and $\varepsilon_3$, the elastic strain from the axial direction is added to 2 times the elastic strain from the lateral direction to obtain total volumetric elastic strain. The same procedure is followed to obtain the total volumetric plastic strain.

With all the tests that define the fixed failure surface plotted in the $J_1$ - $\sqrt{J_{2D}}$ space, the parameter R can be determined to represent two different cap type surfaces. The caps can either define a plastic potential surface or a yield surface (Janardhanam and Desai, 1982).

To define a plastic potential surface, plastic strain increment vectors are plotted along each stress path at convenient points. A plastic potential surface

is drawn normal to those vectors to develop caps. The parameter R is defined as the ratio of the major and minor axes (length over height) for each cap. In most versions of the cap model, the parameter R is assumed to be a constant. In actuality, R probably varies as stress increases and/or decreases, therefore, an average ratio of R is used as the parameter value.

To define a yield surface, total volumetric plastic strain for each test is plotted on its corresponding stress path. Once this plot is completed for all the stress paths, lines of equal total volumetric plastic strains are plotted. The plotted lines should have an elliptical shape and run from the failure surface to the $J_1$ axis. Again, the parameter R is defined as the ratio of the major and minor axes (length over height) for each cap (Zaman et al., 1985). If the soil exhibits associated flow characteristic, the parameter R that defines the plastic potential function should be the same value of R used to define the yield function.

The hardening parameters D, W, and Z are the remaining parameters needed to completely define the cap model. These parameters are associated with the volumetric response and translation of the caps.

The parameter Z can be defined as the point at which the volumetric plastic strain begins or the location of the initial cap. For most soils, this volumetric plastic strain occurs at very low stresses, and is initially taken as zero, at least until the parameters are verified.

The parameters W and D can be determined by using the following equation (Desai and Siriwardane, 1984).

$$\varepsilon_v = W\left(1 - e^{-3pD}\right) + \frac{p}{K} \qquad 5.3$$

where K = bulk modulus

p = mean pressure = $\sigma_{oct.}$

This procedure is a trial and error method in which the values of D and W depend on which values give the best shape of the hardening caps and also satisfy the equation above. With each new value of W, there will be corresponding values of D for each data point along each stress path. W and D are selected as the values which best fit the HC test volumetric strain data points. A least squares type of approach may be used (Desai and Siriwardane, 1984).

## 5.2 Actual Parameter Determination for Sesser Soil

Initially, a preliminary testing plan was developed to determine the ten parameters for the modified cap model (Sture et al., 1979). The plan consisted of the triaxial tests mentioned in Table 5.1 and used the coding system as shown in Figure 5.1.

**Elastic Parameters.** To determine the modulus of elasticity, two CTC tests were run in a load-unload-reload manner. Each test had four unload-reload cycles. The data from these tests were plotted as shown in Figures 5.2 and 5.3. The modulus of elasticity was calculated as follows:

$$E = \frac{\sigma_1 - \sigma_3}{\varepsilon_1} \qquad 5.4$$

**Table 5.1**

**Preliminary Testing Plan**

| Number | Test Type |
|---|---|
| 1 | Conventional Triaxial Compression @ 20 psi (LUR) |
| 2 | Conventional Triaxial Compression @ 20 psi (LUR) |
| 3 | Hydrostatic Compression (LUR) |
| 4 | Hydrostatic Compression (LUR) |
| 5 | Conventional Triaxial Compression @ 10 psi |
| 6 | Conventional Triaxial Compression @ 20 psi |
| 7 | Conventional Triaxial Compression @ 35 psi |
| 8 | Triaxial Compression @ 10 psi |
| 9 | Reduced Triaxial Compression @ 15 psi |
| 10 | Reduced Triaxial Compression @ 30 psi |

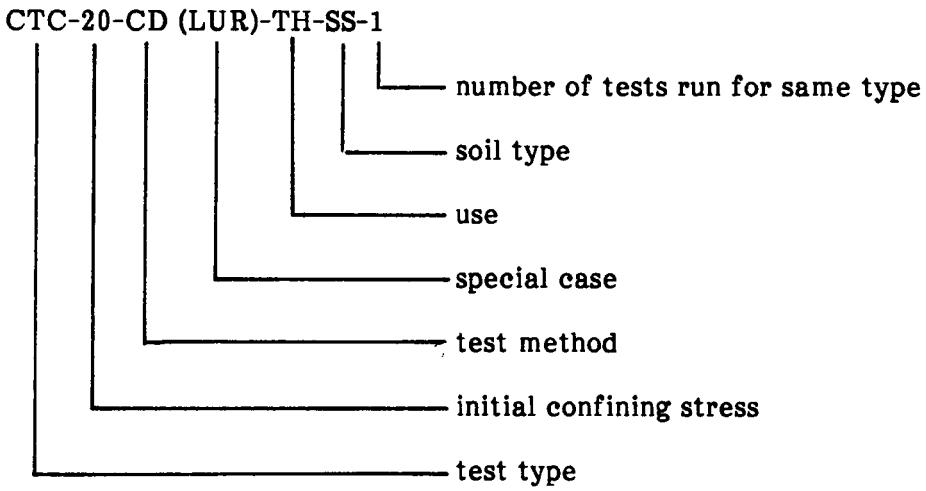


CTC = conventional triaxial compression

HC = hydrostatic compression

RTC = reduced triaxial compression

TC = triaxial compression

CD = consolidated drained

UD = unconsolidated drained (hydrostatic comp. test)

TH = used for thesis research

SS = Sesser soil

LUR = load-unload-reload cycle

PPM = pore pressure measurements

OD = oedometer test (uniaxial compression)

UC = unconfined compression

Figure 5.1 Example of specimen coding system.

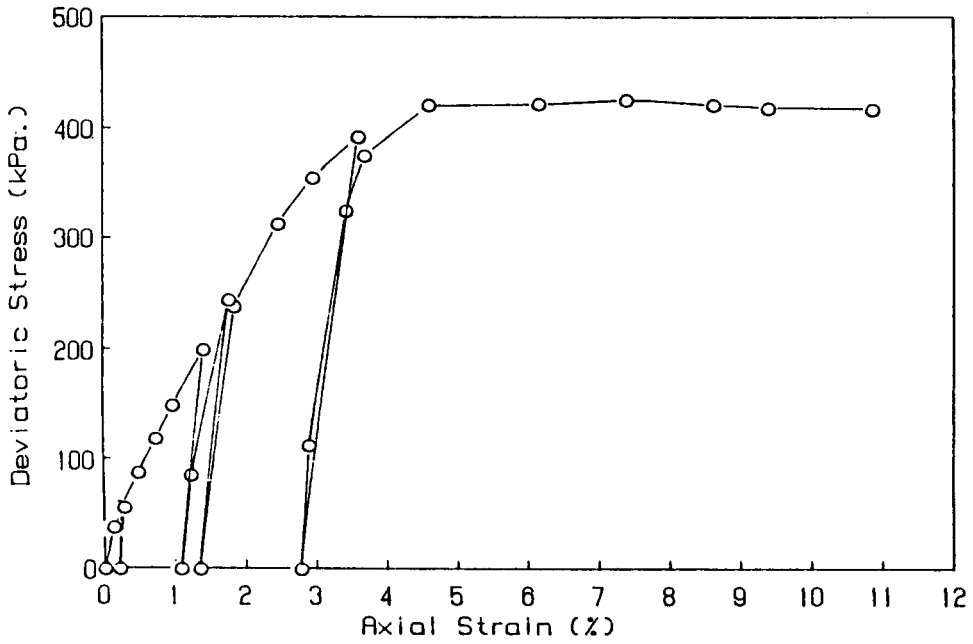


**Figure 5.2 CTC-20-CD (LUR)-TH-SS-1 stress-axial strain curve.**

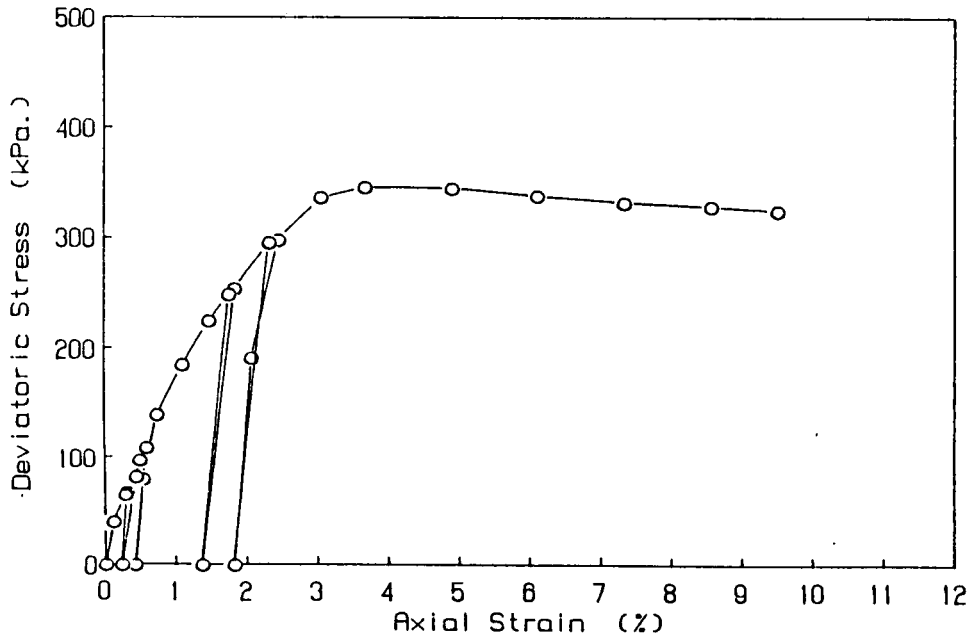


**Figure 5.3 CTC-20-CD (LUR)-TH-SS-2 stress-axial strain curve.**

(from CTC-20-CD (LUR)-TH-SS-1)

$$E_1 = \frac{55.7\ kPa}{0.00286 - 0.00207} = 70{,}475.8\ kPa \qquad 5.4.1$$

$$E_2 = \frac{199.1\ kPa}{0.0149 - 0.0107} = 60{,}333.3\ kPa \qquad 5.4.2$$

$$E_3 = \frac{243.8\ kPa}{0.0177 - 0.0133} = 55{,}409.1\ kPa \qquad 5.4.3$$

$$E_4 = \frac{391.4\ kPa}{0.036 - 0.0277} = 47{,}156.1\ kPa \qquad 5.4.4$$

(from CTC-20-CD (LUR)-SS-TH-2)

$$E_1 = \frac{67.9\ kPa}{0.00298 - 0.00222} = 89{,}342.1\ kPa \qquad 5.4.5$$

$$E_2 = \frac{109.6\ kPa}{0.00586 - 0.00432} = 67{,}239.3\ kPa \qquad 5.4.6$$

$$E_3 = \frac{248.5\ kPa}{0.0175 - 0.0135} = 62{,}125.0\ kPa \qquad 5.4.7$$

$$E_4 = \frac{296.0\ kPa}{0.0232 - 0.0181} = 58{,}039.2\ kPa \qquad 5.4.8$$

Average E = 63,765.1 kPa. (9248.0 psi)

The unloading modulus for the axial direction (UM1), by definition, is the same as the modulus of elasticity, therefore,

$$UM_1 = E = 63{,}765.1\ \text{kPa. (9248.0 psi)} \qquad 5.5$$

The unloading modulus for the lateral direction (UM2,3) is determined from the graphs in Figures 5.4 and 5.5 and calculated as follows:

(from CTC-20-CD (LUR)-SS-TH-1)

$$UM_{2,3} = \frac{391.4\ kPa}{-0.00431 - (-0.000886)} = -114{,}310.7\ kPa \qquad 5.6.1$$

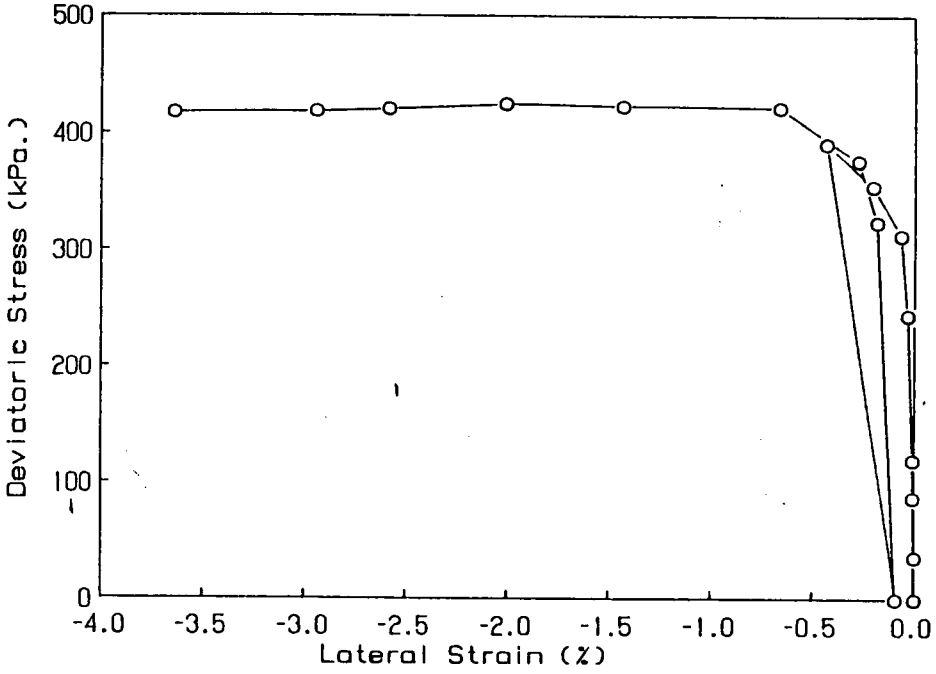


Figure 5.4 CTC-20-CD (LUR)-TH-SS-1 stress-lateral strain curve.

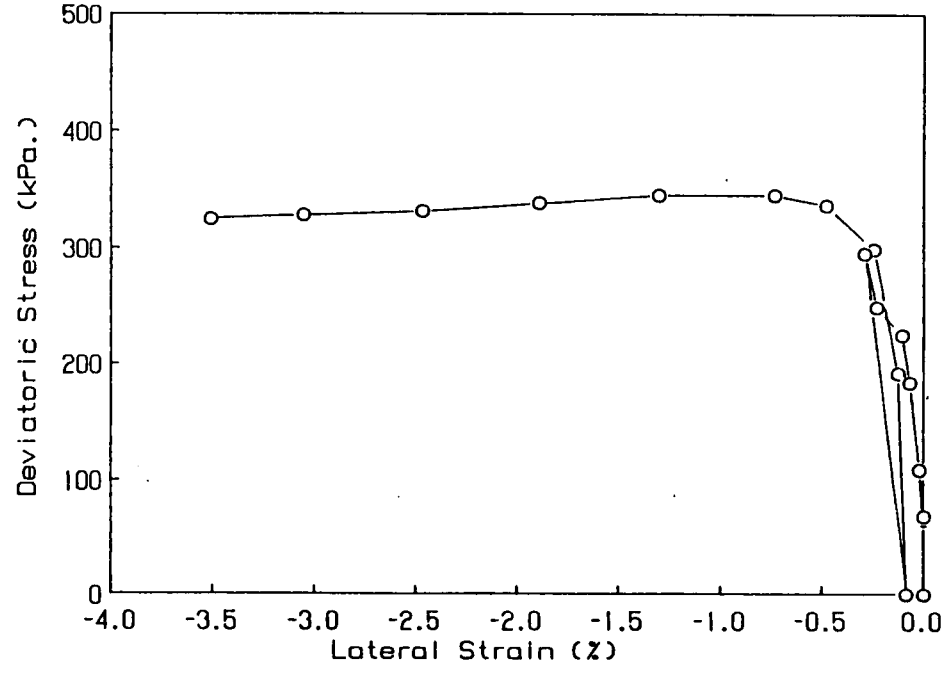


Figure 5.5 CTC-20-CD (LUR)-TH-SS-2 stress-lateral strain curve.

(from CTC-20-CD (LUR)-SS-TH-2)

$$UM_{2,3} = \frac{296.0\ kPa}{-0.00288 - (-0.000868)} = -147{,}104.7\ kPa \qquad 5.6.2$$

Average $UM_{2,3}$ = -130,707.7 kPa. (-18956.9 psi)

It should be noted that the lateral strains for the first three unload-reload cycles were smaller than the resolution of the data acquisition system and did not result in meaningful data, therefore, this data was discarded and only the data from the final unload cycle utilized.

The bulk modulus (K) was determined from the HC test data as shown in Figures 5.6 and 5.7. The bulk modulus was taken as the slope of the unloading curve. Only the second unload-reload cycle for each test will be used for the determination of K due to errors such as pressure loss and data drift, which may occur at low stresses.

The bulk modulus is defined as

$$K = \frac{\sigma_{oct.}}{\varepsilon_v} \qquad 5.7$$

and was determined from the test data as follows:

(from HC-64-UD-TH-SS-1)

$$K_1 = \frac{220.64 - 27.58\ kPa}{0.0818 - 0.0734} = 22{,}983.33\ kPa \qquad 5.7.1$$

(from HC-64-UD-TH-SS-2)

$$K_2 = \frac{220.64 - 27.58\ kPa}{0.0669 - 0.0583} = 22{,}448.8\ kPa \qquad 5.7.2$$

Average K = 22716.1 kPa. (3294.6 psi)

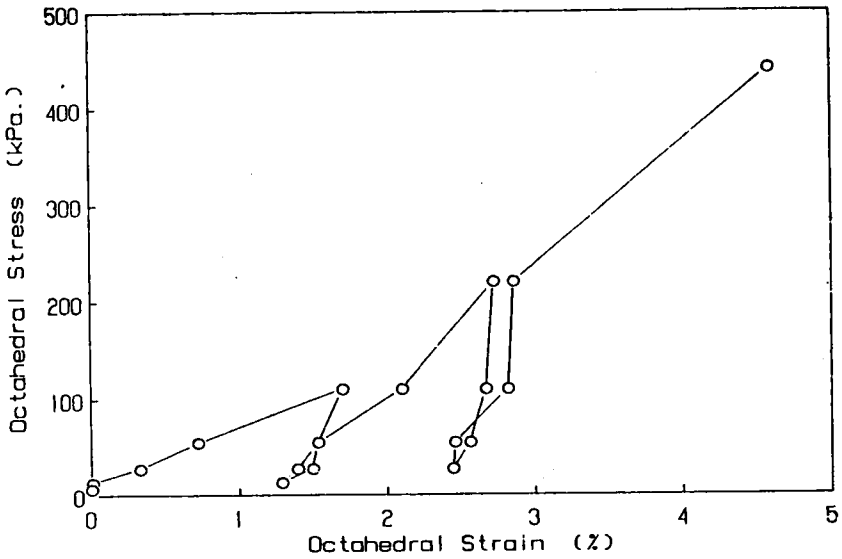


Figure 5.6 HC-1 stress -octahedral strain curve.

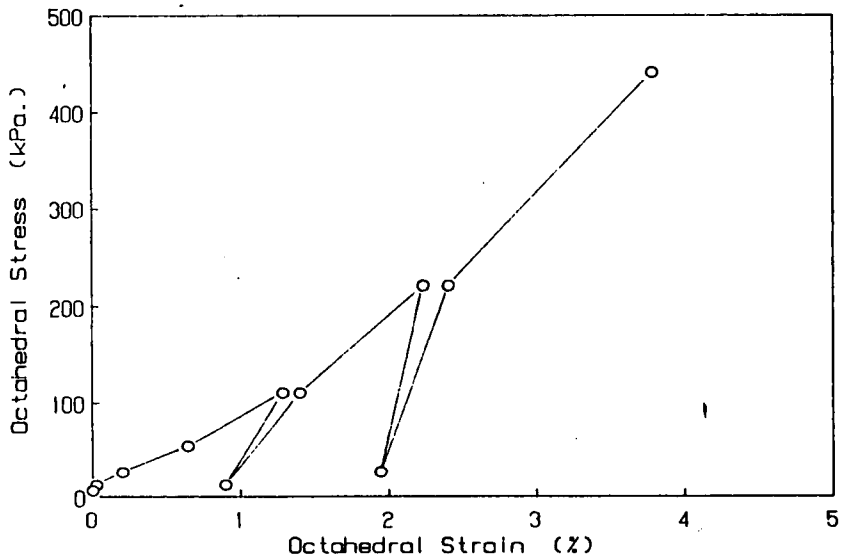


Figure 5.7 HC-2 stress-octahedral strain curve.

Determination of the bulk modulus allows the calculation of Poisson's ratio using Equation 5.1. Rearranging Equation 5.1 yields:

$$\mu = \frac{1}{6}\left(3 - \frac{E}{K}\right) = \frac{1}{6}\left(3 - \frac{9248.0}{3294.6}\right) \qquad 5.8$$

$$\mu = 0.032$$

Since this number is so small compared with the numerous published values of Poisson's ratio for various types of soil, it will be discarded. Poisson's ratio can also be calculated from the CTC unload-reload test data since, by definition, Poisson's ratio is the lateral elastic strain divided by the axial elastic strain, from Figures 5.2 through 5.5.

$$\mu = \frac{lateral\ elastic\ strain}{vertical\ elastic\ strain} \qquad 5.9$$

(from CTC-20-CD (LUR)-SS-TH-1)

$$\mu = \frac{0.00431 - 0.000886}{0.0360 - 0.0277} = 0.412 \qquad 5.9.1$$

(from CTC-20-CD (LUR)-SS-TH-2)

$$\mu = \frac{0.00288 - 0.0008685}{0.0232 - 0.018075} = 0.395 \qquad 5.9.2$$

Average $\mu = 0.403$

When working in the $\sigma_{oct.} - \varepsilon_{oct.}$ space, the bulk modulus can also be used as the unloading modulus for the HC test.

$$K = UM - HC = 22716.1\ kPa\ (3294.6\ psi) \qquad 5.10$$

**Fixed Failure Surface Parameters.** Once the elastic parameters are determined from the CTC and HC tests with unload-reload cycles, the remaining tests, as listed in Table 5.1, were run. The results from these tests, shown in Figures 5.8, 5.9 and 5.10, were plotted in the $J_1$-$\sqrt{J_{2D}}$ stress space as

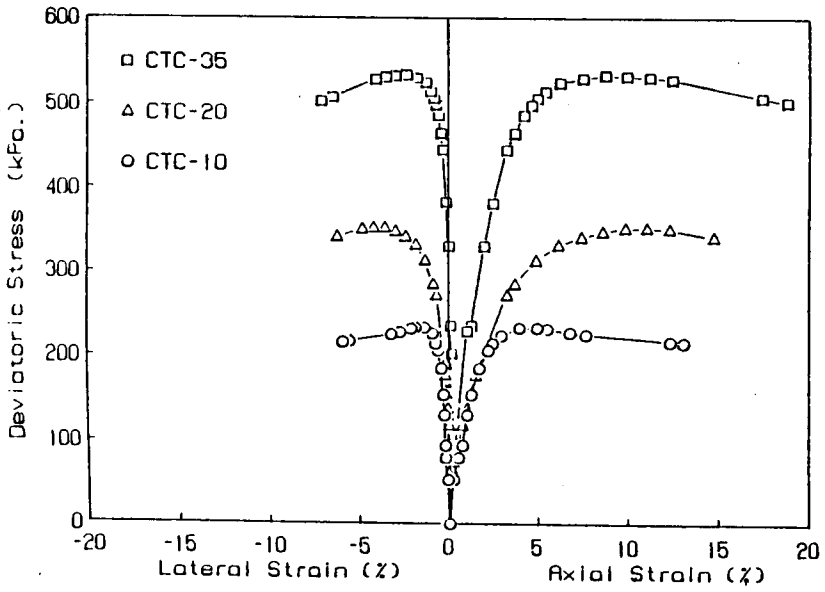


**Figure 5.8 CTC stress-strain curves.**

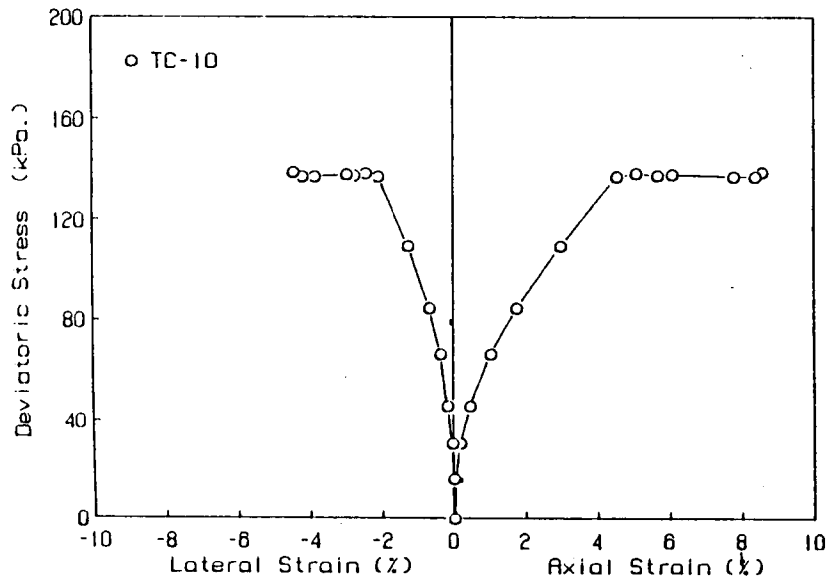


**Figure 5.9 TC stress-strain curves.**

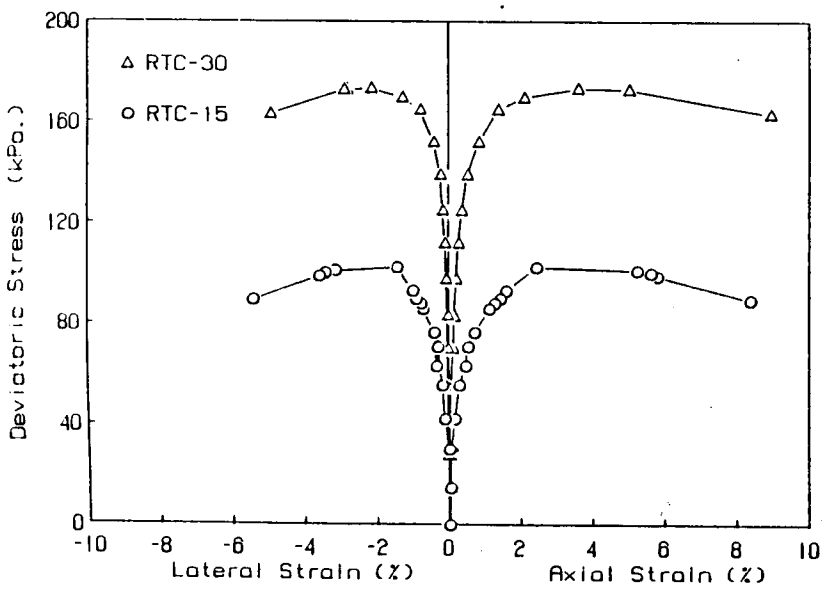


**Figure 5.10 RTC stress-strain curves.**

shown in Figure 5.11. Noting the failure point from each test, a failure surface consisting of a Drucker-Prager I and a Drucker-Prager II surface was fit to those points. The Von Mises surface did not fit the data well and therefore, was not used.

From the geometery of the failure surfaces, usually termed the fixed failure surface, the parameters $\alpha$, $\gamma$, and $\theta$ were determined to be (as shown in Figure 5.12);

$$\alpha = 41.632\ kPa\ (6.038\ psi)$$
$$\gamma = 22.850\ kPa\ (3.314\ psi)$$
$$\theta = 0.212$$

A transition curve connects the two Drucker-Prager surfaces and is defined by parameter $\beta$ using Equation 5.2.

$$\beta = \frac{-1}{J_1} \ln\left(\frac{\alpha - \theta J_1 - \sqrt{J_{2D}}}{\gamma}\right) \qquad (5.2)$$

This transition curve is simply drawn by hand with a French curve. The actual transition curve constructed for this research was too small to be represented on a graph.

Using the three points from the transition curve, having coordinates of $J_1$-$\sqrt{J_{2D}}$, the parameter $\beta$ was calculated as follows;

$J_1 = 224.1\ kPa$, $\sqrt{J_{2D}} = 86.2\ kPa$

$$\beta_1 = \frac{-1}{224.1} \ln\left(\frac{41.632 + (0.212)(224.1) - 86.2}{22.85}\right) \qquad 5.11.1$$

$$\beta_1 = 0.00915\ kPa^{-1}\ \left(0.06309\ psi^{-1}\right)$$

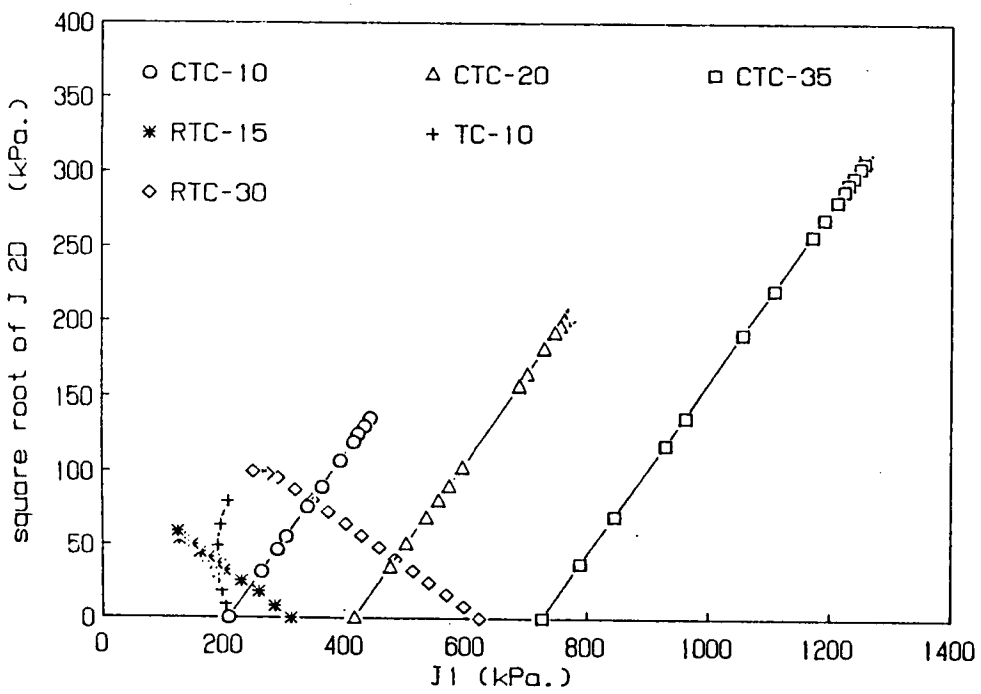


**Figure 5.11 Triaxial stress paths.**

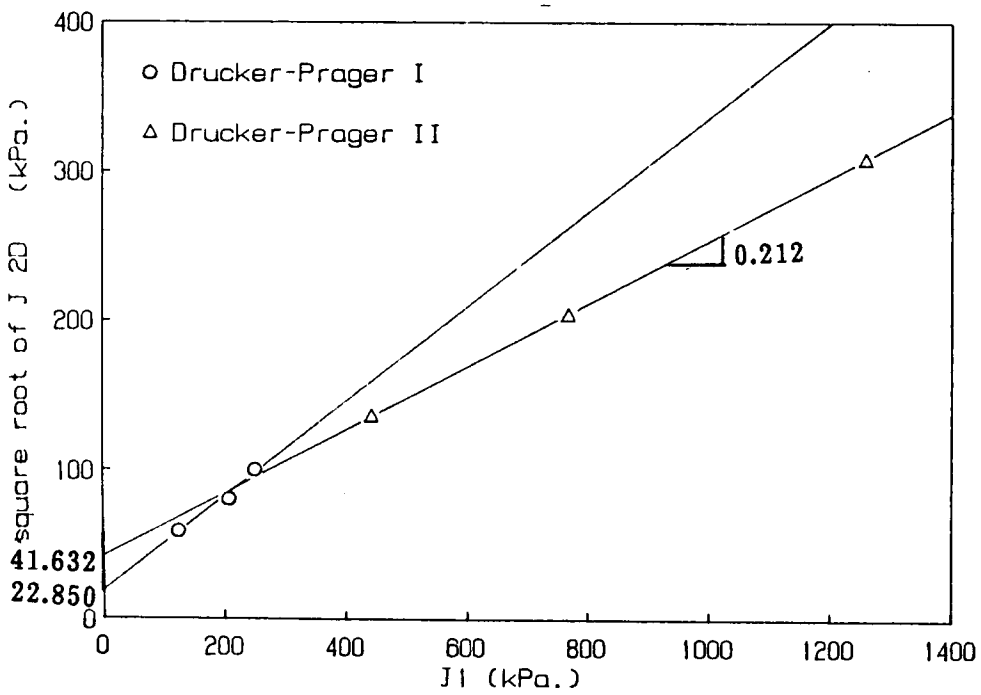


**Figure 5.12 Drucker-Prager I and II surfaces.**

$$J_1 = 237.9\ kPa,\quad \sqrt{J_{2D}} = 90.5\ kPa \qquad \beta_2 = \frac{-1}{237.0}\ ln\left(\frac{41.632 + (0.212)(237.9) - 90.5}{22.85}\right) \quad 5.11.2$$

$$\beta_2 = 0.01126\ kPa^{-1}\ \left(0.07767\ psi^{-1}\right)$$

$$J_1 = 255.1\ kPa,\quad \sqrt{J_{2D}} = 94.8\ kPa \qquad \beta_3 = \frac{-1}{255.1}\ ln\left(\frac{41.632 + (0.212)(255.1) - 94.8}{22.85}\right) \quad 5.11.3$$

$$\beta_3 = 0.01262\ kPa^{-1}\ \left(0.08703\ psi^{-1}\right)$$

Average $\beta$ = 0.01101 kPa.-1 (0.07591 psi -1)

**Yield Surface and Hardening Parameters.** To determine the parameter R, defining the yield caps, the total volumetric plastic strain must be computed. Using the unloading modulus for the HC tests, the total volumetric strains occurring in the HC tests are broken down into total elastic and plastic volumetric strain components as mentioned in Section 5.1. These total volumetric plastic strains are plotted along the HC stress path in the $J_1$-$\sqrt{J_{2D}}$ stress space.

The unloading modulus for the CTC tests is assumed to be equal to the unloading modulus for the RTC and TC tests. Again, the total volumetric strains are broken into the elastic and plastic components. This includes the strains that occurred during the consolidation phase. If volumetric strains were not measured during the consolidation phase, they must be estimated from the HC test data and added to the total volumetric plastic strains that occurred during the shearing phase of the test. The total volumetric plastic strains for each test are plotted on their corresponding stress path.

Contour lines of equal total volumetric plastic strain are plotted. The average aspect ratio (length over height) is taken as the parameter R. Figure 5.13 shows the total volumetric plastic strains, for selected points and the contour lines. The parameter R was determined from the contours as shown in Figure 5.13.

$$R_1 = \frac{189.6\ kPa}{103.4\ kPa} = 1.8333 \qquad 5.12.1$$

$$R_2 = \frac{196.5\ kPa}{137.9\ kPa} = 1.425 \qquad 5.12.2$$

$$R_3 = \frac{427.5\ kPa}{168.9\ kPa} = 2.531 \qquad 5.12.3$$

$$R_4 = \frac{437.8\ kPa}{182.7\ kPa} = 2.396 \qquad 5.12.4$$

Average R = 2.05

The parameters W can be determined directly by running the HC test to very high stresses, stresses near 5000 kPa. (725 psi). These high stresses are nearly unobtainable with most equipment being used, and the test would be very time consuming if it were run at such a high stress. A better method, described in more detail in Chapter 6, is to fit an inverted hyperbolic curve defined by Equation 5.13 to the total volumeteric strain data and use the asymptote of the curve as the value of W.

$$\sigma_{oct.} = \frac{-(a)(\varepsilon_v)}{1 + (b)(\varepsilon_v)} \qquad 5.13$$

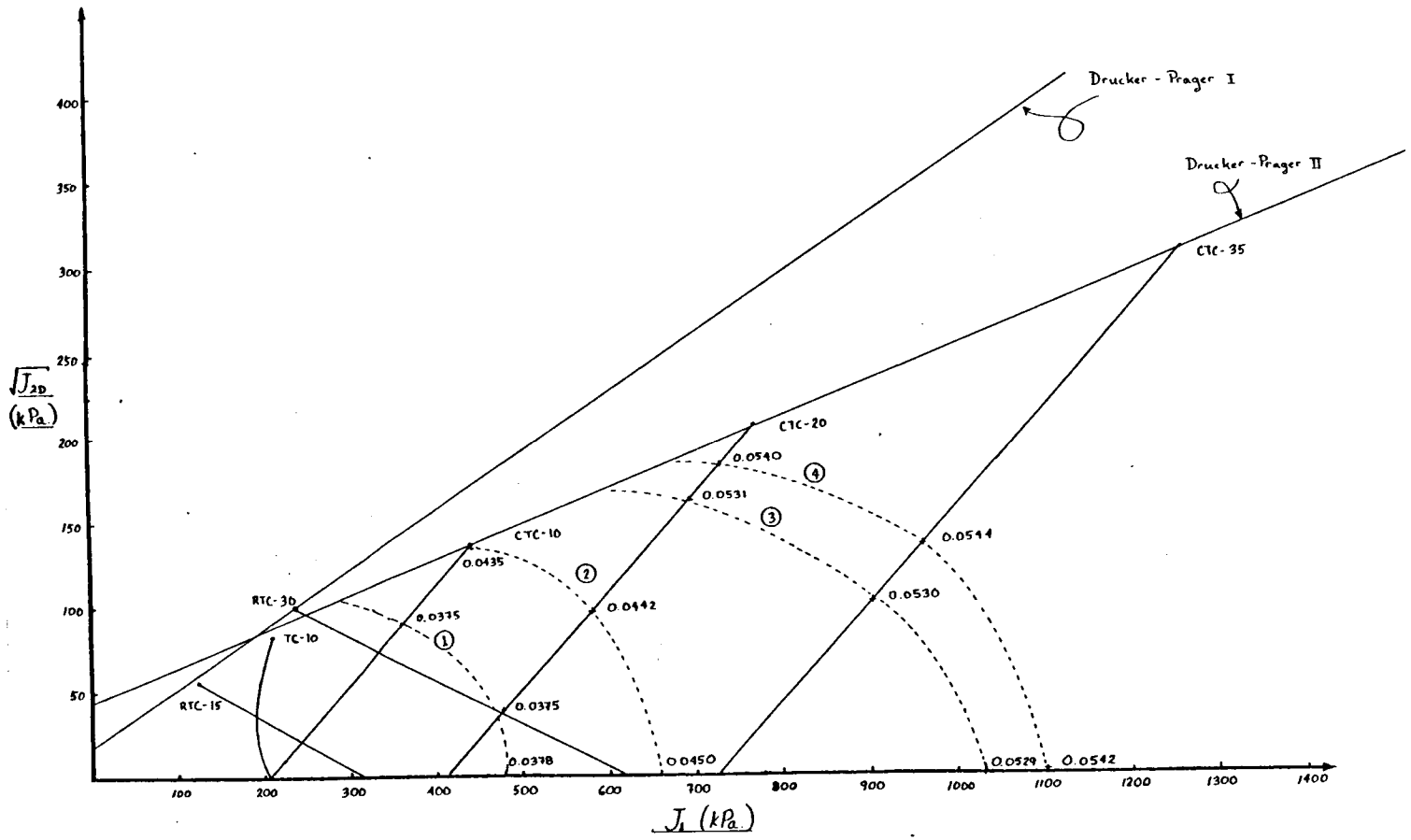


Figure 5.13 Plot of plastic yield caps.

A curve with the form of Equation 5.13 was fit to the total volumetric strain data from both HC tests with the asymtope (1/b) being;;

(from HC-64-UD-TH-SS-1)

W1 = 0.3901 cm/cm

(from HC-64-UD-TH-SS-2)

W2 = 0.3625 cm/cm

Average W = 0.3762 cm/cm

Using Equation 5.3, a trial and error procedure, the parameter D was determined to fit the data shown in Table 5.2. It is usually easier to determine an appropriate D parameter, by trial and error, for each load step. Once a number of suitable D parameters are found, the D parameter is taken as the average. Volumetric strain are then computed using the W and D parameters. The resulting strains should compare well with actual data, and if not, D should be adjusted.

The remaining parameter, Z, is initially assumed to be zero. This parameter is usually estimated for the first trial in the finite element adjustment process (discussed in the next section) and adjusted accordingly to best fit the predicted soil behavior.

The cap model parameters for the Sesser soil are summarized in Table 5.3.

## 5.3 Back Prediction Procedure

To confirm the model parameters, the initial parameters should be used in a finite element code or driver subroutine (Sandler and Rubin 1979) using the

Table 5.2

Volumetric Strain Table for Determination of Parameter D

| $\sigma_{oct.} = p$ (kPa) | $e_v$ = volumetric strain cm/cm | | |
|---|---|---|---|
| | HC - 1 measured | HC - 2 measured | Average $\varepsilon_v$ |
| 6.9 | 0.0 | 0.0 | 0.0 |
| 13.8 | 0.000333 | 0.00073 | 0.00053 |
| 27.6 | 0.00978 | 0.00615 | 0.00797 |
| 55.2 | 0.02169 | 0.01938 | 0.02054 |
| 110.3 | 0.0510 | 0.03846 | 0.04473 |
| 220.6 | 0.08178 | 0.06690 | 0.07434 |
| 441.3 | 0.13746 | 0.11352 | 0.12549 |

| $\sigma_{oct.} = p$ (kPa) | Average $\varepsilon_v$ | Trial D $kPa^{-1}$ | Predicted $\varepsilon_v$ using D = 2.788 E-4 |
|---|---|---|---|
| 6.9 | 0.0 | D = N/A | 0.00246 |
| 13.8 | 0.00053 | D = N/A | 0.00492 |
| 27.6 | 0.00797 | 2.190 E-4 | 0.00978 |
| 55.2 | 0.02054 | 2.990 E-4 | 0.01937 |
| 110.3 | 0.04473 | 3.394 E-4 | 0.03798 |
| 220.6 | 0.07434 | 3.857 E-4 | 0.07304 |
| 441.3 | 0.12549 | 2.509 E-4 | 0.13542 |

Avg. D = 2.788 E-4 $kPa^{-1}$

**Table 5.3**

**Summary of Initial Sesser Soil Cap Model Parameters**

| Parameter | SI | English Units |
|---|---|---|
| E | 63,765.1 kPa | 9248.0 psi |
| $\mu$ | 0.403 | 0.403 |
| $\alpha$ | 41.632 kPa | 6.038 psi |
| $\gamma$ | 22.850 kPa | 3.314 psi |
| $\theta$ | 0.212 | 0.212 |
| $\beta$ | 0.0110 $kPa^{-1}$ | 0.07591 $psi^{-1}$ |
| W | 0.3762 | 0.3762 |
| D | 0.0002788 $kPa^{-1}$ | 0.00192 $psi^{-1}$ |
| R | 2.05 | 2.05 |
| Z | 0.0 | 0.0 |

cap model to back predict the results of other drained triaxial tests conducted on the Sesser soil. From the results of the finite element analysis, the parameters can be adjusted, if need be, to obtain better results. This parameter adjustment is a trial and error procedure and depends heavily on the experience of the modeler (Sandler et al., 1976). Once a set of parameters has given predicted results that simulate the actual soil behavior, that set of parameters will be considered the final set of soil cap model parameters to be used in analysis.

In adjusting the parameters, the sensitivity of each parameter should be considered. Certain parameters can effect the results of an analysis more than others. According to Simo et al., (1988), the parameter sensitivity should follow the following order of decreasing sensitivity,

$$W \rightarrow D \rightarrow R \rightarrow \alpha \rightarrow \theta \rightarrow \gamma \rightarrow \beta$$

Since $\alpha$, $\theta$, $\gamma$, and $\beta$ all define the fixed failure surface, it is unlikely that those parameters should have to be adjusted. This elimination leaves the adjusting confined to W, D, and R. It is the author's view that parameter D should be the first parameter adjusted if W was determined using the alternate, high stress method (or the method proposed in Chapter 6). The reason being that W could then be considered a constant since it was found by a rational method and has some physical significance, whereas D was found by a trial and error method.

## 5.4 Brief Summary of Published Cap Model Parameters for Various Materials

Table 5.4 shows a partial list of cap model parameters that have been published for various soil types, bedding gravel, limestone, and concrete.

Such a table can be useful in estimation of cap model parameters.

**Table 5.4 English Units**

**Brief Summary of Published Cap Model Parameters for Various Materials**

| MATERIAL TYPE | REF. | ELASTIC | | FIXED FAILURE ENVELOPE $f_1 = \sqrt{J_{2D}} + \gamma e^{-\beta J1} - \theta J_1 - \alpha = 0$ | | | | CAP AND HARDENING BEHAVIOR | | | |
|---|---|---|---|---|---|---|---|---|---|---|---|
| | | E ksi | $\mu$ | $\alpha$ psi | $\gamma$ psi | $\beta$ psi$^{-1}$ | $\theta$ | D psi$^{-1}$ | W | Z ksi | R |
| McCormick Ranch Sand (Dry) | A | 100.0 | .25 | 250.0 | 180.0 | 6.7 E$^{-4}$ | 0.0 | 6.7 E-5 | 0.066 | 0.0 | 2.5 |
| Pueblo Colo. Sand | B | 14.966 | 0.36 | 37.22 | 37.22 | -0.00255 | 0.426 | 0.0028 | 7.37 | 0.0 | 1.93 |
| Pueblo Colo. Silty Sand | C | 11.5 | 0.4 | 13.0 | 13.0 | 0.032 | 0.1 | 3.0 E-4 | 0.9 | 0.0 | 1.15 |
| Artificial Soil | D | 3.904 | 0.28 | 5.0 | 5.0 | 0.085 | 0.12 | 5.0 E-4 | 4.4 | 0.0 | 1.67-2.0 |
| Artificial Soil | E | 4.0 | 0.35 | 5.6 | 5.6 | 0.062 | 0.11 | 0.05 | 0.18 | 0.0 | 2.0 |
| Sesser Soil | F | 9.248 | 0.403 | 6.038 | 3.314 | 0.07591 | 0.212 | 0.00192 | 0.3762 | 0.0 | 2.05 |
| Subballast | G | 20.0 | 0.4 | 26.0 | 21.5 | 0.02 | 0.0 | 3.08 E-5 | 0.035 | 0.0 | 1.24 |
| Colorado Concrete | H | N/A | N/A | 3860.0 | 1160.0 | 4.4 E-4 | 0.11 | 3.2 E-6 | 0.42 | 16.0 | 4.43 |
| Indiana Limestone | I | 3258.0 | 0.253 | 1.0 E5 | 9.77 E4 | 2.7 E-6 | 0.0 | 1.0 E-5 | 0.08 | 67.73 | 4.0 |

Table 5.4,

Brief Summary of Published Cap Model Parameters for Various Materials

| MATERIAL TYPE | REF. | ELASTIC | | FIXED FAILURE ENVELOPE $f_1 = \sqrt{J_{2D}} + \gamma e^{-\beta J1} - \theta J_1 - \alpha = 0$ | | | | CAP AND HARDENING BEHAVIOR | | | |
|---|---|---|---|---|---|---|---|---|---|---|---|
| | | E MPa | μ | α kPa | γ kPa | β kPa-1 | θ | D kPa-1 | W | Z MPa | R |
| McCormick Ranch Sand (Dry) | A | 689.5 | .25 | 1723.75 | 1241.1 | 9.72 E-5 | 0.0 | 9.72 E-5 | 0.066 | 0.0 | 2.5 |
| Pueblo Colo. Sand | B | 103.11 | 0.36 | 256.63 | 256.63 | -0.00037 | 0.426 | 4.0 E-4 | 7.37 | 0.0 | 1.93 |
| Pueblo Colo. Silty Sand | C | 79.293 | 0.4 | 89.64 | 89.64 | 0.00464 | 0.1 | 4.35 E-5 | 0.9 | 0.0 | 1.15 |
| Artificial Soil | D | 26.918 | 0.28 | 34.48 | 34.48 | 0.0123 | 0.12 | 7.3 E-5 | 4.4 | 0.0 | 1.67-2.0 |
| Artificial Soil | E | 27.58 | 0.35 | 38.58 | 38.58 | 0.009 | 0.11 | 0.00725 | 0.18 | 0.0 | 2.0 |
| Sesser Soil | F | 63.765 | 0.403 | 41.63 | 22.85 | 0.011 | 0.212 | 2.78 E-4 | 0.3762 | 0.0 | 2.05 |
| Subballast | G | 137.9 | 0.4 | 179.4 | 148.35 | 0.0029 | 0.0 | 4.47 E-6 | 0.035 | 0.0 | 1.24 |
| Colorado Concrete | H | N/A | N/A | 26614.7 | 7998.2 | 6.38 E-5 | 0.11 | 4.64 E-7 | 0.42 | 110.32 | 4.43 |
| Indiana Limestone | I | 22463.8 | 0.253 | 6.9 E5 | 6.74 E5 | 3.92 E-7 | 0.0 | 1.45 E-6 | 0.08 | 467.0 | 4.0 |

**References for Table 5.4**

A DiMaggio and Sandler, 1971

B Zaman et al., 1982

C Desai et al., 1982

D Desai and Siriwardne, 1984

E Desai et al., 1982

F (This Thesis)

G Desai and Siriwardne, 1982

H Ju et al., 1987

I Chu and Brandt, 1987

# CHAPTER 6

# SIMPLIFIED PARAMETER DETERMINATION PROCEDURE

## 6.1 Steps and Justification

To determine cap model parameters in the traditional procedure mentioned in Chapter 5, a series of drained triaxial tests, along different stress paths, must be run. For a fine grained soil, this series may take from three to five weeks to complete and an additional week is needed to determine and tune the parameters. This time period makes using the cap model nonfeasible for many engineering firms; it is for this reason that a simplified procedure is introduced. Recently, several simplified procedures have been introduced (Humphrey and Holtz, 1987; Simo et al., 1988; Drumm, 1989) that associate cap model parameters with existing data such as CTC test data and oedometer test data. However, most of these procedures rely on estimation of one or more soil properties. This introduced procedure should prove feasible time-wise, especially for laboratories with a limited amount of triaxial equipment and eliminate most estimation of properties.

As in the traditional procedure, the first two parameters that should be determined are the modulus of elasticity (E) and Poisson's ratio ($\mu$). The modulus of elasticity is determined using the procedure outlined in Sections 5.1 and 5.2. In addition, the unloading modulus for the axial and lateral direction is also determined using the same procedure as in Sections 5.1 and 5.2. If an appropriate drained loading rate, one in which no pore pressure is built up, is not

known, a loading rate can be estimated from published work, such as (Bishop and Henkel, 1962).

While the CTC test is running, an oedometer test can be conducted, and used to estimate the bulk modulus (Drumm, 1989). The oedometer test is also run in a load-unload-reload manner. The results are then plotted in arithmetic form in the vertical stress - axial strain space. The constrained modulus (M) can be taken as the slope of the unloading curve.

From E and M, Poisson's ratio can be determined by

$$M = \frac{E\left(1 - \mu\right)}{\left(1 + \mu\right)\left(1 - 2\mu\right)} \qquad 6.1$$

and the bulk modulus can be determined using Equation 5.1

$$K = \frac{E}{3\left(1 - 2\mu\right)} \qquad (5.1)$$

Hydrostatic compression tests can be eliminated if at least one of the conventional triaxial tests is run at a high confining stress and volume change measurements are taken during consolidation. The hydrostatic data from the consolidation phase of the CTC can be applied to an inverted hyperbolic curve, mentioned later, to simulate the HC test curve.

Knowing the bulk modulus, total volumetric plastic strains can be computed for the HC data. This computation allows for the plotting of total plastic strains in the $J_1$-$\sqrt{J_{2D}}$ stress space, as described earlier.

Three drained conventional triaxial compression tests, with volume change measurements, are run at different confining stresses, typically 69, 173, and 276 kPa, (10, 25, and 40 psi). These three tests define the fixed failure surface at high stresses, and they help determine the parameter R.

Increments of total volumetric plastic strain, from the CTC and HC tests, are plotted along each of the corresponding stress paths in the $J_1$-$\sqrt{J_{2D}}$ stress space. The parameter R, defining a yield surface, is determined as outlined in Sections 5.1 and 5.2. Contrary to other work, only the CTS and HC plastic strain data is used to determine R. Trying to contour total volumetric plastic strain from other stress paths with the CTC tests is impractical (Munster, 1981).

To better define the fixed failure surface, two options may be considered. If the soil is a cohesionless soil or one that can be saturated fairly easily, undrained triaxial tests with pore pressure measurements, along nontraditional stress paths, such as the TC and RTC, are incorporated. The effective stress paths from undrained triaxial tests can be used since they only help to define the fixed failure surface and are not used to determine the parameter R.

If the soil is a fine grained soil or one that cannot be saturated fairly easily, an unconfined compression test can be run. This test will give at least one point in the low stress range to define the fixed failure surface.

Once the fixed failure surface is defined, the parameters $\alpha$, $\gamma$, $\beta$, and $\theta$ can be determined quite easily as outlined in Section 5.1 and 5.2.

The parameter W is determined by applying the data obtained from the consolidation phase of the CTC test to an inverted hyperbolic curve using a statistical analysis computer program. Octahedral stress data points along with

the corresponding volumetric strain are entered into the computer program. The program should determine appropriate values for a and b for the inputed equation, Equation 5.4. Once two values for a and b are found, the asymptote (1/b) is taken as the maximum total volumetric strain and parameter W.

$$\varepsilon_v = W\left(1 - e^{-3pD}\right) + \frac{P}{K} \tag{5.3}$$

Knowing W, parameter D is determined as outlined in Sections 5.1 and 5.2.

where p = mean pressure

k = bulk modulus

Parameter Z is assumed to be zero (0) initially. This parameter is easily changed during the tuning process.

# CHAPTER 7

# CONCLUSIONS AND SUGGESTIONS

## 7.1 Summary

The main objective of this thesis was to determine the model parameters that will be used in a numerical analysis and suggest an alternate method or simplified procedure by which these parameters can be determined. A review of previous research on various numerical models for soil was conducted and an elastic-plastic model was selected to model the soil from Sesser, Illinois.

Extensive laboratory preparation was conducted to allow testing of partially saturated samples with volume change measurements. This preparation included equipment assembly and calibration, initial testing, and trial testing and verification. Laboratory equipment was also prepared for undrained testing with pore pressure measurements. One undrained test was conducted, using a silty, alluvial soil, for trial testing and equipment verification purposes.

Undisturbed samples of Sesser soil were obtained during the summer of 1988 and transported to Knoxville, Tennessee, where they were stored in a moisture room until testing. Upon testing, samples were extruded, trimmed, measured, weighed, and placed in a triaxial device.

The test series consisted of traditional and non-traditional drained triaxial tests with volume change measurements and required five to six weeks to complete. Traditional, CTC test data was recorded with an electronic X-Y-Y'

plotter. Non-traditional, HC, RTC, and TC test, data was manually recorded and conversely, required extensive monitoring.

The triaxial data was reduced and graphed. From the results, ten cap model parameters for the Sesser soil were determined. An alternate method or simplified procedure was presented and applied to the Sesser results.

## 7.2 Conclusions and Suggestions

Several suggestions should be made concerning the entire process of determining cap model parameters. Several of the suggestions pertain only to The University of Tennessee, Knoxville while the others pertain to the overall process.

1. A new sample extruding device should be built or the old one modified to better fit the sample tubes used for field sampling. The extruder should be shortened to lessen the travel of the piston and there should be a permanent seat for the tube to rest on or fit into while the sample is being extruded. This seat will eliminate the errors induced by hand-holding the tube while the sample is being extruded.

2. Samples should be extruded and resealed as soon as possible. If undisturbed samples are left in their tubes for more than 30 days, they become extremely hard to extrude.

3. The valves on the pressure panel and triaxial frame should be overhauled due to moisture in the air lines. This moisture has

caused the valves to stick and to become non-workable at times. In addition, a new moisture control valve should be installed in the incoming pressurized air line. It is important that water is drained from the compressor on a routine basis. These problems should be reduced with the new, high pressure (850 kPa) air compressor.

4. When running triaxial tests to determine cap model parameters, it is important to run the hydrostatic test(s) as one of the first test(s) in the series. If volume change measurements are not taken during the consolidation phase of the other tests in the triaxial series, these volume changes can be estimated from HC test(s) results.

5. In the proposed cap model parameter determination method, the only reason drained CTC tests should be run is to determine the parameter R. Estimating that this drained series could take up to two weeks to complete, it would be very beneficial if another procedure could be followed to determine R.

As mentioned in Chapter 6, the parameter R has been investigated by Yamada and Abou-Sayed (1979) as being related to Poisson's ratio. If time were a major factor in the parameter determination process, the estimation equation, Equation 7.1, might provide a fair estimate.

$$R^2 = \frac{6(1 + \mu)}{1 - 2\mu} \qquad 7.1$$

It is the author's view that the relationship between Poisson's ratio and the parameter R probably only holds true at small values, less than 0.2, of Poisson's ratio.

One hypothesis that might be explored would be trying to relate R to some other soil property(ies) or other related value. This relationship might be accomplished by running 3 drained CTC tests (at different confining stresses), and 1 drained HC test, all with volume change measurements, on different types of soil. From the results of these tests, R can be determined and can possibly be related to one or more of the following:

1. Plasticity index
2. Soil classification
3. Constrained modulus
4. Bulk modulus
5. Other

If R could be estimated by some type of relationship, no drained tests would have to be conducted to determine cap model parameters, thus cutting the determination process from 2 to 6 weeks down to one week or less.

# REFERENCES

## REFERENCES


American Society of Testing and Materials, (1988). Soil and rock, building stones; geotextiles, *Annual Book of ASTM Standards*, ASTM, Philadelphia, PA, 04.08, 322-326.

Al-Hussaini, M. (1981). "Tensile properties of compacted soils," *Laboratory Shear Strength of Soil*, ASTM STP 740. R.N. Yong and F.C. Townsend, Editors., ASTM, 207-225.

Baldi, G., Hight, D.W., and Thomas, G.E. (1988). "A reevaluation of conventional triaxial test methods," *Advanced Triaxial Testing of Soil and Rock*, ASTM STP 977. R.T. Donaghe et al., Editors., ASTM, 219-263.

Baron, M.L., Nelson, I., and Sandler, I.S. (1973). "Influence of constitutive models on ground motion predictions," *J. of the Engrg. Mech. Div.*, ASCE, 99(12), 1181-1200.

Bishop, A.W., and Henkel, D.J. (1962). *The Measurement of Soil Properties in the Triaxial Test*, William Clowes & Sons, Ltd., London, England.

Chen, W.F., and Baladi, G.W. (1985). *Soil Plasticity, Theory and Implementation.* Elsevier Science Publishing Company Inc., New York, NY.

Chu, H.S. and Brandt, H. (1987). "Constants for an elastic-plastic cap model for limestone," *Int'l. J. Numer. Anal. Meth. Geomech.*, 11, 193-202.

Dafalias, Y.F. and Popov, E.P. (1976). "Plastic internal variables formalism of cyclic plasticity," *J. Appl. Mech.*, 98(4), 645-651.

Das, B. (1986). *Soil Mechanics Laboratory Manual*, Engineering Press, Inc., San Jose, California.

Desai, C.S. and Siriwardane, H.J. (1982). "Analysis of track support structures," *J. Geotech. Eng. Div.*, ASCE, 108(3), 461-480.

Desai, C.S., and Siriwardane, H.J. (1984). *Constitutive Laws for Engineering Materials with Emphasis on Geologic Materials.* Prentice-Hall, Inc., Englewood Cliffs, NJ.

Desai, C.S., Siriwardane, H.J. and Janardhanam, R. (1982). "Interaction and load transfer in track-guide-way systems," Nos. DOT/RSPA/DMA-50/83/11 and 12, Department of Transportation, Washington, DC.

DiMaggio, F.L., and Sandler, I.S. (1971). "Material model for granular soils," *J. of Engrg. Mech. Div.*, ASCE, 97(6), 935-950.

Drucker, D.C. (1950). "Some implications of work hardening and ideal plasticity," *Quarterly of Applied Mathematics*, 7, 411-418.

Drucker, D.C. (1950). "A more fundamental approach to stress strain relations," *Proceeding* 1st U.S. Nat. Congr. Appl. Mech., ASME, 487-491.

Drucker, D.C., and Prager, W. (1952). "Soil mechanics and plastic analysis or limit design," *Quarterly of Applied Mathematics*, 10, 157-175.

Drumm, E.C. (1989). "Determination of cap model parameters from standard laboratory test data," *Int. J. for Numer. and Anal.*, Meth. in Geomech. to appear.

Fung, Y.C. (1969). *A First Course in Continuum Mechanics.* Prentice-Hall, Inc., Englewood Cliffs, NJ.

Haythornthwaite, R.M. (1960). "Mechanics of triaxial tests for soils," *J. of Soil Mech. and Found. Div.*, ASCE, 86(5), 35.

Humphrey, D.N., and Holtz, R.D. (1987). "A procedure to determine cap model parameters," Constitutive Laws for Engineering Materials: Theory and Application. C.S. Desai et al., Editors, Elsevier Science Publishing Co., Inc., 1225-1232.

Janardhanam R., and Desai, C.S. (1982). "Non-associate elasto-plastic material model for compacted soil," *Proceedings*, Int. Symp. on Numer. Models in Geomech., Zurich, Germany, 324-333.

Ju, J.W., Simo, J.C., Pister, K.S., and Taylor, R.L. (1987). "A parameter estimation algorithum for inelastic material models," Constitutive Laws for Engineering Materials: Theory and Application. C.S. Desai et al., Editors, Elsevier Science Publishing Co., Inc., 1233-1240.

Kane, W.F., Bennett, R.M., and Lee, P.A. (1988). "Testing program for earth-structure analysis of mine subsidence," Report prepared for The U.S. Bureau of Mines - Twin Cities Research Center, Minneapolis, MN and Illinois Mine Subsidence Insurance Fund, Chicago, IL, Contract No. S027058.

Ko, H.Y. and Scott, R.F. (1967). "A new soil testing apparatus," *Geotechnique* 17(1), 40-57.

Ko, H.Y. and Sture, S. (1981). "State of the art: data reduction and application for analytical modeling," *Shear Strength of Soil*, ASTM STP 740. R.N. Yong and F.C. Townsend, Editors., ASTM, 329-386.

Konder, R.L. (1963). "Hyperbolic stress-strain response: cohesive soils," *J. Soil Mech. and Found. Div.*, ASCE 89(1), 115-143.

Lade, P.V. and Duncan, J.M. (1975). "Elastoplastic stress-strain theory for cohesionless soil," J. *Geotech. Eng. Div.*, ASCE, 101(10), 1037-1053.

Lade, P.V. (1988). "Automatic volume change and pressure measurement devices for triaxial testing of soils," *Geotech. Testing J.*, GTJODI, No. 4, 11(12), 263-268.

Lowe III, J., and Johnson, T.C. (1960). "Use of back pressure to increase degree of saturation of triaxial test specimens," Reseacrh Conference on Shear Strength of Cohesive Soils - Sponsered by Soil Mech. and Found. Div. of ASCE., (6), 819-836.

Munster Jr., C.L. (1981). "Constitutive modeling of a grandular soil under three-dimensional states of stress," thesis presented to Virginia Polytechnic Institute and State University, Blacksburg, VA, in partial fulfillment of the requirements for the degree of Master of Science in Civil Engineering.

Nayak, G.C. and Zienkiewicz, O.C. (1972). "A convenient form of invariants and its application in plasticity," *Proceedings*, ASCE, No. ST4, 98, 949-954.

Prevost, J.H. (1978). "Plasticity theory for stress-strain behavior," *J. Eng. Mech. Div.*, ASCE, 104(8), 1177-1194.

Roscoe, K.H. and Burland, J.B. (1968). "On the generalized stress-strain behavior of wet clay," *Engineering Plasticity*, J. Heyman and F. Leckie, Editors, Cambridge University Press, Cambridge, England, 535-609.

Roscoe, K.H., Schofield, A., and Wroth, C.P. (1958). "On the yielding of soils," *Geotechnique*, (8), 22-53.

Sandler, I.S., DiMaggio, F.L., and Baladi, G.Y. (1976). "Generalized cap model for geological materials," *J. of the Geotech. Engrg. Div.*, ASCE, 102(7), 683-699.

Sandler, I.S., and Rubin, K.S. (1979). "An algorithm and a modular subroutine for the cpa model," *Int. J. Numer. Anal. Meth. in Geomech.*, 3, 173-186.

Schofield, A.N., and Wroth, C.P. (1968). *Critical State Soil Mechanics.* McGraw-Hill, Inc., London, Eng.

Scott, R.F. (1983). "Plasticity and constitutive relations in soil mechanics," *J. of Geotech. Engrg. Div.*, ASCE, 111(5), 559-605.

Shield, R. T. (1953). "Mixed boundry value problems in soils mechanics," *J. of Mech. and Physics of Solids*, 11, 61-75.

Shield, R. T. (1953). "Mixed boundry value problems in soils mechanics," *J. of Mech. and Physics of Solids*, 11, 61-75.

Simo, J.C., Ju, J., Pister, K.S., and Taylor, R.L. (1988). "Assessment of cap model: consistient return algorithms and rate-dependent extension," *J. Engrg. Mech.*, ASCE, 114(2), 191-218.

Sture, S., Desai, C.S., and Janardhanam, R. (1979). "Development of a constitutive law for an artificial soil," *Proceedings*, Third International Conferenceon Numerical Methods in Geomechanics, Aachen, 309-317.

Taylor, D.W. (1948). *Fundamentals of Soils Mechanics*, John Wiley and Sons, Inc., New York, NY.

Tresca, H. (1872). "Mémoire sur le poinconnage des métaux," Memoires des Savants Etrangers, 20, 617-838.

Truesdell, C. (1955). "Hypoelasticity," *J. Ration. Mech. Anal.*, 4, 83-133.

Yanada, S.E., and Abon-Sayed, A.S. (1979). "Cap model guided by energy concept," *J. of the Geotech. Engrg. Div.*, ASCE, 105(2), 183-200.

Zaman, M.M., Desai, C.S., and Farugue, M.O. (1985). "An algorithm for deteriming parameters for the cap model from raw test data," *Proceedings*, 4th Int. Conf. Numer. Meth. Geomech., Edmonton, Canada, 275-285.

# APPENDICES

# APPENDIX A

## Sesser Soil Properties

| Property | Value |
|---|---|
| USCS Classification | CL |
| Specific Gravity | 2.56 |
| LL | 42 |
| PL | 21 |

Index properties of Sesser soil (Kane et al., 1988)

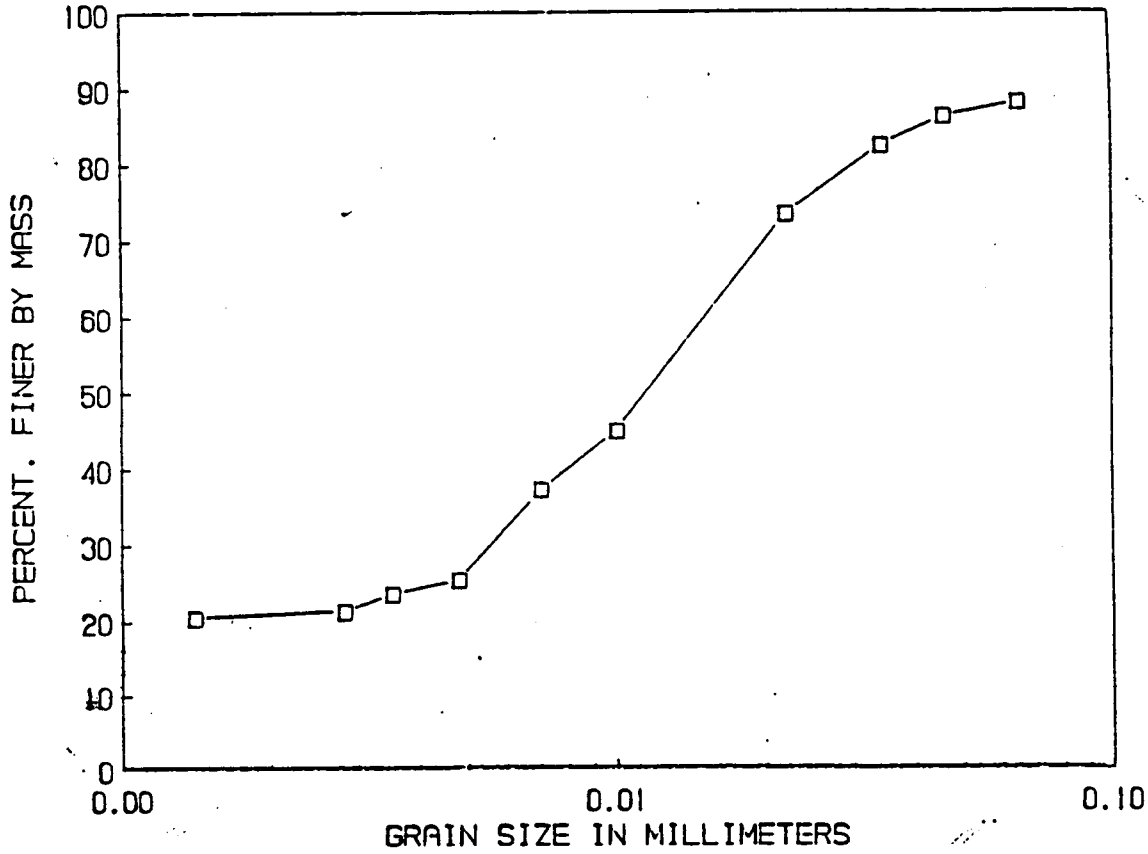


Grain size distribution curve for Sesser soil (Kane, et al., 1988)

# APPENDIX B

## Sample Preparation Data

**Sample Information**

| | |
|---|---|
| Number | CTC-10-CD-TH-SS-1 |
| Height | 4.075 in. |
| Height (after consolidation) | 4.061 in. |
| Diameter | 1.995 in. |
| Weight (before testing) | 402.3 g. |
| Weight (after testing) | 401.8 g. |
| Initial Unit Weight | 120.3 pcf |
| Volume (after consolidation) | 12.413 cu. in. |
| Initial Moisture Content | 26.0 % |
| Final Moisture Content (middle) | 26.3 % |
| Final Moisture Content (bottom) | 25.2 % |

**Sample Information**

| | |
|---|---|
| Number | CTC-20-CD-TH-SS-1 |
| Height | 4.100 in. |
| Height (after consolidation) | 4.069 in. |
| Diameter | 1.990 in. |
| Weight (before testing) | 404.3 g. |
| Weight (after testing) | 403.6 g. |
| Initial Unit Weight | 120.8 pcf |
| Volume (after consolidation) | 12.041 cu. in. |
| Initial Moisture Content | 26.8 % |
| Final Moisture Content (middle) | 26.7 % |
| Final Moisture Content (bottom) | 26.1 % |

**Sample Information**

| | |
|---|---|
| Number | CTC-35-CD-TH-SS-1 |
| Height | 4.080 in. |
| Height (after consolidation) | 4.026 in. |
| Diameter | 2.000 in. |
| Weight (before testing) | 402.3 g. |
| Weight (after testing) | -------- |
| Initial Unit Weight | 119.6 pcf |
| Volume (after consolidation) | 11.784 cu. in. |
| Initial Moisture Content | 24.9 % |
| Final Moisture Content (middle) | 25.8 % |
| Final Moisture Content (bottom) | 25.3 % |

**Sample Information**

| | |
|---|---|
| Number | TC-10-CD-TH-SS-1 |
| Height | 4.100 in. |
| Height (after consolidation) | 4.086 in. |
| Diameter | 1.965 in. |
| Weight (before testing) | 399.2 g. |
| Weight (after testing) | 401.7 g. |
| Initial Unit Weight | 122.3 pcf |
| Volume (after consolidation) | 12.108 cu. in. |
| Initial Moisture Content | 26.1 % |
| Final Moisture Content (middle) | 27.2 % |
| Final Moisture Content (bottom) | 26.9 % |

**Sample Information**

| | |
|---|---|
| Number | RTC-15-CD-TH-SS-1 |
| Height | 4.160 in. |
| Height (after consolidation) | 4.137 in. |
| Diameter | 1.980 in. |
| Weight (before testing) | 406.9 g. |
| Weight (after testing) | 409.8 g. |
| Initial Unit Weight | 121.0 pcf |
| Volume (after consolidation) | 12.276 cu. in. |
| Initial Moisture Content | 28.7 % |
| Final Moisture Content (middle) | 28.1 % |
| Final Moisture Content (bottom) | 26.2 % |

**Sample Information**

| | |
|---|---|
| Number | RTC-30-CD-TH-SS-1 |
| Height | 4.079 in. |
| Height (after consolidation) | 4.035 in. |
| Diameter | 1.990 in. |
| Weight (before testing) | 394.2 g. |
| Weight (after testing) | 392.7 g. |
| Initial Unit Weight | 118.4 pcf |
| Volume (after consolidation) | 11.800 cu. in. |
| Initial Moisture Content | 27.6 % |
| Final Moisture Content (middle) | 28.1 % |
| Final Moisture Content (bottom) | 27.8 % |

**Sample Information**

| | |
|---|---|
| Number | CTC-20-CD (LUR)-TH-SS-1 |
| Height | 4.092 in. |
| Height (after consolidation) | 4.061 in. |
| Diameter | 1.985 in. |
| Weight (before testing) | 407.3 g. |
| Weight (after testing) | -------- |
| Initial Unit Weight | 122.5 pcf |
| Volume (after consolidation) | 11.952 cu. in. |
| Initial Moisture Content | 22.8 % |
| Final Moisture Content (middle) | 23.0 % |
| Final Moisture Content (bottom) | 23.8 % |

**Sample Information**

| | |
|---|---|
| Number | CTC-20-CD (LUR)-TH-SS-2 |
| Height | 4.125 in. |
| Height (after consolidation) | 4.094 in. |
| Diameter | 2.050 in. |
| Weight (before testing) | 412.6 g. |
| Weight (after testing) | 409.6 g. |
| Initial Unit Weight | 115.4 pcf |
| Volume (after consolidation) | 12.904 cu. in. |
| Initial Moisture Content | 28.0 % |
| Final Moisture Content (middle) | 25.2 % |
| Final Moisture Content (bottom) | 22.0 % |

**Sample Information**

| | |
|---|---|
| Number | HC-64-UD-TH-SS-1 |
| Height | 4.100 in. |
| Height (after consolidation) | N / A |
| Diameter | 1.995 in. |
| Weight (before testing) | 406.9 g. |
| Weight (after testing) | 404.1 g. |
| Initial Unit Weight | 121.0 pcf |
| Volume (after consolidation) | N / A |
| Initial Moisture Content | 26.7 % |
| Final Moisture Content (middle) | 25.2 % |
| Final Moisture Content (bottom) | 26.1 % |

**Sample Information**

| | |
|---|---|
| Number | HC-64-UD-TH-SS-2 |
| Height | 4.085 in. |
| Height (after consolidation) | N / A |
| Diameter | 1.980 in. |
| Weight (before testing) | 402.85 g. |
| Weight (after testing) | 400.8 g. |
| Initial Unit Weight | 122.0 pcf |
| Volume (after consolidation) | N / A |
| Initial Moisture Content | 25.0 % |
| Final Moisture Content (middle) | 25.6 % |
| Final Moisture Content (bottom) | 25.2 % |

# APPENDIX C

## Additional Data Plots

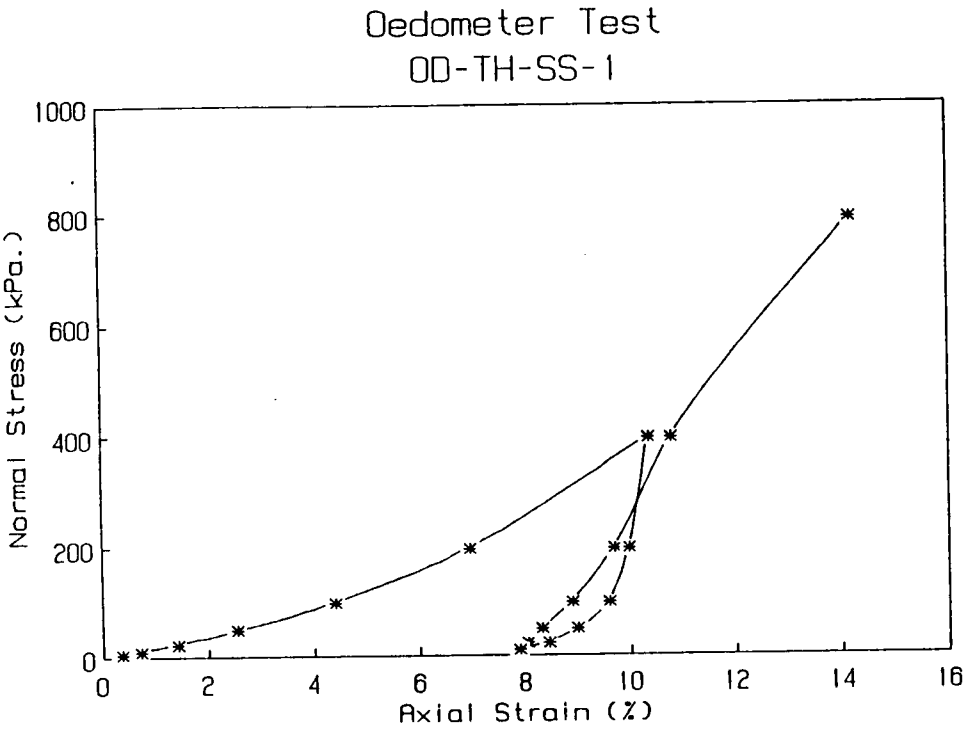
Oedometer Test
OD-TH-SS-1
Normal Stress (kPa.)
1000
800
600
400
200
0
0
2
4
6
8
10
12
14
16
Axial Strain (%)

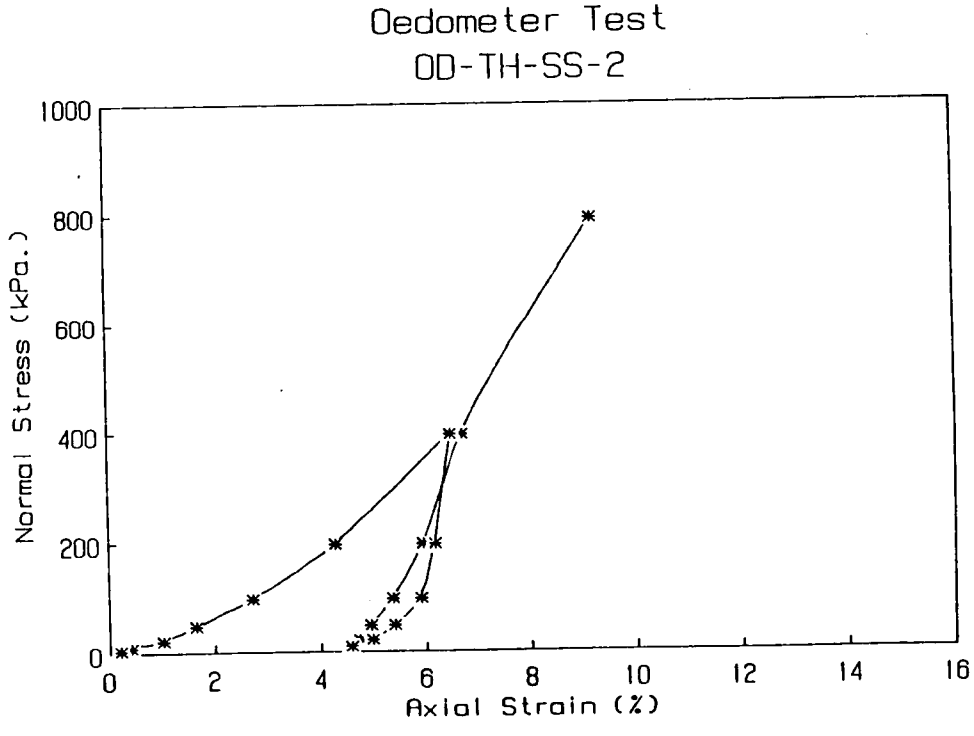
Oedometer Test
OD-TH-SS-2
Normal Stress (kPa.)
1000
800
600
400
200
0
0
2
4
6
8
10
12
14
16
Axial Strain (%)

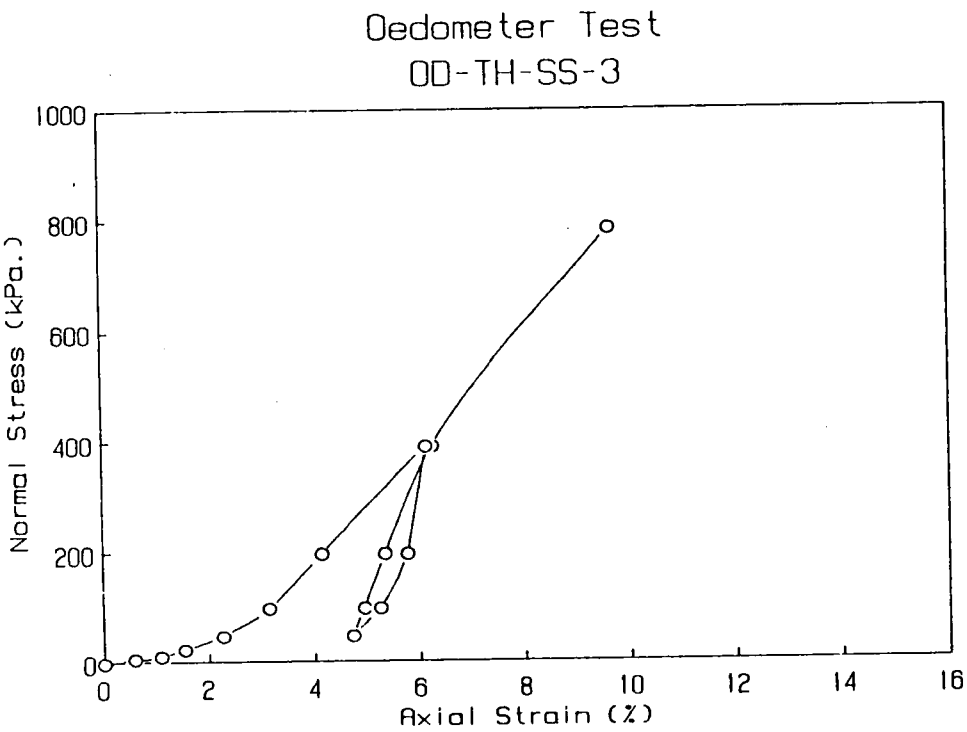
Oedometer Test
OD-TH-SS-3
Normal Stress (kPa.)
1000
800
600
400
200
0
0
2
4
6
8
10
12
14
16
Axial Strain (%)

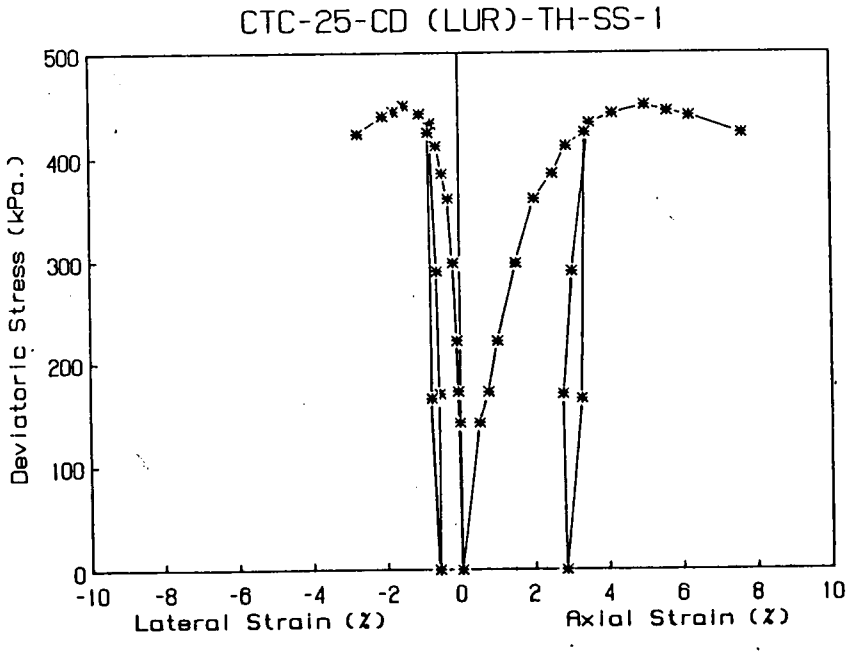
CTC-25-CD (LUR)-TH-SS-1
Deviatoric Stress (kPa.)
500
400
300
200
100
0
-10
-8
-6
-4
-2
0
2
4
6
8
10
Lateral Strain (%)
Axial Strain (%)

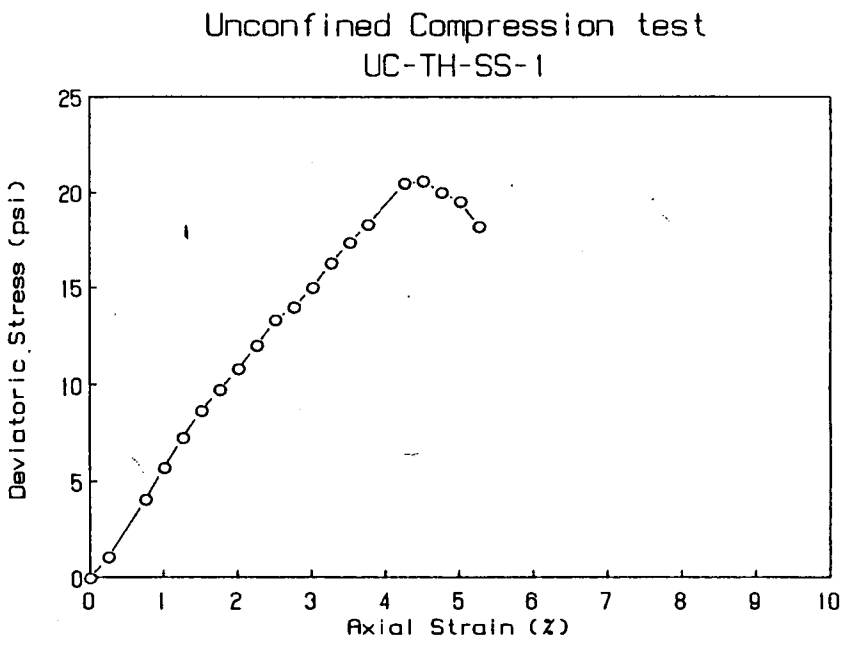
Unconfined Compression test
UC-TH-SS-1
Deviatoric Stress (psi)
Axial Strain (%)
0
5
10
15
20
25
0
1
2
3
4
5
6
7
8
9
10

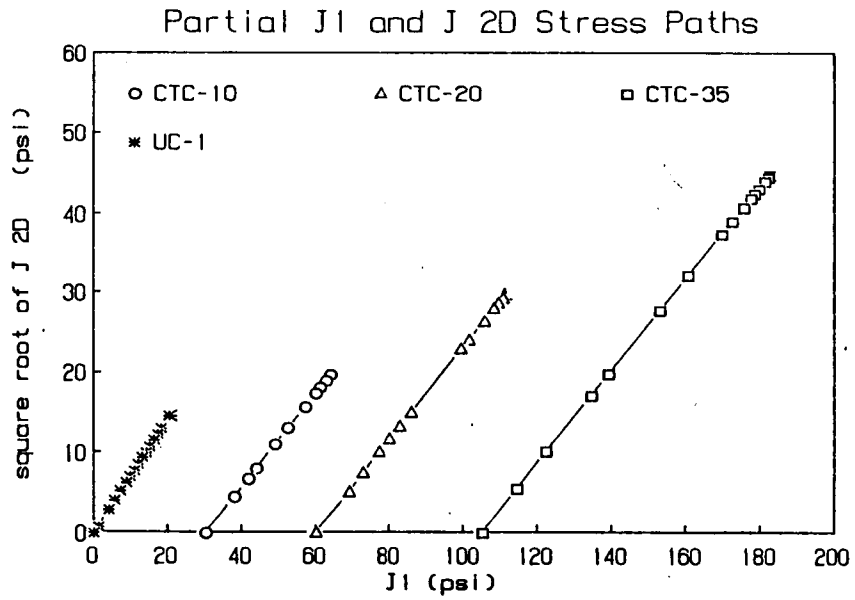
Partial J1 and J 2D Stress Paths
o CTC-10
Δ CTC-20
□ CTC-35
* UC-1
square root of J 2D (psi)
J1 (psi)
0
10
20
30
40
50
60
0
20
40
60
80
100
120
140
160
180
200

# APPENDIX D

## REDUC Computer Program

```
10 DIM LLOAD(100) ,AAXDIS(100) ,VVOLCH(100) ,CELLEXP(100)
20 DIM PVOLCH(100) ,VOLCH(100) ,EPSILON1(100) ,SIGMA1(100) ,TVOLSTR(100)
30 DIM INCTVSTR(100) ,J1(100) ,J2DSR(100) ,DEVSTRS(100), SIGMA3(100)
40 DIM EPSILON3(100) ,DELI1P(100) ,DELI2DP(100) , TOTALI1P(100)
50 DIM DELI1E(100) ,DELI2DE(100) ,TOTALI1E(100) ,VECTOR(100)
60 DIM ELAS1(100) ,ELAS3(100) ,DELI2DE4(100) ,DELI2DE6(100)
70 DIM PLAS1(100) ,PLAS3(100) ,DELI2DP4(100) ,DELI2DP6(100)
80 DIM OCTSTRES(100) ,OCTSTRAN(100) ,CCONF(100)
90 REM
100 REM
110 REM   PRROGRAM TO REDUCE THE DATA FROM A TRIAXIAL SOIL TEST.  THE
120 REM   RESULTS WILL BE GIVEN AS DATA POINTS IN THE FOLLOWING FORMAT:
130 REM     FOR: 1. CTC
140 REM          2. RTC
150 REM          3. TC
160 REM               - Sigma 1,2,3 - Epsilon 1,2,3   (stress - strain)
170 REM               - J1-(sq. root of) J2D Space
180 REM               - Total Volume Change
190 REM               - Incremental & Total Volumetric Strain
200 REM               - Incremental, Deviatoric, & Total Plastic Strain
210 REM               - Incremental, Deviatoric, & Total Elastic Strain
220 REM
230 REM     FOR: 4. HC
240 REM
250 REM               - Octahedral Normal Stress & Strain
260 REM               - Epsilon 1,2,3  (strain)
270 REM               - Total Volume Change
280 REM               - Incremental & Total Volumetric Strain
290 REM               - Incremental, Deviatoric, & Total Plastic Strain
300 REM               - Incremental, Deviatoric, & Total Elastic Strain
310 REM
320 REM   PROGRAM WRITTEN BY:   JAMES D. HOSKINS III      24 JANUARY 1989
330 REM                         UNIVERSITY OF TENNESSEE - KNOXVILLE
340 REM
350 FOR I=1 TO 40
360 PRINT
370 NEXT I
380 PRINT "This program reduces the data from a triaxial soil test.  The"
390 PRINT "results will be given as data points in the following format:"
400 PRINT
410 PRINT "   For: CTC, RTC, & TC type of tests
420 PRINT "           - Sigma 1,2,3 - Epsilon 1,2,3   (stress - strain)"
430 PRINT "           - J1-(sq. root of) J2D Space"
440 PRINT "           - Total Volume Change"
450 PRINT "           - Incremental & Total Volumetric Strain"
460 PRINT "           - Incremental, Deviatoric, & Total Plastic Strain"
470 PRINT "           - Incremental, Deviatoric, & Total Elastic Strain"
480 PRINT
```

```
490 PRINT "   For: HC type of test"
500 PRINT "           - Octahedral Normal Stress & Strain"
510 PRINT "           - Epsilon 1,2,3  (strain)"
520 PRINT "           - Total Volume Change"
530 PRINT "           - Incremental & Total Volumetric Strain"
540 PRINT "           - Incremental, Deviatoric, & Total Plastic Strain"
550 PRINT "           - Incremental, Deviatoric, & Total Elastic Strain"
560 FOR I=1 TO 4
570 PRINT
580 NEXT I
590 INPUT "Project Name : ";NAM$
600 PRINT
610 INPUT "Test Date / Todays Date : ";DAT$
620 PRINT
630 INPUT "Test Number : ";TESTNUM$
640 PRINT
650 INPUT "Data Entry by : ";DATNAM$
660 PRINT
670 PRINT
680 PRINT "Enter the Height of the sample before consolidation (inches)"
690 INPUT HIGH
700 PRINT
710 PRINT "Enter the Height of the sample after consolidation (inches) "
720 PRINT "     (Enter 0 or skip if HC test)"
730 INPUT HIGHAF
740 PRINT
750 PRINT "Enter the average Diameter of the sample (inches)"
760 INPUT DIA
770 PRINT
780 VOLUME=(HIGH*(((DIA/2)^2)*3.14159))
790 PRINT "Enter the volume of the sample after consolidation (cubic inches)"
800 PRINT "     (Enter 0 or skip if HC test)"
810 INPUT CONSLVOL
820 PRINT
830 PRINT "Enter the initial water content of the sample (%)"
840 INPUT INWC
850 PRINT
860 PRINT "Enter the final water content of the sample, at the failure plane (%)
"
870 INPUT FINWCFP
880 PRINT
890 PRINT "Enter the final water content of the sample, at the bottom (%)"
900 INPUT FINWCBT
910 PRINT
920 PRINT "Enter the weight of the sample (grams)"
930 INPUT GWT
940 LBWT=(GWT*.0022046)
950 VOLCF=(((((DIA/2)^2)*3.14159)*HIGH)/1728)
```

```
960 UNIT=LBWT/VOLCF
970 PRINT
980 PRINT "Enter the Conversion Factor for the Load (volts x Factor = lbs.)"
990 INPUT CFLOAD
1000 PRINT
1010 PRINT "Enter the Conversion Factor for the Axial Displacement"
1020 PRINT "(volts x Factor = inches)"
1030 INPUT CFDISPL
1040 PRINT
1050 PRINT "Enter the Conversion Factor for the Volume Change"
1060 PRINT "(volts x Factor = cubic inches)"
1070 INPUT CFVOL
1080 PRINT
1090 PRINT "Enter the diameter of the loading piston (0.5 in. -DEFAULT)"
1100 INPUT PDIA
1110 IF PDIA=0 GOTO 1120 ELSE 1130
1120 PDIA=.5
1130 PRINT
1140 PRINT "Enter the type of test run (1,2,3, or 4)"
1150 PRINT
1160 PRINT "     1. Conventional Triaxial Compression (CTC)"
1170 PRINT "     2. Triaxial Compression (TC)"
1180 PRINT "     3. Reduced Triaxial Compression (RTC)"
1190 PRINT "     4. Hydrostatic Compression (HC)"
1200 INPUT TYPE
1210 IF TYPE=1 THEN TYPE$="Conventional Triaxial Compression"
1220 IF TYPE=2 THEN TYPE$="Triaxial Compression"
1230 IF TYPE=3 THEN TYPE$="Reduced Triaxial Compression"
1240 IF TYPE=4 THEN TYPE$="Hydrostatic Compression"
1250 PRINT
1260 PRINT "Was this a Drained test (Y/N) ?"
1270 INPUT DRAIN$
1280 IF DRAIN$="Y" THEN DUD$="Drained"
1290 IF DRAIN$="y" THEN DUD$="Drained"
1300 IF DRAIN$="N" THEN DUD$="Undrained"
1310 IF DRAIN$="n" THEN DUD$="Undrained"
1320 IF TYPE=1 GOTO 1330 ELSE 1850
1330 REM
1340 REM  ******  CONVENTIONAL TRIAXIAL COMPRESSION SECTION  *******
1350 REM
1360 PRINT
1370 PRINT "Enter the Confining Stress (psi)"
1380 INPUT CONF
1390 PRINT
1400 PRINT "Enter the number of Data Points to be entered"
1410 INPUT NUM
1420 PRINT
1430 PRINT
```

```
1440 PRINT "Enter the digitized voltage readout points for the following :"
1450 PRINT "   Load, Axial Displacement, Volume Change"
1460 PRINT
1470 REM      EPSILON1 = TOTAL AXAIL STRAIN, EPSILON 1, e1 (plas. & elas.)
1480 REM      EPSILON3 = TOTAL LATERAL STRAIN, (epsilon 3 = epsilon 2), e3
1490 REM      TVOLSTR  = TOTAL VOLUMETRIC STRAIN, ev
1500 REM      AREA     = SURFACE AREA OF SAMPLE END, CONTACT AREA
1510 REM      CORAREA  = CORRECTED AREA ONCE AXIAL DEFORMATION BEGINS
1520 REM      DEVSTRS  = DEVIATORIC STRESS, SIGMA 1 - SIGMA 3
1530 REM      INCTVSTR = INCREMENTAL TOTAL VOLUMETRIC STRAIN
1540 REM      J1       = FIRST INVARIENT OF STRESS
1550 REM      J2DSR    = SQUARE ROOT OF SECOND INVARINET OF DEVIATORIC STRESS
1560 REM      AXDIS    = AXIAL DISPLACEMENT OF THE SAMPLE IN INCHES
1570 REM      PVOLCH   = VOLUME OF THE PISTON ENTERING THE CELL DURING TESTING
1580 REM      DELTAR   = THE CHANGE IN THE SAMPLE RADIUS, USED TO CALCULATE
1590 REM                    THE INCREMENTAL CROSS SECTIONAL AREA OF THE SAMPLE
1600 REM      SIGMA1   = AXAIL STRESS + CELL PRESSURE (sigma 1)
1610 REM      SIGMA3   = CELL PRESSURE (sigma 3 = sigma 2), LATERAL STRESS
1620 REM
1630 FOR I=1 TO NUM
1640 RR=RR+1
1650 T=RR-1
1660 PRINT RR
1670 INPUT LLOAD(I), AAXDIS(I), VVOLCH(I)
1680 LOAD1=LLOAD(I)*CFLOAD
1690 AXDIS=AAXDIS(I)*CFDISPL
1700 PVOLCH(I)=AXDIS*((PDIA/2)^2)*3.14159
1710 VOLCH(I)=(((VVOLCH(1)-VVOLCH(I))*CFVOL)+PVOLCH(I))
1720 EPSILON1(I)=(AXDIS/HIGHAF)
1730 TVOLSTR(I)=(VOLCH(I))/CONSLVOL
1740 EPSILON3(I)=((TVOLSTR(I)-EPSILON1(I))/2)
1750 DELTAR=(((TVOLSTR(I)-EPSILON1(I))*(DIA/2))/2)
1760 CORAREA=((((DIA/2)-DELTAR)^2)*3.14159)
1770 DEVSTRS(I)=LOAD1/CORAREA
1780 SIGMA3(I)=CONF
1790 SIGMA1(I)=DEVSTRS(I)+SIGMA3(I)
1800 INCTVSTR(I)=TVOLSTR(I)-TVOLSTR(T)
1810 J1(I)=(DEVSTRS(I)+CONF)+(2*CONF)
1820 J2DSR(I)=(((DEVSTRS(I))^2)*.33333)^.5
1830 NEXT I
1840 GOTO 2640
1850 IF TYPE=2 GOTO 1910 ELSE 1860
1860 IF TYPE=3 GOTO 1910 ELSE 2290
1870 REM
1880 REM   ********** TRIAXIAL COMPRESSION SECTION **********
1890 REM   ******* REDUCED TRIAXIAL COMPRESSION SECTION *******
1900 REM
1910 PRINT
```

```
1920 PRINT
1930 PRINT "Enter the number of Data Points to be entered"
1940 INPUT NUM
1950 FOR K=1 TO 15
1960 PRINT
1970 NEXT K
1980 PRINT "Enter the digitized voltage readout points for the following :"
1990 PRINT "   Load, Ax. displ., Volume change, Cell Expan. (cubic in.), Conf. S
tress"
2000 PRINT
2010 PRINT "The following sign convention is used in this program"
2020 PRINT "   + (pos.) = decrease in volume"
2030 PRINT "   - (neg.) = increase in volume"
2040 PRINT
2050 PRINT "NOTE: Therefore, enter the cell expan. numbers as positive."
2060 PRINT
2070 FOR I=1 TO NUM
2080 RR=RR+1
2090 T=RR-1
2100 PRINT RR
2110 INPUT LLOAD(I), AAXDIS(I), VVOLCH(I), CELLEXP(I), CCONF(I)
2120 LOAD1=LLOAD(I)*CFLOAD
2130 AXDIS=AAXDIS(I)*CFDISPL
2140 PVOLCH(I)=AXDIS*((PDIA/2)^2)*3.14159
2150 VOLCH(I)=((((VVOLCH(I)-VVOLCH(I))*CFVOL)+CELLEXP(I))+PVOLCH(I))
2160 EPSILON1(I)=(AXDIS/HIGHAF)
2170 TVOLSTR(I)=(VOLCH(I))/CONSLVOL
2180 EPSILON3(I)=((TVOLSTR(I)-EPSILON1(I))/2)
2190 DELTAR=(((TVOLSTR(I)-EPSILON1(I))*(DIA/2))/2)
2200 CORAREA=((((DIA/2)-DELTAR)^2)*3.14159)
2210 DEVSTRS(I)=LOAD1/CORAREA
2220 SIGMA3(I)=CCONF(I)
2230 SIGMA1(I)=DEVSTRS(I)+SIGMA3(I)
2240 INCTVSTR(I)=TVOLSTR(I)-TVOLSTR(T)
2250 J1(I)=(DEVSTRS(I)+CCONF(I))+(2*CCONF(I))
2260 J2DSR(I)=(((DEVSTRS(I))^2)*.33333)^.5
2270 NEXT I
2280 GOTO 2640
2290 REM
2300 REM   ****** HYDROSTATIC COMPRESSION SECTION  *********
2310 REM
2320 PRINT
2330 PRINT
2340 PRINT "Enter the number of steps, loading and unloading and including"
2350 PRINT "the initial confining stress, in which the test was conducted."
2360 INPUT NUM
2370 PRINT
2380 PRINT "Enter the following:  "
```

```
2390 PRINT " Confining stress, Axial Defor., Vol. Change, Cell Expansion (cubic
in.)"
2400 PRINT
2410 PRINT "The following sign convention is used for this program"
2420 PRINT "  + (pos.) = decrease in volume"
2430 PRINT "  - (neg.) = increase in volume"
2440 PRINT
2450 PRINT "NOTE: Therefore, enter the cell expan. numbers as negative."
2460 PRINT
2470 FOR I=1 TO NUM
2480 RR=RR+1
2490 T=RR-1
2500 PRINT RR
2510 INPUT CCONF(I), AAXDIS(I), VVOLCH(I), CELLEXP(I)
2520 AXDIS=AAXDIS(I)*CFDISPL
2530 PVOLCH(I)=AXDIS*((PDIA/2)^2)*3.14159
2540 VOLCH(I)=((((VVOLCH(I)-VVOLCH(I))*CFVOL)+CELLEXP(I))+PVOLCH(I))
2550 TVOLSTR(I)=(VOLCH(I))/VOLUME
2560 INCTVSTR(I)=TVOLSTR(I)-TVOLSTR(T)
2570 OCTSTRES(I)=CCONF(I)
2580 OCTSTRAN(I)=TVOLSTR(I)/3
2590 EPSILON1(I)=AXDIS/HIGH
2600 EPSILON3(I)=(TVOLSTR(I)-EPSILON1(I))/2
2610 J1(I)=CCONF(I)*3
2620 NEXT I
2630 GOTO 4830
2640 REM
2650 REM  ************ SECTION TO CALCULATE *************************
2660 REM  ************ ELASTIC & PLASTIC STRAINS ********************
2670 REM
2680 REM
2690 REM      MODELAS1 = MODULUS OF ELASTICITY IN THE AXAIL DIRECTION AS TAKEN
2700 REM                    FROM THE CTC - UNLOAD/RELOAD TEST
2710 REM      MODELAS3 = MODULUS OF ELASTICITY IN THE LATERAL DIRECTION AS
2720 REM                    TAKEN FROM THE CTC - UNLOAD/RELOAD TEST
2730 REM      ALPHA1   = ARCTAN OF MODELAS1
2740 REM      ALPHA3   = ARCTAN OF MODELAS3
2750 REM      THETA1   = (PI - PI/2) - ALPHA1
2760 REM      THETA3   = (PI - PI/2) - ALPHA3
2770 REM      TOTALI1E = TOTAL ELASTIC STRAIN
2780 REM      DELI1E   = INCREMENTAL TOTAL ELASTIC STRAIN
2790 REM      DELI2DE  = INCREMENTAL DEVIATORIC STRAIN
2800 REM      ELAS1    = ELASTIC STRAIN IN THE EPSILON-1 DIRECTION
2810 REM      ELAS3    = ELASTIC STRAIN IN THE EPSILON-3 DIRECTION
2820 REM      DELI2DE4 = INCREMENTAL ELASTIC STRAIN IN THE EPSILON-1 DIRECTION
2830 REM      DELI2DE6 = INCREMENTAL ELASTIC STRAIN IN THE EPSILON-3 DIRECTION
2840 REM      TOTALI1P = TOTAL PLASTIC STRAIN
2850 REM      DELI1P   = INCREMENTAL TOTAL PLASTIC STRAIN
```

```
2860 REM      DELI2DP  = INCREMENTAL DEVIATORIC STRAIN
2870 REM      PLAS1    = PLASTIC STRAIN IN THE EPSILON-1 DIRECTION
2880 REM      PLAS3    = PLASTIC STRAIN IN THE EPSILON-3 DIRECTION
2890 REM      DELI2DP4 = INCREMENTAL PLASTIC STRAIN IN THE EPSILON-1 DIRECTION
2900 REM      DELI2DP6 = INCREMENTAL PLASTIC STRAIN IN THE EPSILON-3 DIRECTION
2910 REM
2920 REM
2930 PRINT
2940 PRINT
2950 PRINT "Do you want to calculate and printout the incremental, deviatoric,"
2960 PRINT "and total elastic and plastic strains  (Y/N)"
2970 INPUT EPANSW$
2980 IF EPANSW$="Y" GOTO 3020 ELSE 2990
2990 IF EPANSW$="y" GOTO 3020 ELSE 3000
3000 IF EPANSW$="N" GOTO 3420 ELSE 3010
3010 IF EPANSW$="n" GOTO 3420 ELSE 3420
3020 PRINT
3030 PRINT "Enter the unloading modulus in the axial direction (E-1)"
3040 PRINT "and the lateral direction (E-3) in (psi)"
3050 INPUT "E-1   (positive)  "; MODELAS1
3060 INPUT "E-3   (negative)  "; MODELAS3
3070 IF TYPE=4 GOTO 3080 ELSE 3110
3080 FOR I=1 TO NUM
3090 DEVSTRS(I)=OCTSTRES(I)
3100 NEXT I
3110 ALPHA1=ATN(MODELAS1)
3120 ALPHA3=ATN(MODELAS3)
3130 THETA1=(1.570796-ALPHA1)
3140 IF MODELAS3<0 GOTO 3150 ELSE 3170
3150 THETA3=(1.570796+ALPHA3)
3160 GOTO 3180
3170 THETA3=(1.570796-ALPHA3)
3180 FOR I=1 TO NUM
3190 ZZ=ZZ+1
3200 S=ZZ-1
3210 ELAS1(I)=((SIN(THETA1)*DEVSTRS(I))/SIN(ALPHA1))
3220 ELAS3(I)=((SIN(THETA3)*DEVSTRS(I))/SIN(ALPHA3))
3230 IF ABS(ELAS3(I))>ABS(EPSILON3(I)) GOTO 3240 ELSE 3250
3240 ELAS3(I)=EPSILON3(I)
3250 TOTALI1E(I)=(ELAS1(I)+(2*ELAS3(I)))
3260 DELI1E(I)=(TOTALI1E(I)-TOTALI1E(S))
3270 DELI2DE4(I)=ELAS1(I)-ELAS1(S)
3280 DELI2DE6(I)=ELAS3(I)-ELAS3(S)
3290 DELI2DE(I)=(((DELI2DE4(I)-DELI2DE6(I))^2)/3)
3300 TOTALI1P(I)=(TVOLSTR(I)-TOTALI1E(I))
3310 DELI1P(I)=(TOTALI1P(I)-TOTALI1P(S))
3320 PLAS1(I)=EPSILON1(I)-ELAS1(I)
3330 PLAS3(I)=EPSILON3(I)-PLAS3(I)
```

```
3340 DELI2DP4(I)=PLAS1(I)-PLAS1(S)
3350 DELI2DP6(I)=PLAS3(I)-PLAS3(S)
3360 DELI2DP(I)=(((DELI2DP4(I)-DELI2DP6(I))^2)/3)
3370 NEXT I
3380 IF TYPE=4 GOTO 3990 ELSE 3390
3390 REM
3400 REM  ***************** end elastic/plastic strain section ********************
3410 REM
3420 REM
3430 REM ******************* OUTPUT to PRINTER Section ***********************
3440 REM
3450 LPRINT "Project Name                : ";NAM$
3460 LPRINT "Test Date / Todays Date     : ";DAT$
3470 LPRINT "Test Number                 : ";TESTNUM$
3480 LPRINT "Data Entry by               : ";DATNAM$
3490 LPRINT
3500 LPRINT "Test Type : "; TYPE$ " - "; DUD$
3510 LPRINT
3520 LPRINT
3530 LPRINT "Entered Data: "
3540 LPRINT
3550 LPRINT "   - sample height before consoildation (inches)    = ";HIGH
3560 LPRINT "   - sample height after consolidation (inches)     = ";HIGHAF
3570 LPRINT "   - sample diameter (inches)                       = ";DIA
3580 LPRINT "   - sample volume after consolidation (cubic in.)  = ";CONSLVOL
3590 LPRINT "   - sample unit weight (pcf)                       = ";UNIT
3600 LPRINT "   - inital water content (%)                       = ";INWC
3610 LPRINT "   - final water content at the failure plane (%)   = ";FIWCFP
3620 LPRINT "   - final water content at the bottom (%)          = ";FIWCBT
3630 IF TYPE=1 GOTO 3660 ELSE 3640
3640 LPRINT "   - confining stress (psi)                         = CHANGING"
3650 GOTO 3670
3660 LPRINT "   - confining stress (psi)                         = ";CONF
3670 LPRINT
3680 LPRINT
3690 LPRINT "Epsilon-1      Epsilon-2     Sigma-1      Sigma 2       Dev. Stress
"
3700 LPRINT "               Epsilon-3                  Sigma-3      Sigma 1 - Si
gma 3"
3710 LPRINT "  (%)            (%)          (psi)        (psi)           (psi)"
3720 LPRINT "-------------------------------------------------------------------
----"
3730 LPRINT
3740 FOR I=1 TO NUM
3750 LPRINT EPSILON1(I)*100, EPSILON3(I)*100, SIGMA1(I), SIGMA3(I), DEVSTRS(I)
3760 NEXT I
3770 FOR P=1 TO 4
3780 LPRINT
```

```
3790 NEXT P
3800 LPRINT "                                                    Total"
3810 LPRINT "    J1       sq. root J2D    Vol. Change      Vol Strain"
3820 LPRINT "  (psi)         (psi)        (cubic in.)        (%)"
3830 LPRINT "-----------------------------------------------------"
3840 LPRINT
3850 FOR I=1 TO NUM
3860 LPRINT J1(I), J2DSR(I), VOLCH(I), TVOLSTR(I)*100
3870 NEXT I
3880 LPRINT
3890 LPRINT
3900 LPRINT
3910 LPRINT "The following sign convention is used in this program:"
3920 LPRINT "    + (pos.) = decrease in volume"
3930 LPRINT "    - (neg.) = increase in volume"
3940 FOR I=1 TO 10
3950 LPRINT
3960 NEXT I
3970 IF EPANSW$="Y" GOTO 3990 ELSE 3980
3980 IF EPANSW$="y" GOTO 3990 ELSE 4510
3990 REM
4000 REM  ******************** OUTPUT SECTION FOR :  ************************
4010 REM  ****************** ELASTIC & PLASTIC STRAINS  ***********************
4020 REM
4030 LPRINT "Elastic & Plastic Strain Output"
4040 LPRINT "--------------------------------"
4050 LPRINT "--------------------------------"
4060 LPRINT
4070 LPRINT
4080 LPRINT "E-1 = "; MODELAS1 "    (unloading modulus in the axial direction)"
4090 LPRINT "E-2 = "; MODELAS3 "    (unloading modulus in the lateral direction)
"
4100 LPRINT
4110 LPRINT
4120 LPRINT "Total I-1      Delta I-1         Delta I2D"
4130 LPRINT " plastic        plastic           plastic"
4140 LPRINT "   (%)            (%)               (%)"
4150 LPRINT "-----------------------------------------"
4160 LPRINT
4170 FOR I=1 TO NUM
4180 LPRINT TOTALI1P(I)*100, DELI1P(I)*100, DELI2DP(I)*100
4190 NEXT I
4200 LPRINT
4210 LPRINT
4220 LPRINT
4230 LPRINT "Total I-1      Delta I-1         Delta I2D"
4240 LPRINT " elastic        elastic           elastic"
4250 LPRINT "   (%)            (%)               (%)"
4260 LPRINT "-----------------------------------------"
```

```
4270 LPRINT
4280 FOR I=1 TO NUM
4290 LPRINT TOTALI1E(I)*100, DELI1E(I)*100, DELI2DE(I)*100
4300 NEXT I
4310 LPRINT
4320 LPRINT
4330 LPRINT
4340 LPRINT "Vector       Total Vol.   Incremental Total"
4350 LPRINT "Angle         Strain         Vol. Strain"
4360 LPRINT "(deg.)          (%)             (%)"
4370 LPRINT "-----------------------------------------"
4380 LPRINT
4390 FOR I=1 TO NUM
4400 VEC1=((DELI2DP(I)^.5)*2)
4410 VEC2=(DELI1P(I)/3)
4420 VECTOR(I)=ATN(VEC1/VEC2)
4430 LPRINT VECTOR(I)*57.29578, TVOLSTR(I)*100, INCTVSTR(I)*100
4440 NEXT I
4450 FOR I=1 TO 5
4460 LPRINT
4470 NEXT I
4480 REM
4490 REM  ********** End of Elastic/Plastic Output Section ************
4500 REM
4510 REM
4520 LPRINT "********************************* INPUT DATA ************************
*********"
4530 LPRINT
4540 LPRINT
4550 LPRINT "Load Conversion Factor              = "; CFLOAD
4560 LPRINT "Axial Displacement Conversion Factor = "; CFDISPL
4570 LPRINT "Volume Change Conversion Factor      = "; CFVOL
4580 LPRINT
4590 LPRINT
4600 IF TYPE=1 GOTO 4610 ELSE 4690
4610 LPRINT "Load      Axial Displ.    Vol. Change"
4620 LPRINT "       (all units in m. Volts)"
4630 LPRINT "-----------------------------------"
4640 LPRINT
4650 FOR I=1 TO NUM
4660 LPRINT LLOAD(I), AAXDIS(I), VVOLCH(I)
4670 NEXT I
4680 GOTO 4760
4690 LPRINT "Load     Conf. Stress    Axial Displ.    Vol. Change   Cell Expansi
on"
4700 LPRINT " mV.        (psi)           mV.             mV.         (cubic in.
)"
4710 LPRINT "-----------------------------------------------------------------
--"
```

```
4720 LPRINT
4730 FOR I=1 TO NUM
4740 LPRINT LLOAD(I), CCONF(I), AAXDIS(I), VVOLCH(I), CELLEXP(I)
4750 NEXT I
4760 LPRINT
4770 LPRINT
4780 LPRINT "############################ END OF INPUT DATA SECTION ###############
############"
4790 IF TYPE=4 GOTO 4800 ELSE 5530
4800 IF EPANSW$="Y" GOTO 5530 ELSE 4810
4810 IF EPANSW$="y" GOTO 5530 ELSE 4820
4820 RETURN
4830 REM
4840 REM  ########## OUTPUT SECTION FOR HYDROSTATIC COMPRESSION ###########
4850 REM
4860 LPRINT "Project Name                : ";NAM$
4870 LPRINT "Test Date / Todays Date     : ";DAT$
4880 LPRINT "Test Number                 : ";TESTNUM$
4890 LPRINT "Data Entry by               : ";DATNAM$
4900 LPRINT
4910 LPRINT "Test Type : "; TYPE$ " - "; DUD$
4920 LPRINT
4930 LPRINT
4940 LPRINT "Entered Data: "
4950 LPRINT
4960 LPRINT "   - sample height  (inches)                    = ";HIGH
4970 LPRINT "   - sample diameter (inches)                   = ";DIA
4980 LPRINT "   - initial volume (cubic in.)                 = ";VOLUME
4990 LPRINT "   - sample unit weight (pcf)                   = ";UNIT
5000 LPRINT "   - inital water content (%)                   = ";INWC
5010 LPRINT "   - final water content at the middle (%)      = ";FIWCFP
5020 LPRINT "   - final water content at the bottom (%)      = ";FIWCBT
5030 LPRINT
5040 LPRINT
5050 LPRINT
5060 LPRINT "Octahedral     Octahedral    Vol. Change"
5070 LPRINT "Nor. Stress    Nor. Strain"
5080 LPRINT "  (psi)           (%)        (cubic in.)"
5090 LPRINT "----------------------------------------"
5100 LPRINT
5110 FOR I=1 TO NUM
5120 LPRINT OCTSTRES(I), OCTSTRAN(I)*100, VOLCH(I)
5130 NEXT I
5140 LPRINT
5150 LPRINT
5160 LPRINT "  Total        Incremental Total"
5170 LPRINT "Vol. Strain      Vol. Strain"
5180 LPRINT "   (%)              (%)"
```

```
5190 LPRINT "------------------------------"
5200 LPRINT
5210 FOR I=1 TO NUM
5220 LPRINT TVOLSTR(I)*100, INCTVSTR(I)*100
5230 NEXT I
5240 LPRINT
5250 LPRINT
5260 LPRINT "Epsilon 1     Epsilon 2"
5270 LPRINT "              Epsilon 3"
5280 LPRINT "  (%)           (%)"
5290 LPRINT "----------------------"
5300 LPRINT
5310 FOR I=1 TO NUM
5320 LPRINT EPSILON1(I)*100, EPSILON3(I)*100
5330 NEXT I
5340 LPRINT
5350 LPRINT
5360 PRINT
5370 PRINT
5380 PRINT "Do you want to calculate and printout the total, incremental,"
5390 PRINT "and deviatoric elastic and plastic strains  (Y/N)"
5400 INPUT EPANSW$
5410 IF EPANSW$="Y" GOTO 3020 ELSE 5420
5420 IF EPANSW$="y" GOTO 3020 ELSE 5430
5430 IF EPANSW$="N" GOTO 5450 ELSE 5440
5440 IF EPANSW$="n" GOTO 5450 ELSE 5450
5450 LPRINT
5460 LPRINT "The following sign convention is used in this program:"
5470 LPRINT "    + (pos.) = decrease in volume"
5480 LPRINT "    - (neg.) = increase in volume"
5490 LPRINT
5500 LPRINT
5510 LPRINT
5520 GOSUB 4510
5530 LPRINT
5540 LPRINT
5550 PRINT
5560 PRINT
5570 PRINT "END"
5580 END
```

# APPENDIX E

## Equipment Usage Procedure

## Sampling & Equipment Usage Procedure

I. Sample Preparation Procedure

A. Undisturbed Samples from thin wall tubes

1. Thin wall sample tubes should be smoothed with steel wool and then well lubricated.

2. The top layer of soil (approximately 3 to 5 inches) should be stripped off with a flat blade shovel.

3. The tubes should be pushed slowly into the soil and NOT pounded. A scissors jack or hydraulic jack are good devices to drive the tubes into the soil.

4. Once the tube is filled with soil, the surrounding soil is excavated and the tube removed.

5. The tube is then placed in a plastic bag, sealed, placed in another plastic bag and sealed again. The sample is then placed in PVC sample tubes (if available) and the samples are identified by placing a piece of numbered paper in the PVC tube, numbering the plastic bags, and recording the number of the PVC tube. The samples are transported back to the laboratory to be tested or stored in the moisture room.

6. If the samples are not going to be used immediately, (within a month) they should be extruded, sealed, and stored in the moisture room until used.

7. When a sample is to be tested, it is removed from the moisture room and taken out of the PVC tube and plastic bags.

8. Using a piston type of extruding device, the sample is extruded by placing a metal disc, usually 1.0 inches thick and just a hair smaller in diameter than the inside diameter of the sample tube, placed at the end of the sample tube. The other end of the sample tube is placed in the tube holder (the tube holder is a piece of metal with a hole cut in it and another hole counter sunk so that the end of the tube will fit in the hole but cannot be pushed through.

9. The piston is then allowed to advance forward and push the disc through the tube, pushing out the soil sample.

10. The sample is then trimmed, measured, and weighed. The trimmings are quickly placed in a pre-weighed container, weighed, and placed in the oven in order to get an initial moisture content.

11. A rubber membrane is carefully placed over the sample. This is accomplished easiest by turning the membrane so that half of the membrane is inside its self. Then the folded end is placed over one end of the sample and the membrane rolled over the remaining portion of the sample.

B. Remolded Samples

1. With the soil in bulk form, it must be crushed by use of mortar and pedestal.

2. An "as is" moisture content is taken for the soil. Once this moisture content is determined, the soil is mixed with an appropriate amount of water to achieve some predetermined moisture content.

3. This soil is then double bagged, sealed, and placed in the moisture room to allow the water to distribute evenly throughout the sample. A small portion of the sample is saved in order to check the moisture content.

4. Before removing the soil from the moisture room, the remolding equipment must be prepared. This preparation entails placing a pre-weighed rubber membrane in the remolding mold. The membrane is held in place by hose clamps. The mold and membrane is then placed in the mold stand and fastened down. It is usually best to lubricate the metal disc at the bottom of the mold stand so that soil does not stick to it.

5. By trial and error or volume-unit weight relationship, a certain amount of soil is weighed out and and divided into four equal portions and each placed in four plastic bags. Each portion will become one layer or the remolded sample, therefore, enough soil must be present to create four layers thus filling the mold.

6. The mold and plastic bags with the soil are carried to the kneading compacting device. Again by trial and error, the first layer of soil is placed in the mold and compacted a certain amount of times (14 to 20) at a certain foot pressure. Once each layer is compacted in the mold, the top of that layer is scuffed to allow better cohesion with the next layer. The final layer is usually compacted with twice the blows and the earlier three layers.

7. The remolded sample is then carefully removed from the mold, the membrane pulled back and the sample trimmed. The sample is then weighed.

II. Volume Change Device Operation

1. The directions of filling the volume change device should initially be followed when starting a new test series in which the volume change device has been sitting for over 2 months. Always use deaired water when filling the device.

2. Once the volume change device is filled and connected to the wall, it should be calibrated. The calibration of the volume change device should be in accordance with guidelines described by Lade (1988). The calculations to determine volume change resolution can be found at the end of this appendix. This calibration usually involves hooking the line from the right port to the pressure panel. A pipette on the pressure panel should be filled slowly with deaired water. The pipette, when filling should be VENTED or under very small pressure, and the line control valve OFF. Turn the annulus\pipette valve to OFF. The other line, from the left port, should be connect to the bottom of a graduated pipette of at least 50 ml.

3. In the volume change device is a inner piston. If the piston is at the bottom of the volume change device, pull both knobs out all the way, turn the flow valve (yellow handled knob) to the vertical position, and turn the line control valve, very slowly, from OFF to ON. This will allow water to flow through the volume change device and raise the piston. When the piston reaches about the half way point, turn the line control valve from ON to OFF, turn the flow valve to the horizontal position, and push both knobs in to the midway position. Turn the line control valve from OFF back to ON to allow water to flow through the lines and clear them of any trapped air. This will also allow the pipette to be filled with water. NOTE: If the piston is at the top of the device it should still be moved to the middle. This is accomplished by following the same procedure as above except initially switch the line connections. That is, connect the line from the left port to the pressure panel and connect the line from the right port to the pipette.

4. Now the volume change device is ready for calibration. With the line control valve in the OFF position and the WATER control valve in the OFF position, turn the annulus\pipette valve to PIPETTE. Move the pressure control valve from VENT to PRESSURE and turn the pressure knob clockwise until about 5.0 psi is reached. Empty the standing pipette (not the one on the pressure panel) so that only about 10.0 ml. of water is in it. Connect the digital read out and the 3-pen plotter. Pull both knobs on the volume change device out all the way and move the flow control valve to the vertical position.

5. Slowly move the line control valve from the OFF position to the ON position. One should see the water level in the pipette on the pressure panel drop slowly and the water level in the standing pipette rise as the water flows through the volume change device. One will also see the inner piston rising in the chamber. The numbers on the digital readout should also change along with the movement of one of the pens of the 2-pen plotter. The SPAN screw in the digital readout can be turned to increase or decrease the gain setting of the meter. It is best to have the resolution of the volume change device between 40 to 60 mV. per cc (cubic centimeter).

6. Once a gain setting is determined, press the CAL. button on the digital readout to get a calibration number. This number should be recorded and checked before each triaxial test is run. It should be noted that all of the calibration numbers should be checked for each channel before each triaxial test.

III. Pressure Panel

NOTE: It should be noted that the pressure panel is explained in some detail in the B-K manual that came with the pressure panel. The following proceedure is only helpful tips that the author has found through trial and error workings of the panel.

A. Deaired Water Setup

1. When filling the 5 gallon bottle with tap water, make sure that the deaired water controls are turned to VENT and FILL.

2. Watch the water level rise in the bottle, and turn the water off when the level reaches a point about 6 inches below the mouth (opening) of the bottle. If the bottle is filled higher than this point, there is a chance that the water will be sucked up into the vacuum lines.

3. The deaired water controls are then turned to VACUUM and OFF. The pump is turned on and should reach 25.0 inches of Mercury.

4. The vacuum is left on for about a 24 to 36 hour period. One should periodically tap the sides of the bottle to release air bubbles. It is usually a good idea to let a seperate fan blow on the pump the entire time it is turned on. This is due to the fact that the pump will become very hot over such a long time span.

5. When the deairing period is over, the deaired control valve is switched from VACUUM to PRESSUE. This pressurizes the bottle.

B. Pressure Panel Controls

1. Again, the B-K manual that came with the pressure panel should be read thoroughly. This text should not be used as a complete proceedure guide to the operation of the pressure panel.

2. When filling the triaxial chamber with deaired water, all the control valves should be at the OFF position. The fill line is then connected to the bottom fitting on the chamber and the air release valve at the top of the chamber opened. The line control valves are then turned to WATER and ON. This will allow water to flow from the deaired water bottle into the chamber.

3. The water is allowed to fill the chamber until it reaches ALMOST to top of the chamber. At this point the line control valve is turned to OFF and the ANNULUS/PIPETTE valve turned to BOTH. While the pipette and annulus is VENTED, both the pipette and annulus is filled with water to the top of the annulus. Make sure not to over fill them. Once they are filled, the line control valves are then turned from WATER to OFF.

4. The pipette and annulus is then pressurized by turning the valve from VENT to PRESSURE. The pipette and annulus are pressurized at 1.0 psi. This is done because the 5 gallon deaired water bottle is pressurized at a much higher pressure. If the chamber was allowed to be filed to the top from the deaired water bottle, the sample would be consolidating under the same pressure as the bottle is pressurized at, and this probably is not the pressure that one wishes to consolidate the sample at.

5. With the pipette and annulus pressurized at 1.0 psi, the line control valves should be in the following position, starting from the top BOTH, OFF, OFF. Then the bottom valve is turned from OFF to ON slowly. Water will flow from the pipette and annulus again into the chamber. When the water reaches the top of the chamber, the chamber should be moved around to try and get the air bubbles to go out the air release valve which must be constantly pressed in order to release water. (It should be noted that when using the aluminum plattens, it is a good idea to unscrew the loading piston from the top platten while filling the chamber since air tends to get trapped in that space and may come out during the test).

6. When there are no air bubbles visable in the chamber, the air release valve is closed and the chamber allowed to be filled with water. The chamber will only continued to be filled if there is a male part of the quick release valve inserted at the top of the chamber. This become the air release valve now. When water flows from the male end of the quick release valve, the chamber is full, and the male end is removed.

7. The chamber is now ready for testing.

IV. Digital Readout & X-Y-Y' Plotter

A. The workings of the digital readout and X-Y-Y' plotter will not be described in complete detail due to the author's limited knowledge of these devices.

1. The gain setting for the load is usually set at 2 mV. per lbs.. The gain setting for the axial displacement is usually 1.0 mV per 0.001 inch. Again, the calibration number, found by pressing the calibration button on the digital readout, should be recorded for each channel. These calibration numbers should be checked before each triaxial test.

2. Concerning the X-Y-Y' plotter, the X-Y pen is used for load and axial displacement measurements. The Y' pen is used for either volume change measurements or pore pressure measurements.

3. It should be noted that the gain sttings marked (stated) on the X-Y-Y' plotter are not in calibration with actual output. Before each series of triaxial tests, calibration curves should be constructed for each of the three channels. The calibration numbers should be checked during each test by manually recording the data at some point and marking that point on the plot be recorded. This manual check should be done at least two to five times for each test, especially at the final point of each test.

**Volume Change Device Calibration/Resolution Chart**
**(After Lade, 1988)**

| Quantity | Specimen |
|---|---|
| Sample Diameter, cm | 5.08 |
| Sample Height (H), cm | 10.16 |
| Sample Cross-sectional Area, $cm^2$ | 20.2683 |
| Sample Volume (V), $cm^3$ | 205.926 |
| Desired Volumetric Strain Capacity: $\Delta V = (\varepsilon_v/100)(V)$, $cm^3$ | 20 |
| Volume Capacity | ~ 45 |
| Precision on axial displacement measurement $\Delta H$, cm | 0.00254 |
| Axial Strain Precision $\varepsilon_1 = (\Delta H/H)(100\%)$, % | 0.025 |
| Volume Strain Precision $\Delta \varepsilon_v = \Delta\varepsilon_1$, % | 0.025 |
| Volume Change Precision $\Delta V = (\Delta\varepsilon_v/100)(V)$, $cm^3$ | 0.05148 |
| Actual Volume Change Precison, cm3 | 0.01667 |

# APPENDIX F

## Triaxial Test Procedures

I. Conventional Triaxial Compression (CTC)

A. Once the sample was ready to be tested, the drain lines were opened, and the cell pressure was applied. The cell pressure was applied to a column of water in a pipette which fed water through the volume change device and into the cell, as shown in Figure 3.1. Thus, the volume change which occurred during consolidation could be measured with both the pipette and the volume change device. For samples at low confining stresses, the sample was usually consolidated in 8 to 12 hours; for samples at high confining stresses, the sample was usually consolidated in 12 to 18 hours. In all cases, the sample was allowed to consolidate for a period of 24 hours to assure full consolidation. The final axial deformation and volume change readings after consolidation were recorded. Following the consolidation phase, the sample was loaded axially at a predetermined rate of 0.0254 cm (0.01 inches) per hour.

B. Since no initial oedometer test was conducted using the Sesser soil, a Cc or Cv value could not be determined to find an appropriate loading rate to be considered a drained test; a drained test is defined as a test in which no pore pressure is built up within the sample. Referring to work by Bishop and Henkel (1962), true clays such as Wield clay and Cambridge clay failed in about 48 hours for drained triaxial tests. From this failure data and assuming the soil would begin to fail at an axial strain of approximately 10 %, a loading rate of 0.0254 cm (0.01 inch) per hour was selected, giving a failure time of about 35 to 55 hours, depending on the confining stress.

C. During the test, the load, axial deformation, and volume change were constantly recorded by an electronic two pen plotter (X-Y-Y' plotter). Periodic manual readings were taken to check the calibration factors and as a back up method. Once the test was complete, data points from the recorded graph were entered into a data reduction program and reduced into appropriate stress and strain units.

II. Hydrostatic Compression (HC)

A. In the hydrostatic compression test, there is no consolidation phase, but the sample may become slightly consolidated when the chamber is filled with water. For water to flow into the chamber, the water must be under pressure, unless gravity filling is used. During filling, when the fill water reaches the top of the chamber and air is being bled out, the fill pressure is transferred to the sample.

B. As mentioned when describing the CTC test, the fill pressure was 6.895 kPa. (1.0 psi). Therefore, the sample can be considered to be consolidated at 6.895 kPa. (1.0 psi). Once the chamber was filled with deaired water, all the measuring devices were zeroed, and the cell pressure was increased to 13.79 kPa. (2.0 psi).

C. Recording axial deformation at set time intervals, a dial reading verus square root of time graph was plotted and t90 was determined, as shown in Figure 5.2. Described by Taylor (1948), t90 is the point at which 90% consolidation has occurred. Once this point was reached, the final axial deformation and volume change for that step was recorded and the next load step was applied to the sample and another graph started. This procedure was followed for each increasing (loading) load step. In the case of decreasing (unloading) load steps, a similar graphing procedure was used to determine t90, although t90 cannot truely be called 90% consolidation, but rather 90% of the axial unloading movement had occured. Again, at t90, the next unload or load step was applied.

D. The loading steps should be similar to that of a traditional oedometer test. The load steps, in kPa., were 6.895, 13.79, 27.58, 55.16, 110.32, 55.16, 27.58, 13.79, 27.58, 55.16, 110.32, 220.64, 110.32, 55.16, 27.58, 13.79, 27.58, 55.16, 110.32, 220.64, 441.28 (in psi: 1.0, 2.0, 4.0, 8.0, 16.0, 8.0, 4.0, 2.0, 4.0, 8.0, 16.0, 32.0, 16.0, 8.0, 4.0, 2.0, 4.0, 8.0, 16.0, 32.0, and 64.0. The final axial deformation and volume change for each step was recorded. This data was then reduced and graphed in a similar fashion as the conventional triaxial compression test data.

E. Hydrostatic compression tests were stopped at 441.28 kPa. (64.0 psi) since 551.6 kPa. (80.0 psi) was the limit of the pressurized air supply. The HC test may be run to even higher stresses to make certain cap model parameter evaluations less complicated and time consuming.

F. It was found through testing that it is important to unload to the same stress each cycle. For example, on the first cycle if the sample is unloaded to 13.79 kPa. (2.0 psi) and on the next cycle unloaded to only 4.0 psi, the slopes of the unloading curve will not be consistent, as shown in Figure 4.3. This inconsistency is due to the nonlinearity of the unload behavior. When unloading in the second cycle to only 27.58 kPa. (4.0 psi), 27.58 kPa. (4.0 psi) was on the hysteresis loop on the first unloading cycle. The HC test was not unloaded to 6.895 kPa. (1.0 psi) due to unavoidable drift which may occur in the pressure system, thus unloading the smaple below the initial starting stress of 6.895 kPa. (1.0 psi).

G. It was also found through testing that when samples were unloaded below 13.79 kPa. (2.0 psi), an apparent drift in the data aquisition system occurred. The author does not know if this is attributed to the resolution of the testing equipment or actual behavior of the soil.

III. Triaxial Compression (TC)

A. As stated in an earlier section, the triaxial compression test is run along a stress path such that the octahedral stress remains constant. This test is started by first consolidating the sample at some predetermined consolidation pressure as described previously.

Following the consolidation phase, the triaxial compression test was run immediately. Initially, the octahedral stress is equal to the consolidation stress, then the cell pressure (lateral stress) is decreased as the axial stress is increased, keeping the octahedral stress constant.

B. The octahedral stress is kept constant by first loading the sample axially at the same rate the CTC drained tests were loaded. As the axial stress reaches convenient intervals, usually 1.724 to 3.448 kPa. (0.25 to 0.5 psi), the cell pressure is decreased accordingly to keep the octahedral stress constant. Again at convenient intervals, such as 6.895 kPa. (1.0 psi), the axial and lateral stress is recorded along with the axial displacement and volume change.

C. It is usually easier to predetermine what the digital display should read for each stress level. With these numbers written down beside the DDU, the researcher can easily know when to unload the lateral stress and take readings. This is also true for the RTC tests.

D. This procedure requires an extensive amount of monitoring, since load steps must be applied manually and the data must be recorded manually. This extensive monitoring is especially realized if the soil being tested is a fine-grained soil, to allow complete sample drainage. Sleeping in the laboratory room with an alarm clock should become familiar before the testing series is complete.

IV. Reduced Triaxial Compression (RTC)

A. The reduced triaxial compression test is similar to the TC test, with the exception of the variation of axial stress. In the TC test, the axial stress is increased to keep the octahedral stress constant; conversely, in the RTC test, the axial stress is increased to maintain the same value at which it was consolidated.

B. The axial stress is kept constant by first loading the sample axially at the same rate as the CTC drained tests. As the axial stress reaches convenient intervals, usually 1.724 to 3.448 kPa. (0.25 to 0.5 psi), the cell pressure is decreased accordingly to keep the axial stress the same as the consolidation stress. Again at convenient intervals, such as 1.0 psi, the axial and lateral stress is recorded along with the axial displacement and volume change.

C. This procedure, as for the TC test, requires an extensive amount of monitoring.

V. Sample Saturation Procedure

A. Several methods of saturation were used in trying to saturate the samples.

B. The first method of saturation is a method using back pressure to increase the degree of saturation (Lowe and Johnson, 1960). In this

method, deaired water is forced into the sample, thus driving the air in the sample into solution. This is accomplished by incrementally increasing the cell pressure and pore pressure at a constant rate; the difference in the two pressures being the effective stress. It is important to use intervals in which no consolidation, beyond the planned consolidation, takes place. This method can be modified by placing a vacuum at the top of the sample to expedite the saturation process.

C. Another method used is similar to the previously mentioned procedure except that, instead of using a vacuum, a second back pressure line forces deaired water into the top of the sample (Lowe and Johnson, 1960). A differential of no more than 13.79 kPa. (2.0 psi) is used in the back pressure lines.

D. With soils such as low permeability clays, these methods may not provide complete saturation of the soil, unless extremely high back pressures are used. In this case, very small holes are drilled, running 3/4 the length of the sample around the premeter of the sample and stuffed with woolen wicks. The sample is then turned over and a single hole is drilled, running 3/4 the length of the sample down the middle of the sample and stuffed with woolen yarn. The wicks are placed at these set intervals to reduce the length of the path the water must travel through the sample (Lowe and Johnson, 1960).

E. The author does not have enough experience to completely describe the workings of the pore pressure transducer and readout. One suggestion is to use plumbers tape with all connections.

F. Several trial tests should be conducted using the pore pressure transducer on sand samples to check the system.

# VITA

James D. Hoskins, III was born in Charleston, South Carolina on January 29, 1965. He and his family moved to Charlotte, North Carolina, in 1967. In Charlotte he attended Park Road Elementary, Piedmont Middle, and graduated from Myers Park High School in June 1983. The following August, he entered The Citadel in Charleston, South Carolina. During the summers of 1984, '85, and '86 he worked at Law Engineering Company in Charlotte, North Carolina as an engineering technician. Following his graduation from The Citadel in May 1987 with a B.S. in civil engineering, he took a position as a materials staff engineer at Law Engineering.

In September 1987 the author accepted an assistantship at The University of Tennessee, Knoxville and began study toward a Master's degree. In the spring of 1988, he accepted a research assistantship sponsored by the United States Bureau of Mines Twin Cities Research Center. He completed his studies during the summer of 1989 and received his M.S. degree in civil engineering in December of 1989.

The author is a member of Chi Epsilon, American Society of Civil Engineers, and Tau Beta Pi. Mr. Hoskins will be employed by Trigon Engineering Consultants, Inc. in Greensboro, N.C..